UNIVERSIDADE ESTADUAL PAULISTA
"JÚLIO DE MESQUITA FILHO"
CAMPUS DE GUARATINGUETÁ

FELLIPE SARTORI DA SILVA

Energy generation systems under unexpected operational conditions : consequences in view of components and consideration of resilience in the design phase

Guaratinguetá

2022

Fellipe Sartori da Silva

Energy generation systems under unexpected operational conditions : consequences in view of components and consideration of resilience in the design phase

Tese apresentada à Faculdade de Engenharia do Campus de Guaratinguetá, Universidade Estadual Paulista, para obtenção do título de Doutor em Engenharia Mecânica na área de Energia.

Orientador: Prof. Dr. José Alexandre Matelli

Guaratinguetá
2022

unesp ✦

UNIVERSIDADE ESTADUAL PAULISTA
CAMPUS DE GUARATINGUETÁ
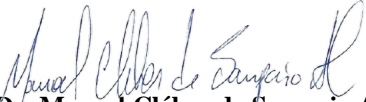
FELLIPE SARTORI DA SILVA

ESTA TESE FOI JULGADA ADEQUADA PARA A OBTENÇÃO DO TÍTULO DE
"DOUTOR EM ENGENHARIA MECÂNICA"

PROGRAMA: ENGENHARIA MECÂNICA
CURSO: DOUTORADO

APROVADA EM SUA FORMA FINAL PELO PROGRAMA DE PÓS-GRADUAÇÃO

Prof. Dr. Manoel Cléber de Sampaio Alves
Coordenador

B A N C A   E X A M I N A D O R A:

Prof. Dr. JOSE ALEXANDRE MATELLI
Orientador - UNESP
participou por videoconferência

Prof. Dr. KAI GOEBEL
Luleå Tekniska Universitet
participou por videoconferência

Prof. Dr. CARLOS DIAS MACIEL
USP São Carlos
participou por videoconferência

Prof. Dr. JOSE ANTONIO PERRELLA BALESTIERI
UNESP
participou por videoconferência

Prof. Dr. MICHEL BESSANI
UFMG
participou por videoconferência

FEVEREIRO de 2022

<div align="center">

DADOS CURRICULARES

FELLIPE SARTORI DA SILVA

</div>

NASCIMENTO   16/10/1991 - São Paulo / SP

FILIAÇÃO   Edson Pereira da Silva
Alva Valéria Sartori

2018 / 2022   Doutorado em Engenharia Mecânica (Energia)
Universidade Estadual Paulista – Faculdade de Engenharia de Guaratinguetá

2016 / 2018   Mestrado em Engenharia Mecânica (Energia)
Universidade Estadual Paulista – Faculdade de Engenharia de Guaratinguetá

2010 / 2015   Graduação em Engenharia Mecânica
Universidade Estadual Paulista – Faculdade de Engenharia de Guaratinguetá

I dedicate this work to those that supported me during this path: my parents Alva and Edson, my best company and biggest enthusiast Ana Júlia, and my siblings Frederico and Ana Beatriz. I would also like to dedicate to the real and unbiased scientists: it is not easy to stand up against lobby. Keep going.

ACKNOWLEDGEMENTS

I would like to thank some important parts of my path.

My advisor, José Alexandre Matelli, for trusting this project to me and for the patience during this path.

The professors that were somehow part of my graduate courses, specially José Antônio Perrella Balestieri and Eliana Vieira Canettieri, who assisted me from the beginning.

The employees of the School of Engineering of Guaratinguetá (FEG).

Some friends that I made during the course, specially Fábio Roberto Vieira, Ana Cláudia Cipriano and Mateus Dias Ribeiro. I also include here all my fraternity friends that lived with me during my undergraduation in República Arapuca, but highlighting the closest ones: Matheus Pedrosa da Silva, Friedrich Sander Giatti, Pedro Cadorin Falleiros, and the outsider Luiz Henrique Torres da Costa. It is really important for me to mention some special people that the city of Guaratinguetá gave me, as Roberta Peres, Valéria Monteiro, and Mirela Monteiro.

My family, for the moments of joy and care, and my daily partner, Ana Júlia Mendes de Oliveira, who tolerated me in every way during this project. I will never be able to thank you enough, Ana.

Many other important people have spent at least some precious time with me during my PhD, and I would like them to know that they are also part of it. I do remember all of you with affection. All. Know that. Also my mention to my good friend Davi Furcolin Alvim.

CAPES and FAPESP for their indispensable financial support during the project.

ABSTRACT

Energy systems are part of the critical infrastructures, and therefore any dysfunctionality can cause reactions in crucial societal fields. The more frequent and severe natural and man-made disasters increased the frequency of unexpected events, affecting these systems and exposing their vulnerability by leading them to abrupt disruptions. Resilience is a relatively recent concept in the thermal engineering field that is receiving attention due to the consideration of these high-impact, low-probability (HILP) events. This work aims to investigate the consequences of unexpected situations under these systems and establish a new method composed by seven quantitative metrics and a graphical analysis for resilience evaluation. The method was applied in four previously proposed cogeneration plants, two of them presenting redundancies. Both quantitative metrics and graphs converged to the same systems as the most and the least resilient ones, proving the robustness and reliability of the method. The inclusion of repairing actions hardly enhanced resilience of all the systems, mostly the less resilient ones, indicating that improving repairing conditions can be a great alternative to systems already in operation. The variation of input parameters revealed that operating time presents strong relation to resilience, indicating that systems projected to operate for shorter periods do not need significant investment in this field. Redundancy proved to be one of the important aspects for resilience evaluation, not being the major one under more detrimental scenarios, overcoming a possible initial idea that it is the main influence factor. Higher lifetimes provided extreme adverse environments, in which none of the configurations was able to continue its operation at an acceptable level. The graphical analysis pointed to the most resilient system as the one not only achieving more operating time, but also with highest energy generation along its lifetime. It also indicated that, for the analyzed scenarios, decreasing the failure rate could be more beneficial than invest in repair actions. In this evaluation, it became clear that the redundancy improved better the system availability, maintaining its operation for longer, compared to energy availability.

KEYWORDS: Resilience. Energy system. Energy generation. Natural disaster. Man-made disaster. Graphical analysis.

RESUMO

Sistemas de energia são parte das chamadas infraestruturas críticas e, portanto, qualquer alteração ou interrupção em sua operação pode ter alto impacto negativo em campos importantes da sociedade. Maiores frequência e intensidade de desastres naturais e antrópicos causaram um aumento de eventos inesperados, os quais afetam esses sistemas e expõem sua vulnerabilidade ao perturbá-los abruptamente durante sua operação. Por considerar essas situações extremas de baixa probabilidade de ocorrência e alto impacto operacional, o conceito de resiliência foi recentemente introduzido à engenharia térmica. O presente trabalho se propõe a investigar as consequências de situações inesperadas para sistemas de geração de energia, além de estabelecer um novo método de análise de resiliência, composto de sete métricas quantitativas e análise gráfica de parâmetros estabelecidos. O método foi aplicado em quatro plantas de cogeração previamente desenvolvidas, duas delas apresentando redundância. Tanto as métricas quantitativas quanto a análise gráfica convergiram para os mesmos sistemas mais e menos resilientes, provando a robustez e confiabilidade do método desenvolvido. A inclusão de ações de reparo aumentaram consideravelmente a resiliência de todos os sistemas, especialmente aqueles menos resilientes, indicando que melhorar as condições de reparo pode ser uma alternativa para plantas já em operação. A variação de parâmetros de entrada revelou que a vida útil esperada da planta apresenta forte relação com a resiliência, apontando que sistemas projetados para operar por curtos períodos não precisam de alto investimento nesse quesito. A redundância se destacou como um dos aspectos importantes para avaliação da resiliência, não sendo, entretanto, o principal sob condições adversas, fato que contraria uma possível ideia inicial de que esse é o fator de maior influência. Maiores tempos de vida útil criaram situações operacionais desfavoráveis, sob as quais nenhum sistema apresentou desempenho aceitável do ponto de vista prático. A análise gráfica apontou para o sistema mais resiliente como aquele não apenas que opera por maiores tempos, mas também que gera mais energia durante sua operação. Adicionalmente, ela também indicou que, para as condições simuladas, diminuir a taxa de falha pode ser mais benéfico que investir em ações de reparo. Por meio dessa análise, foi possível identificar que a redundância afeta de maneira mais acentuada a disponibilidade do sistema, mantendo sua operação por mais tempo, comparada à disponibilidade de energia.

PALAVRAS-CHAVE: Resiliência. Sistemas de energia. Geração de energia. Desastres naturais. Desastres antrópicos. Análise gráfica.

LIST OF FIGURES

LIST OF TABLES

LIST OF ABBREVIATIONS AND ACRONYMS

ACP	Absorption chiller pump
CDT	Condensate tank
CDP	Condensate pump
CHP	Combined heat and power
CT	Cooling tower
CTP	Cooling tower pump
CWP	Chilled water pump
E	Internal combustion engine
EM-DAT	International Disaster Database
EP	Engine pump
G	Generator
GT	Gas turbine
HEX	Heat exchanger
HILP	High-impact, low-probability
HRSG	Heat recovery steam generator
HWAC	Single effect absorption chiller
IT	Information technology
LHV	Lower heating value
MDC	Mechanical-driven chiller
PER	Primary energy rate
R	Radiator
SAC	Double effect absorption chiller
SARS	Severe Acute Respiratory Syndrome
SJR	SCImago Journal Rank
UNDRR	United Nations Office for Disaster Risk Reduction
USGS	United States Geological Survey

LIST OF SYMBOLS

Latin Letters

c	Round counter
c_v	Coefficient of variation
$\bar{D}$	Average downtime
d	Time counter when the system is stagnant (downtime)
d_k	Downtime time of kth simulation
E_g	Momentary total generated energy
E_{rc}	System rated capacity
EGR	Energy generation rate
F	Momentary system functionality
$\bar{f}$	Time until failure
m_f	Fuel consumption
N	Number of simulations
n	Time counter when the system operation is normal
N_d	Number of simulations in which $d_k > 0$ and $t_k = T$
$N_{d,T}$	Number of simulations in whith $d_k > 0$
N_f	Numbers of simulations in which $t_k < T$
NFx	Number of simulations that avoided failing when $p_{cr} = x$
N_r	Numbers of simulations in which $r_k > 0$ and $t_k = T$
p_b	Component failure probability
p_{cnr}	Component unsuccessful repair probability
p_{cr}	Component repair probability
p_d	Probability of system recovery
$p_{d,T}$	Probability of the system to recover and reach lifetime
p_f	System probability of failure

p_i	Probability of normal operation of component i
p_r	Probability of system resilient operation
Q	Thermal energy
r	Time counter when the system operation is resilien
$\bar{r}$	System resilient operating time
r_k	Resilient time of kth simulation
rt	Component repair time
st	Time spent in repair
T	System expected lifetime
t	Simulation time
$\bar{t}$	Average operating time
t_k	Simulation time of kth simulation
W	Power

Greek letters

θ	Resilient-stagnant ratio
ρ	Normalized resilience index
$\bar{\sigma}$	Standard deviation

CONTENTS

1 INTRODUCTION

Global energy demand is increasing in past years, mainly due to technological and industrial activities in both developed and developing countries [1], along with expansion of urban spaces, which currently consume around 75% of the generated energy [2]. Besides being associated with development, energy plays an important role by maintaining the other vital societal functions, fully dependent on its utilization [3]. Energy systems, those responsible for energy generation, transmission and distribution, are then classified as part of critical infrastructures [4].

Simultaneously with rapid development in all fields, the world experiences an increasing frequency of unexpected adverse conditions, threatening both people and functionality of society. These scenarios are basically consequences of disasters, which are unexpected, undesirable, and in some cases, unmanageable events [5]. The United Nations Office for Disaster Risk Reduction (UNDRR) defines disaster as:

> A serious disruption of the functioning of a community or a society at any scale due to hazardous events interacting with conditions of exposure, vulnerability and capacity, leading to one or more of the following: human, material, economic and environmental losses and impacts. [6].

Disasters can be classified in two groups, according to their origin: natural and man-made [7]. While the former covers events originated by processes of nature, the latter is caused by human actions or a direct consequence of them. Regardless their source, disasters are becoming more frequent in past decades, as it can be seen in Figure 1.

Figure 1 – Yearly frequency of disasters
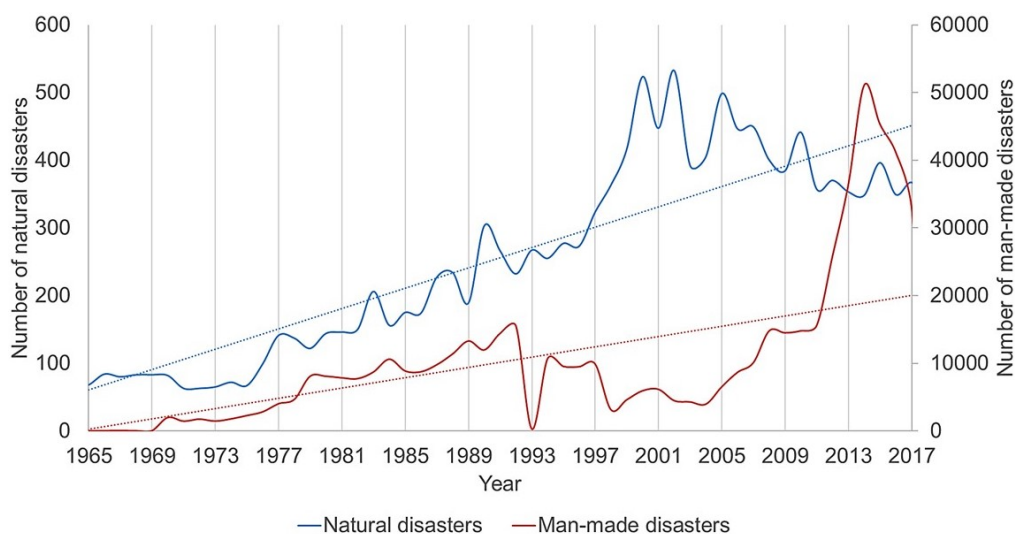
Source: [8, 9]

Figure 1 depicts a global critical situation, in which the humankind is exposed to more frequent unexpected adverse scenarios. The raise of natural disasters occurrence is associated with climate

changes and population growth [10, 11], while the recent increase of man-made disasters is related to the development of novel technologies, which led to unintended and uncalculated consequences [12], and a higher number of terrorist attacks and conflicts [9].

The potential losses and impacts can affect society in all levels and disrupt the functionality of several sectors, including energy infrastructure. Some examples of damage to energy systems are presented in Table 1 along with each corresponding consequence.

Table 1 – Examples of disasters and consequences to energy systems

Year	Country	Event	Consequence	Reference
2005	Iran	Cyber attack	Damaging of several centrifuges in uranium enrichment site	[13]
2008	China	Ice storm	Collapse of substations and towers	[14]
2009	France	Heat wave	Substantial decrease of nuclear power generation	[15]
2010	Mexico	Explosion	Destruction of part of an oil pipeline	[16]
2011	Japan	Earthquake / tsunami	Multiple failures in cooling system of nuclear power stations and collapse of power generators	[17]
2012	Colombia	Bomb attack	Decrease of energy production and negative affect on economic growth	[18]
2012	US	Hurricane (Sandy)	Destruction of electrical wires, transformers and substations	[14]
2014	US / Western Europe	Cyber attack	Disfunctionality of energy producers and oil distribution	[13]
2016	China	Tornado	Disruption of 14 transmission lines	[19]
2020	Bangladesh	Cyclone	Blackout and normalization of distribution lines in one month	[20]

Source: Author's elaboration

The above described scenario indicates potential threats for the operation of systems in general, including energy ones. However, as the conventional design of energy systems does not include high-impact, low-probability events (HILP events) [21, 22], they are not prepared to withstand unexpected adverse conditions, and therefore any abrupt disturbance can lead to severe and unpredictable outcomes. By focusing on prepare systems to operate under these circumstances, resilience has been attracting a high amount of attention in engineering in past years, especially in energy field [23].

Referring to energy systems, resilience can be defined as their ability to absorb unexpected external disturbances, withstand operationally and structurally the impacts, recover quickly in case of disruption and/or damages, and adapt to further hazards [24, 25, 26]. Panteli and Mancarella [27] defined as short-term resilience the features analyzed from the moment before the event until system recovery, while the long-term resilience covers the learning and adaptation after the occurrence. A resilient system keeps generating the total or a part of its energy demand under adverse conditions.

The introduction of resilience in system design fills a gap of covering eventual components random failure. Reliability is currently the main concept considered by structural analysis, which relies on predictable events under static operating conditions, following expected failure rates [23, 28]. In other words, HILP events are not suitable within reliability analysis [29]. Figure 2 represents a concept map

that describes the relation of both resilience and reliability to the design of energy systems, differing both concepts.

Figure 2 – Application of resilience and reliability in the design of energy systems
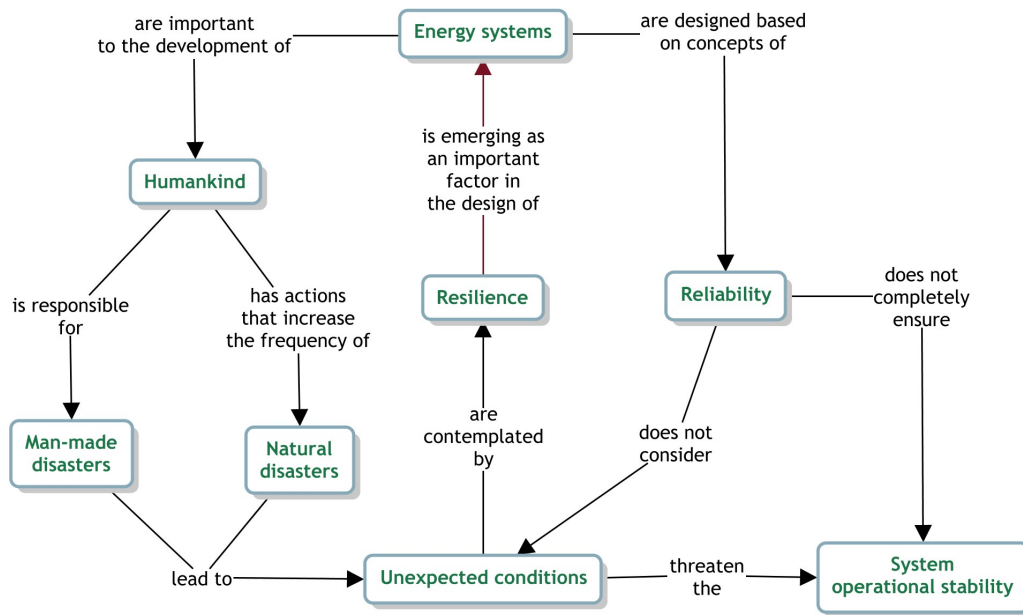
Source: Author's elaboration

As contained in Figure 2, the main difference between the concepts of resilience and reliability within the energy context is the consideration of unexpected conditions, mainly as a consequence of disasters, which threaten the system operational stability. This novel awareness evidences the necessity of a distinct and innovative approach to be contemplated during system design.

As a recently introduced concept in energy field, the evaluation of resilience is not consensual in the scientific community and there is no standard method to analyze this parameter in energy systems. However, several works address this topic, being optimization models [30, 31, 32] and graph network analysis [33, 27, 34] the most commonly found methods in literature. In addition, power distribution structures and natural gas pipelines are the most studied systems [35]. Besides the evident scientific gap regards a consistent resilience evaluation in engineering systems, there is also a significant lack of discussion of resilience in energy generation systems, which is the focus of this work. In the next chapters, these systems are mentioned as "cogeneration systems", a term covering both electrical and thermal energy generation.

1.1 OBJECTIVES

This work aims to develop a method capable of evaluating resilience in energy generation systems by proposing both quantitative metrics and graphical analysis for different configurations. The specific objectives of the research are:

- Analyze possible hazards and their corresponding consequences to energy systems;

- Propose actions to reduce the operational risk;

- Investigate the design and operational factors that influence resilience in these systems;

- Identify the sectors that demand resource allocation;

- Verify the behavior of the system under several operational conditions.

2 LITERATURE REVIEW

This chapter presents the existing hazards threatening energy systems and their consequences at component level. In addition, the concept of resilience is introduced and the state-of-the-art in scientific literature is analyzed.

2.1   THREATS TO ENERGY SYSTEMS

2.1.1   Natural disasters

Unavoidable and abrupt events presenting destructive potential originated by natural processes are defined as natural disasters. According to the International Disaster Database (EM-DAT) [8], along with an increase of natural disasters frequency – covered by Figure 1 –, both number of people affected by these events and associated economic losses also experienced a substantial growth worldwide, as illustrated by Figure 3. A scientific consensus on the higher number of both frequency and severity of natural disasters point to human activities, as population growth, urbanization and climate changes [36]. It is important to inform that the estimated economic damage in Figure 3 refers to impairment of property, crops and livestock.

Figure 3 – Number of people affected and economic losses due to natural disasters
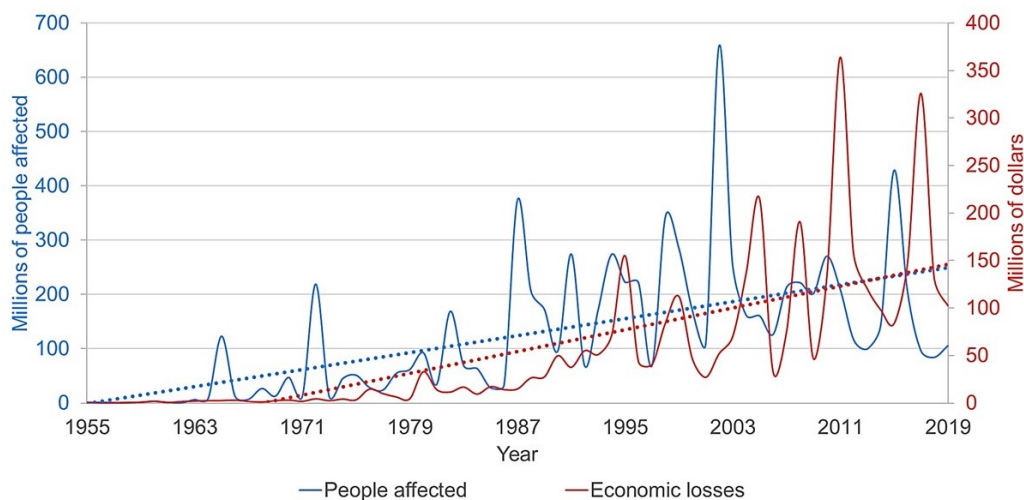
Source: [8]

The highest peaks in economic losses occurred in 2011 and 2017. In 2011, storms, floods and earthquakes caused severe economic damage in Asian and American countries. In the same year, Colombia lost almost US$ 8 billion in infrastructure damage and governmental actions due to a La Niña phenomena [37]. In 2017, the main losses were caused by Hurricanes in United States and Puerto Rico. India and China experienced severe droughts, floods and storms in 2002, which affected more than 620 million people and contributed to the associated highest blue peak in Figure 3.

There are natural disasters difficult to foresee, as storms and earthquakes; while others may be seasonal, like droughts and floods. For instance, a severe drought that took place in India in 2002

occurred over the same period in several years [38]. On the other hand, an unexpected earthquake in 2011 hit coastal areas in Japan with harsh outcomes [39]. In addition, the former example was seven months long, while the latter took a few minutes. The large number of disasters and their different features need to be considered in actions focused on risk reduction and society protection, and therefore separate and understand them are important steps. According to the UNDRR [40], disaster risk profile, local context and government structure are crucial factors to implement strategies.

Currently, as illustrated by Figure 4, Asia – especially South and Southeast – is the most affected continent by natural disasters, experiencing almost 40% of all reported events, followed by Africa and Americas. Areas located on the earthquake belt [41], fast urbanization and population growth [42], and severe seasonal monsoon pattern [43] are factors that contribute for this high occurrence rate. The curves represented in Figure 4 also demonstrate the increased frequency of natural disasters worldwide, except for Oceania, that presents stable numbers since the 80s.

Figure 4 – Frequency of natural disasters by continent
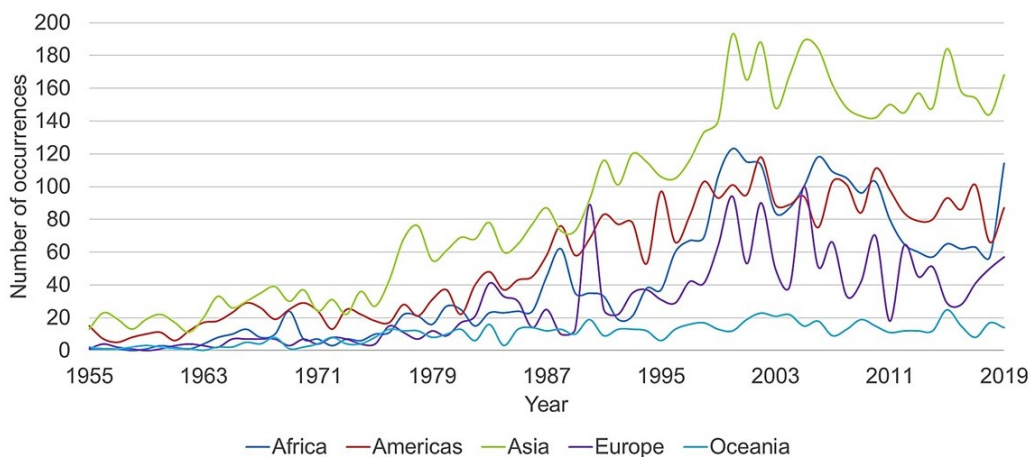
Source: [8]

Despite observing the frequency of the events, the consideration of the local context also includes the analysis of disaster types. This work follows the arrangement of EM-DAT [8], which differs them by their origins in the following subgroups: geophysical, hydrological, meteorological, climatological and biological. Although a sixth type named extra-terrestrial is also considered by EM-DAT, only one case is reported since 1900, and therefore it is not significantly relevant. A concept map represented by Figure 5 illustrates an overview of natural disasters and their corresponding types.

Figure 5 – An overview of natural disasters and their corresponding types
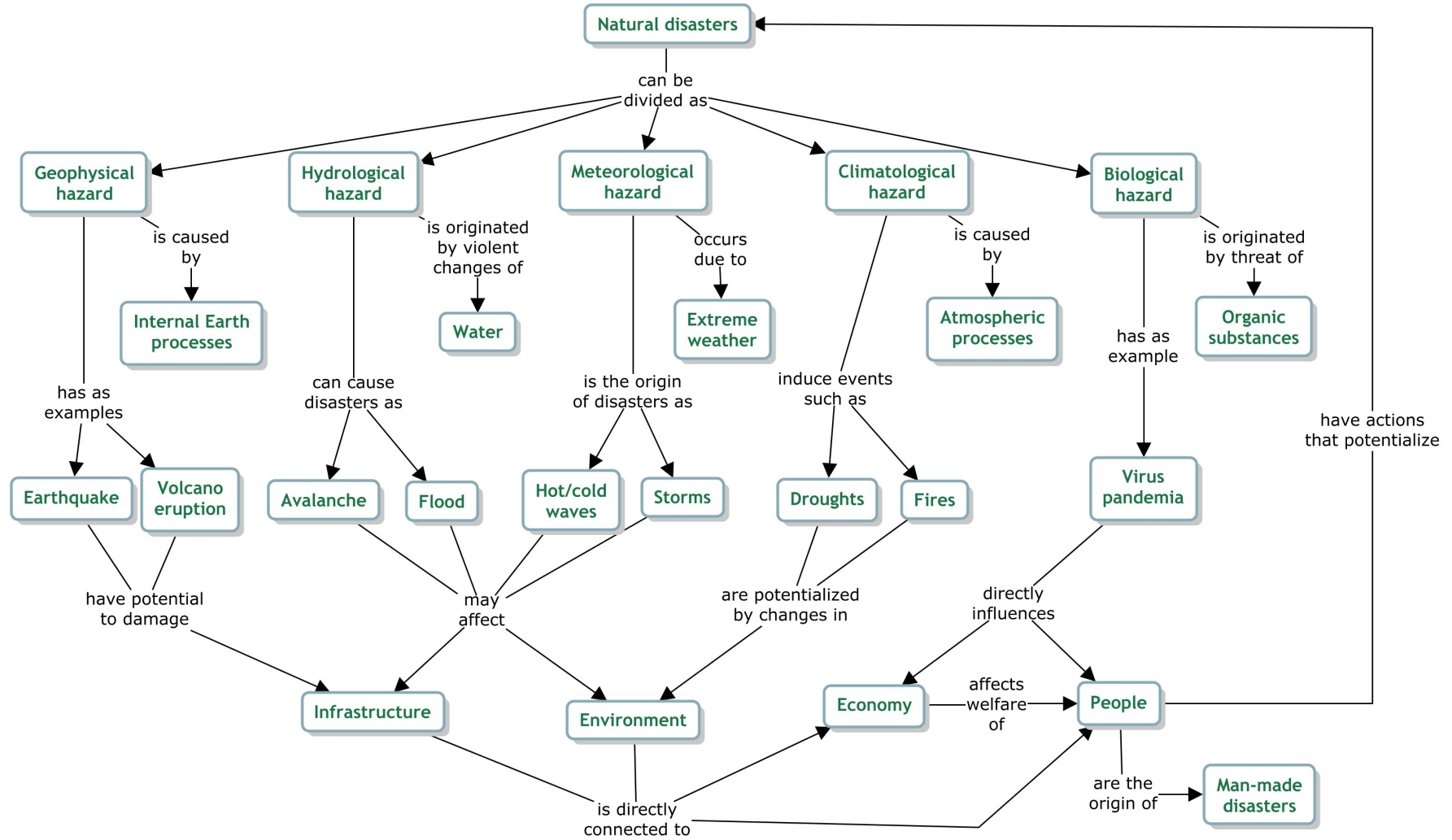
Source: Author's elaboration

It is noted in Figure 5 that all the types of natural disaster are related to disruptions in vital sectors of society, such as infrastructure, environment and economy. Regardless the affected part, the outcome always interferes in people, who themselves are responsible for intensifying the frequency and severity of the occurrences.

The frequency of each type of natural disaster is depicted by Figure 6. It is possible to notice that in past years, hydrological and meteorological events are those with the most substantial growth, then becoming the most common threats. Although all the types present increased number of occurrences, there is a recent stabilization of climatological and geophysical disasters.

Figure 6 – Frequency of each type of natural disaster
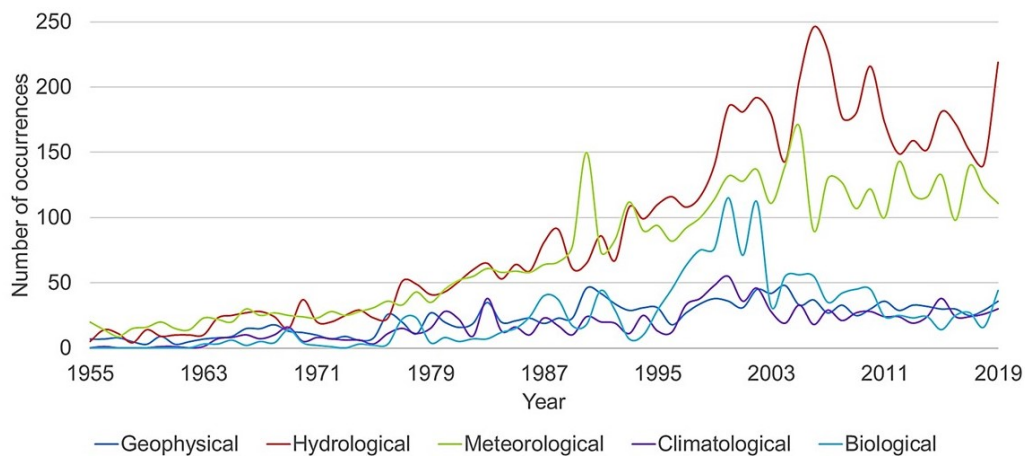
Source: [8]

The following sections describe and discuss each type of natural disaster.

2.1.1.1 Geophysical

Underground tectonic and seismic activities can cause abrupt movement in Earth surface – which may lead to earthquakes and dry mass movement, depending on the region in which the processes originate – and activation of volcanoes. These events are defined as geophysical disasters, and they are divided into the three above mentioned subgroups: earthquakes, dry mass movement and volcanic activity.

As the occurrence of geophysical disasters depends on underground activities, they are distinctly widespread over the Earth [44]. Asia is the most affected continent by these events, with 54% of the reported geophysical disasters [8], mainly due to the location of its South and Southeast regions along the earthquake belt, an active tectonic plate boundary [45, 41]. Asia, America and Oceania reported 88% of the volcanic activity, as a consequence of the distribution of volcanoes along the coastal regions of these continents [46].

The frequency of each subgroup is illustrated by Figure 7. It is possible to see a higher frequency of reported earthquakes in past decades and a light stabilization of volcanic activity and dry mass movement. The U.S. Geological Survey (USGS) attributes this increase in earthquakes frequency not to the higher number of occurrences itself, but to the greater quality and quantity of the instruments to record these data [47]. Seismic and tectonic activities usually occur according to geophysical features

of the Earth, and although some human activities can possibly release some internal stress and trigger earthquakes [48], it is accepted that there is no relation between the occurrence of these disasters and human activities.

Figure 7 – Frequency of geophysical disasters
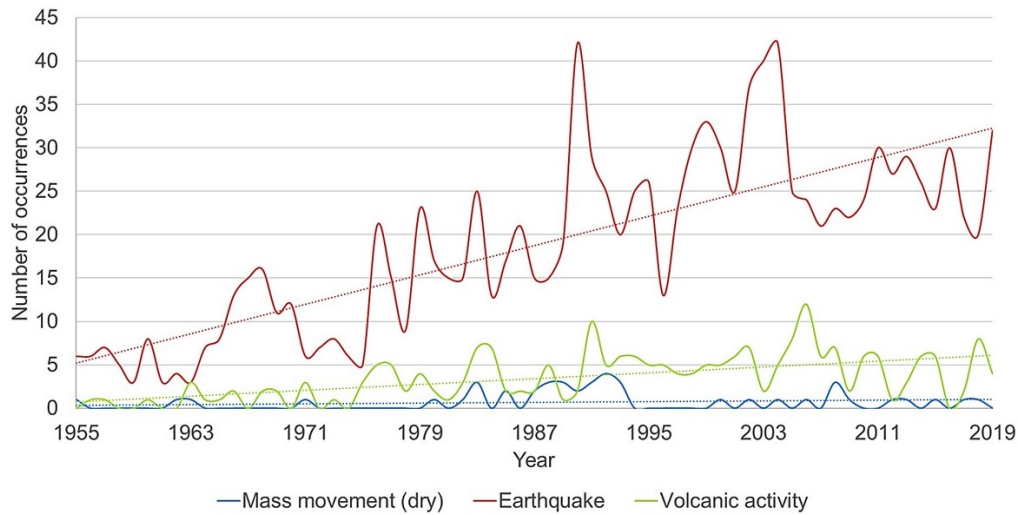
Source: [8]

The sudden behavior of geophysical disasters increases their potential of destruction by quickly disrupting systems operation and reducing the accuracy of disaster mitigation actions [49]. Local infrastructures and people are susceptible to severe outcomes that can last for many years. In addition, adverse effects can be induced after the event, such as tsunamis, which can deteriorate the condition of both soil and air, as well as damage the local buildings and infrastructure; modification in local hydrology and destruction of fauna and flora, through salty water, lava flow or abrupt mass movement; pollution of air and water; and fires [50].

2.1.1.2 Hydrological

Hydrological disasters are those caused by violent and sudden changes in water quality, distribution or movement due to intense modification in hydrological cycle. In socio-economic terms, these type of disaster can be classified as the most devastating [51]. They are typically divided into two main subgroups: wet mass movement and flood, as represented by Figure 8 along with the most common occurrences.

Data of EM-DAT [8] point to a considerably prevalence of flood among the occurrences of these events since 1950, being 88% of the total amount, among which 43% took place in Asia. South and Southeast of this continent have typical monsoon and structural problems [52, 53], while the Central Asia is affected by concentrated annually precipitations [54]. The frequency of these disasters is also affected by human activities, as rapid urbanization [55], public mismanagement [53] and global warming [56]. Climate changes are expected to both alter the rainfall patterns, modifying the occurrence of hydrological events worldwide [57], and increase the surge flood level of Coastal locations by rising sea level [58].

Figure 8 – Subgroups of hydrological disasters and common occurrences
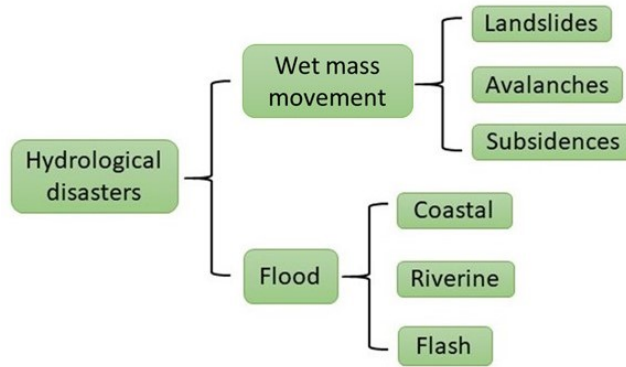
Source: Author's elaboration

Severe consequences are related to hydrological disasters. Movement of a large amount of sediment, threatening local infrastructure, people and ecosystems [59], contamination of water sources and arable areas [60, 61], growth of infectious diseases [62], erosion and loss of vegetation [63], and interruption of business activity [64] are among the outcomes.

2.1.1.3 Meteorological

Meteorological disasters are short-lived damaging events caused by extreme weather and sudden changes in atmospheric conditions. The most common hazard is storm, a generic term covering a high variability of catastrophes, including thunderstorm, sandstorm, snowstorm, tornadoes, cyclones, severe rainfalls, among others. The other type is extreme temperature, originated by heat and cold waves, as well as severe winter conditions [8].

Figure 9 – Frequency of meteorological disasters
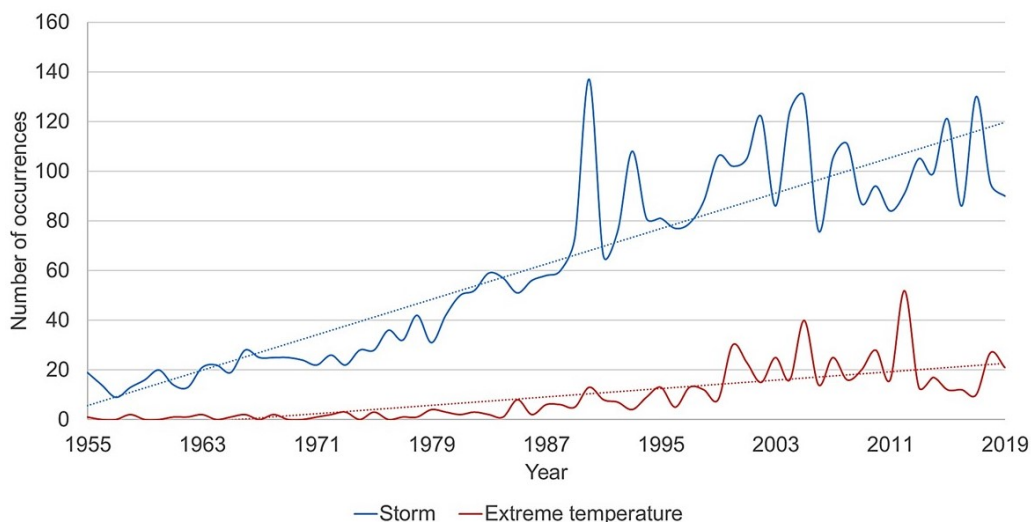
Source: [8]

It is possible to notice in Figure 9 the significant increase in reported storms, especially since the 80s, along with a slight upward trend in occurrences of extreme temperatures. According to Global Climate Projections [65], it is expected that both heat waves become longer, more frequent and severe,

and cold waves become less frequent, due to global warming. The behavior of storms under climate changes remain uncertain, although it is consensual that their intensity increases [66, 67] while they tend to move to other areas [68, 69]. Although their reported cases increased, there is still questions about the relation between climate changes and storms frequency [70, 71].

Extreme temperatures can affect local fauna and flora – including destruction of vegetation, impairment of livestock and alteration of soil conditions –, change the local precipitation and induce fires and droughts [72, 73]. Storms have potential to induce flood, damage buildings, infrastructure, arable lands and partially cease production activities [74, 75].

2.1.1.4 Climatological

Long-lived – up to several years [76] – incidents induced by natural atmospheric processes are classified as climatological. Droughts and wildfire are the prevalent subgroups, the former being responsible for 62% of the reported events [8].

Droughts are important to the functionality of some forests, since they allow a vegetation cycle [77]. However, as human activities and climate changes are altering hydrological patterns and rising global temperature, both frequency and intensity of droughts tend to increase [78], affecting the functionality of society. Food security and economy of some agriculture-dependent countries are strongly affected by the occurrence of severe droughts, especially by reducing water quality and availability and damaging the soil [79, 76], leading to famine and economic losses [38, 80]. In addition, local hydrology can be altered, which modifies the local climate [76].

Wildfires are also natural processes, which can be intensified in dry conditions [77]. Their frequency also depends on temperature, soil and air moisture and aspects of vegetation [81]. These events lead to emissions that cause air pollution and threaten people health [82], in addition to potentially destroy a large forest area [83], affecting local vegetation and soil.

2.1.1.5 Biological

Biological disasters are those caused by living organisms, organic substances and their respective vector-bone threats. These organisms invade spaces and disturb the normal function of ecosystems [84]. Epidemics and insect infestation are the prevalent subgroups, although the former itself is the subject 94% of the reported data worldwide since 1955 [8]. As these events have both uncertain and random behavior, their forecast is a difficult task and the risk analysis is mainly based on historical data [85].

The most harmful reported pandemic was the flu pandemic of 1918, which was responsible for around 50 million deaths and 500 million infected people [86]. World experienced heavy impacts in economy [86], science [87], public health [88], and other crucial societal fields. Other pandemics and epidemics happened over time, as Severe Acute Respiratory Syndrome (SARS) and influenza A (H1N1) [89]. The most recent one is the COVID-19 pandemic [90], with effects on several sectors. These unexpected events have the potential to impact regions up to several years.

Regarding insect infestation, this incident has been a concern for a long time, as it can be found in written records from 3000 BC [91]. Infestations can cause up to 20% of losses in the global agrofood

industry production [92, 93]. The increase in surface temperature tends to alter some features of the insects, as well as the population dynamics, which may difficult the predictability even more [94].

2.1.2 Man-made disasters

Man-made or anthropogenic disasters are those caused by human actions or a direct consequence of them. Although the definition is consensual in literature, several authors and organizations differ about the division of the subgroups. UNDRR [95] states that armed conflicts and terrorism need to be treated as humanitarian issues and therefore are not included in this term, while other researches [96, 97, 98, 99] consider these hazards as man-made. As conflicts and terrorist attacks meet the disaster definition as unexpected cause of disruptions in society, they are considered as man-made disasters in this work.

Basically, man-made disasters can be intended or unintended. Conflicts and both physical and cyber terrorism are defined as intended, once the attacks are planned by the terrorists, although they are unexpected by the receiver. Accidents originated by equipment malfunction or mismanagement and other types of disasters caused by human error are classified as unintended. The concept map presented by Figure 10 illustrates an overview of man-made disasters.

Figure 10 – An overview of man-made disasters
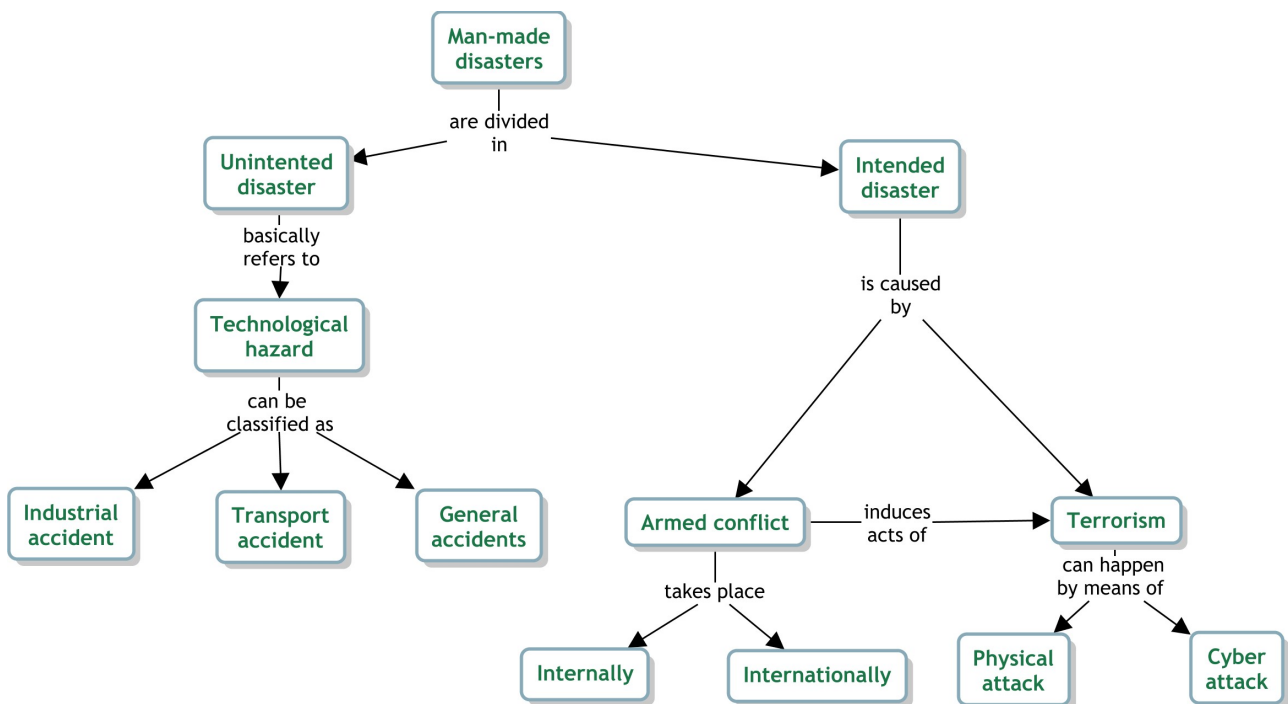
Source: Author's elaboration

2.1.2.1 Technological disasters

Technological disasters are unintended, severe consequences emerging from mistakes, failures and accidents regarding technology, industrial activity and natural environment manipulation [100, 101]. In contrast with natural disasters, most of these accidents can be mitigated – even prevented – by technical and organizational actions [7].

In addition to increase productivity, efficiency and safety of systems and processes, the development of novel technologies also creates unusual situations, which lead to higher probability of unintended and uncalculated events [12]. With the intensified and widespread use of technological systems, it is inevitable that both intensity and frequency of this hazard increase [102]. As illustrated by Figure 11, technological disasters, especially those related with transport systems, became more frequent in past decades.

Figure 11 – Frequency of technological disasters by subgroup
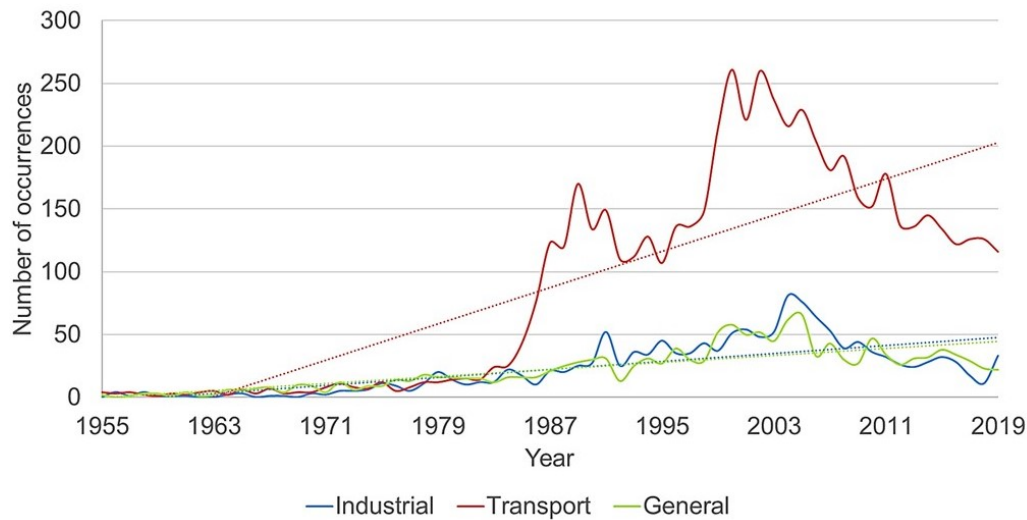
Source: [8]

The development of transportation technologies and the importance of transport systems to the current society are within the reasons for the increased number of occurrences in past decades [100, 103]. In addition, atypical weather conditions influence these occurrences [104], which take place mostly in developing countries [105]. Besides the deadly potential, transport disasters can damage infrastructure and buildings, interrupt the supply of essential products and release hazardous materials, which can be explosive, toxic or radioactive [106, 107, 108].

Industrial accidents occur as consequences of dysfunctionalities in industrial processes, generally in the form of explosions, spills, leaks and waste [8, 109]. One of the catastrophic examples is the Bhopal disaster [110], which happened in 1984, in India. In this event, 30 metric tons of methyl isocyanate escaped from the storage tanks, hurting and killing people and destroying part of the flora. An accidental reaction of the storage gas with water caused the leaking, and it is certain that it could be prevented with safety measures and some attenuation strategies [111].

The frequency of these disasters was intensified by the rapid economic growth of some countries, along with globalization and technological development [112, 113]. The term "general" in Figure 11 refers to the same events, but those which take place outside the industrial environment.

Regardless the type of technological disaster, there are three possible causes: human, organizational or technological, being the first two responsible for 70-80% of the accidents [101]. The human factor refers to bad decisions in system operation, managerial errors and negligent actions; organizational errors include deficiencies in communication, policies and strategies that contribute to

failures; and technological factor consists of errors in design and operation of these systems, leading to a compromised integrity.

2.1.2.2 Intended disasters

It is classified as intended disasters those planned by intelligence sector of offensive groups, i.e., that are intended to cause damage to a specific location or people, aiming maximum social disruption [114]. Terrorism and conflicts, both subgroups of this disaster type, increased in past decades, as illustrated by Figure 12. It is important to point that the data source [9] does not include terrorism data from 1993.

Figure 12 – Frequency of intended disasters by subgroup

Source: [9]
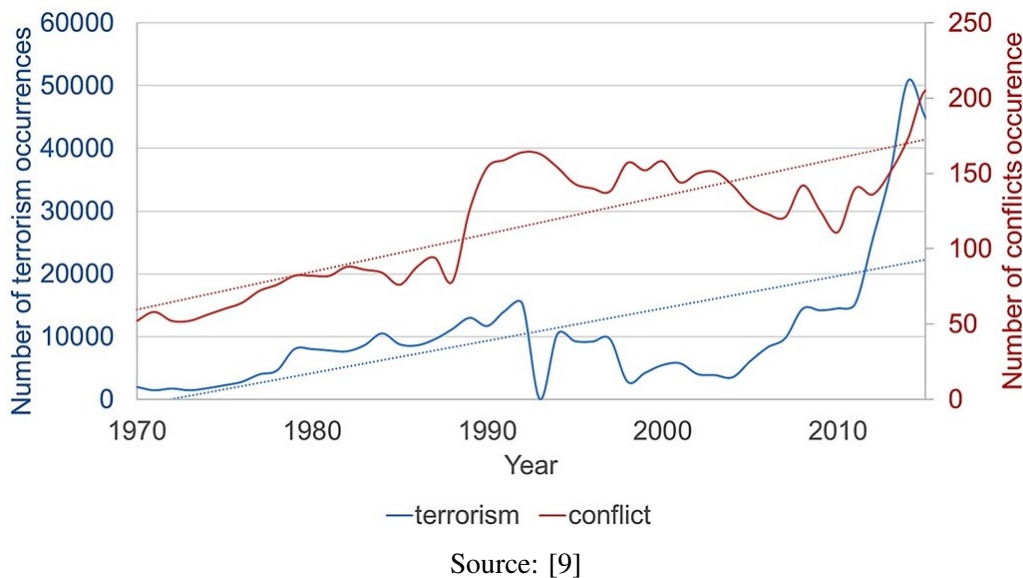
Terrorist attacks were not largely emphasized in design of buildings and systems until the 09/11 events, when the idea of analyzing this scenario in project phase spread worldwide, being treated as priority in some cases [115]. These offensives focus not only on harming people directy, but also on damaging critical infrastructure, as energy systems [116], manufacturing [117], transportation [118], water systems [117], among others. With this strategy, terrorists intend to cause severe damages to the functionality of society. Recent expansion of radical groups are increasing the risks of systems disruption [116].

Besides physical damage to critical infrastructure, terrorists also threat these systems with cyber attacks. Recent technology advances brought new vulnerabilities, as the systems reliance on information technology (IT), which are the focus of these offensives [119]. Unauthorized access to devices in order to alter and steal important data, as well as attacks on communication systems are two of the most common strategies [120]. Disruption of vital sectors, as energy, water and gas supply are among the goals of these violations [121].

As another source of threats, armed conflicts also have potential to damage local infrastructure and cause injuries and deaths. Currently, more countries are involved in armed conflicts than in past great wars in 20th century [122]. Additionally, the continuous growth behavior shown in Figure 12 can be magnified in next years, also related with increased frequency of natural disasters [123]. Therefore,

regions under constant conflict and those nearby are permanent candidates of having their infrastructure severely damaged.

2.1.3 Possible failures in cogeneration systems

Under the risk of unexpected conditions, as described in the last section, the operation of energy generation systems is threatened by the possible induction of failures in their components. Detect and understanding the vulnerability of these components is crucial to prepare them to withstand adverse situations and keep the system operating at an acceptable functional level.

Although the development of novel technologies relying on alternative energy vectors is being widely investigated [124], oil, coal and natural gas are currently responsible for 81% of global energy sources [125]. This data reflects the still great dependence on power plants based on fossil fuels. In this context, turbines are the most used components for electrical energy generation [126]. Engine-based systems are also numerous in smaller applications [127], while fuel cells recently became an attractive option due to their operational advantages, including fuel flexibility [128, 129]. As the prevalent prime movers operate at high temperatures, cogeneration units stand out as feasible and favorable options.

Cogeneration or combined heat and power (CHP) systems are those that simultaneously generate both thermal and electrical energy from a single fuel source. Besides being economically and technically attractive, cogeneration technologies are widely explored due to their flexibility, since various configurations can be proposed using several types of prime movers in different scales [130, 131, 132].

Regardless the type of demanded energy, the basic operation of power plants essentially follows the fundamental thermodynamic processes of compression, heating, expansion, and cooling [133]. Generally, a component suits a purpose of variation of pressure, temperature, molar composition and/or rate of a specific stream, within a specification based on a projected demand. Technical specifications, working fluid, cost and feasibility are within the features considered in component selection [134, 135]. However, due to the multi-criteria condition, the synthesis of an energy system is not trivial and there is no consensual method in scientific literature [133].

In cogeneration systems, the basic configuration includes the prime mover coupled to a power generator to generate electricity, and a component or system that recovers the residual heat from the prime mover, which can be heat exchangers, steam cycles and absorption chillers [127, 136]. Table 2 presents the prevalent prime movers, their complementary components, and the additional components, which are normally used to expand the plant, allowing new configurations proposals.

Abrupt disruption in any component listed in Table 2 can cause a cascade effect, leading to possibility of system total disruption and significant productive and economic losses, as well as sequential overloads. It is then important to recognize the possible failures that disasters can induce to these components.

As a proposal of this work, the possible failures are divided in three main groups: changes in operating environment, caused by sudden alterations in the system operating environment; direct physical failure, originated from impact, vibration or disconnections of the components; and damage in control system, induced by failures in equipment responsible for communication, operation management and

Table 2 – Typical components for cogeneration systems

Prime mover	Complementary components	Additional components
Gas turbine	Compressor Combustion chamber	Chiller Steam generator
Steam turbine	Steam generator Condenser Pump	Generator Heat exchanger Splitter/mixer
Internal combustion engine	-	Valve
Fuel cell	Reformer	

Source: Author's elaboration

supervision. Table 3 presents these groups, along with possible consequences and derivative effects, which are further detailed and discussed.

2.1.3.1 Changes in operating environment

The system operational environment is susceptible to changes as the local environment is affected by disasters. Any unexpected event that alters physical and/or chemical aspects of natural resources, reduces availability of substances used by internal processes or causes an extreme condition is a threat to system performance.

Inside the system, reaction processes can present anomalies due to environmental changes and alteration in reagents properties, which can be consequences of sudden modifications in temperature and air condition due to hot/cold waves, fires, droughts and contamination. Specific reagents can also suffer from a sudden change in its availability, which may unbalance the reaction. Components that operate with combustion, such combustion chambers, boilers and engines, can experience not only reaction performance decrease, but also structural damage as erosion and overheating, which can lead to fractures and explosions [137, 138]. Additionally, the temperature variation can change mechanical properties of the component materials [139], leading to unexpected behavior.

Air and water pollution, as eventual outcome of fires, floods, volcano activities or other alterations, also affect the operation. Polluted external flows influence compressors and pumps, which can present deposition and material degradation [140, 141] and overload in filtration system. Once inside the system, a flow containing sand, ashes or dust rubs the pipeline and the materials surface, leading to structure degradation. A contaminated external flow used for cooling may be less effective, causing overheating and damaging to the structure of the component by friction.

Modifications in local hydrology can prejudice the water availability, disturbing the components that operate with internal or external water flows – like pumps, condensers and heat exchangers – for not meeting the demand, which overload the component and consequently cause malfunction. On the other hand, an excess of water in the operating environment is also undesirable. Tsunamis and coastal floods induce increasing chloride content in local environment, a favorable condition to material corrosion [142]. In addition, a high moisture condition can also be detrimental to component materials, compromising its structural integrity [143].

Table 3 – Occurrences and consequences to the system

Occurrence	Possible consequences	Derivative effect
Changes in operating environment	Reaction anomalies	Overheating Explosion Poor generation
	Overheating	Deformation/fractures Component collapse
	Corrosion/oxidation	Fractures Leaking Contamination
	Excessive fouling	Contamination Overheating
Direct physical failure	Coupling failure	Overheating Fractures Overload Contamination Sudden pressure drops
	High vibration	Resonance Disconnections Fatigue acceleration
	Creep/fracture	Contamination Sudden pressure drops Overheating Explosion Leaking Component collapse
Damage in control system	Malfunction	Overload Component collapse Preventable failure acceleration
	Sudden variations	Malfunction Overload

Source: Author's elaboration

2.1.3.2   Direct physical damage

Among the three groups of occurrences presented in Table 3, direct physical damage is possibly the most abrupt. It considers impacts, vibrations and disconnections, and can affect all the components.

Sudden impacts can be consequence of earthquakes, targeted terrorist attacks or sediments and objects carried by the following: severe windstorms; lava, in case of volcano activity; or violent water flows, in case of tsunamis, floods or severe rainfalls. The brunts potentially cause immediate damages to the affected components with disconnections and instantaneous fractures, leading to leaking, sudden alteration in system parameters, contamination, malfunction and, in some cases, explosion. Flammable and toxic substances, which can be released with an eventual impact on their pipelines or components that are fed with them, as combustion chambers, fuel cells, engines and boilers, provide even more risk to the operating environment in these scenarios. Isolated systems can be exposed to a unexpected operating environment with the destruction of the local structure, leading to consequences described in section 2.1.3.1.

Earthquakes also lead to high vibration and resonance conditions, which accelerate cracking in components that operate with rotating movement, like turbines and pumps [144, 145, 146]. All the components are eventually affected under this condition with eventual disconnections and rupture of internal parts.

2.1.3.3   Damage in control system

The design of modern systems includes control of some parameters and processes, which provide useful information for the operators to take corrective actions. Although there are still on site management, the development of a communication network connected all the information to a central monitoring room [147]. This practice can concentrate the system control into a single space, increasing the vulnerability in case of an unexpected external impact.

The control system can be affected by a sensor failure, mainly in case of physical impact, or by an eventual dysfunctionality of the communication network, leading to disruption of information flow. The latter can be consequence of a targeted cyber attack. Events impacting the operators are also threats to control systems in cases when a human action is needed. All kinds of disasters can affect the operators in both physical and productive ways [148].

Table 4 presents the usual control types and controlled parameters. Internal system flow sensors can alert altered values of temperature, pressure and flow rate, which can lead to component malfunction and long term significant failures in its structure. Low pH water flow has potential to damage heat exchangers [149], while water and air altered compositions compromise the functionality of components operating with these substances and can lead to deposition and friction. An inoperative control of operational environment may not predict modifications in ambient temperature, pressure and composition, leading to malfunction and long term overload and overheating of the components. Monitoring the component structural aspects is also important, as the rotation speed of turbines [140] and their physical position in the system, since they can be evidences of dysfunctionalities.

Table 4 – Usual types of control

Control type	Controlled parameters
Flow	Temperature Pressure Flow rate Water pH Composition
Operational environment	Temperature Pressure Composition
Component structure	Rotation speed Position

Source: Author's elaboration

2.1.4 Reducing the risk

Several investigations converge in stating that disasters, followed by unexpected catastrophic conditions, are real threats to people either directly, by damaging their physical and psychological conditions; and indirectly, by disturbing the environment, infrastructure and economy. These events became more frequent and their occurrences are expected to keep increasing, which represents, along with the acceleration of climate changes, higher vulnerability of society and critical infrastructures. This situation requires actions taken by government, corporations and research institutions, aiming risk reduction and system protection. Some of the relevant actions are illustrated by Figure 13.

Figure 13 – Actions for risk reduction and system protection

Source: Author's elaboration

The risk analysis in energy systems in this context implies basically two approaches: reduction and forecast of disasters and adaptation of the system to withstand and recover from the possible effects.

Natural disasters are not always avoidable, as discussed in section 2.1.1, but novel methods and

technologies are being developed in order to forecast some of them [150, 151, 152]. Security models against cyber and terrorist attacks are also being widely investigated as possibilities to predict and avoid these events [153, 154]. This development is important to provide additional information before the adverse situation, in order to give time to adapt the system to withstand the possible impacts and attenuate the consequences. Governments play an important role in this topic not only by supporting researches in this field, but also by establishing both anti-conflict positions and sustainable policies, aiming to reduce the possibility of a disaster.

Threats also include human error and organizational mistakes – responsible for the most part of the technological disasters, as discussed in section 2.1.2.1. Therefore, investment in both error minimization and operational security enhancement are within the actions that corporations can take to reduce the risk of adverse scenarios. Sustainable policies, as the appropriate waste management, improve environmental issues and also reduce disaster occurrences.

It is important that investigations on impacts of disasters in systems operation consider local context. As pointed in section 2.1.1, Asia is the continent with more occurrences of natural disasters, totalizing 40% of the global events, specially regions located in South and Southeast [41]. Hydrological disasters, the most frequent ones worldwide, occur mainly in riverside locations. Seasonality of extreme conditions is also an important factor to be considered, since some regions are susceptible to seasonal variations in precipitation, droughts and other hazards, which can be intensified by rapid urbanization, industrialization and population growth [155]. Regarding terrorist attacks, it is essential to point that one of the terrorism goals is to transmit a specific message [156], and therefore places with high visibility and conflict regions are within the risky positions.

It is consensual that natural disasters currently occur more often due to human activities, such as rapid urbanization, combined with detrimental land usage [157]; greenhouse gas emission [158]; deforestation [159], and other types of destructive actions. Debates about climate changes mitigation, as the Paris Agreement [160], and investment in researches addressing this topic are essential steps to sustain policies focused on attenuate the causes, reducing the associated risks and consequently enhancing both operational stability and critical infrastructure protection.

At system level, it is important for the further investigations to focus on resilience. It is a relatively new concept that contemplates unexpected adverse conditions in system operation. In the energy context, it can be defined as the ability of the system to keep operating totally or partially under unexpected conditions by withstanding the impact, adapting and recovering [24, 161]. Therefore, considering this scenario of growing disasters frequency, including resilience in the design phase of energy systems becomes important to ensure a safer performance and a consequently safer energy supply.

Given the extensive range of disasters and effects, it was evident the requirement of elements covering these unexpected situations. The investigation of resilience in energy systems, together with policies contemplating both climate changes mitigation and terrorism extenuation, becomes important to increase system operational stability and ensure energy generation under unexpected conditions. It is a tendency that the exposed vulnerability of energy systems motivates new analysis at the system design phase, increasing its ability to withstand impacts and softening the abrupt consequences.

2.2   THE CONCEPT OF RESILIENCE

The term "resilience" has been largely used during the last decades. Material sciences referred to resilience as a mechanical property at least since the 19th century [162] , while the socio-ecological field firstly introduced this concept in the late 20th century [163], when Holling stated that resilience is a measure of the ability of populations of an ecological system to absorb disturbances and continue their relationships. Over the years, this terminology was adapted to different fields due to its broad nature, in a way that covers several definitions. Resilience is currently related to different contexts, such as anthropology [164], psychology [165], urbanism [166], business [167], engineering [26], among others [168]. There are minor changes between the definitions used by each field, so that the basic idea of dealing with disturbances without compromising a system or a group remains similar.

In energy field, resilience is emerging as an attractive study object. Giving this recent introduction, the definition is not entirely clear and several interpretations can be found in literature [169]. In this work, the definition of resilience is adapted from the ones proposed by Haimes [170] and Azzuni and Breyer [171] as it follows: resilience is the ability of the system to withstand disruptions and recover within an acceptable time without discontinuing the delivering services. These disruptions are originated by HILP events.

As a consequence of the lack of consensus, the key properties that should be covered by resilience also vary according to the research line [172]. In this work, an adaptation of the proposals of the US Department of Homeland Security and the US National Infrastructure Advisory Council is considered. The former organized a Risk Steering Committee, which stated that resilience should cover phases of withstanding, absorption and recovery [173]; while the latter proposed as the key features of resilience the anticipation, absorption, adaptation and recovery [174]. Herein, a resilient system is intended to absorb the initial impact, withstand structurally and operationally and recover as quickly as possible from failures and disruptions. After the recovery process, the system can be adapted to better cope with next events.

In order to illustrate the resilience key properties, the performances of two energy systems are represented by Figure 14. Initially, the systems operate with performance P_0, when a sudden HILP event occurs, interfering in their functionality and instantaneously decreasing their performance. The first phase after the disruption is the impact absorption, when the systems needs to attenuate the initial effects. The intensity of this initial decrease is associated with the system vulnerability. After the occurrence, they continue to withstand the consequences, with the goal of keep operating at an acceptable functional level until recovery actions are taken, focusing on returning them to initial performance. The increase of the performance, which is associated with the system recoverability, can even lead the system to a lower/better performance compared to the initial one, depending on the proceedings taken. Finally, the acquired experience and further developments support an adaptation process, so that they can increase their resilience and reduce the performance degradation under the forthcoming catastrophic scenarios.

In Figure 14, the resilience of the system 2 is higher than the one associated with system 1, since system 2 present a slighter performance decrease during absorption phase, maintains a higher performance during withstanding phase, and recover quicker to initial operation. Under the scenario

Figure 14 – Performance of energy systems under unexpected scenario
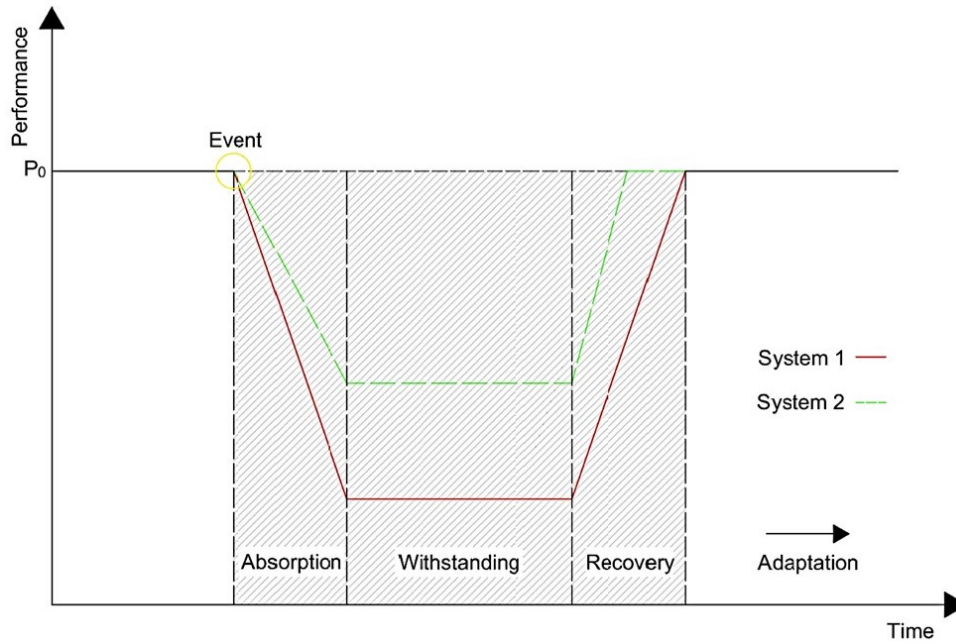
Source: Author's elaboration

covered by the figure, system 2 exhibits lower functional degradation than system 1.

2.2.1 State-of-the-art

As an emerging term, it is important to understand the way that resilience is addressed in scientific literature, whether as a generic topic or associated with a particular field. A bibliometric survey is carried out using the Scopus database, with refinements shown in Table 5. As a synonym of resilience, the term "resiliency" was considered in the survey. The document type and language limitations aimed to cover a more reliable identification of scientific development. The data analyses were run in VOSviewer, a software for bibliometric mapping [175].

Table 5 – Survey information and refinement

Database	Scopus
Search terms / occurrences	"resilience" or "resiliency" / 89713 results ("resilience" or "resiliency") ǀ Energy field / 3781 results ("resilience" or "resiliency") and ("power plant" or "energy generation" or "cogeneration" or "power system" or "power generation") / 1158 results (excluding transmission lines: 187 results)
Search fields	Article title, abstract, and keywords
Period	Until 2021
Language	English
Document type	Article

Source: Author's elaboration

Figure 15 – Subjected areas of published papers related to resilience
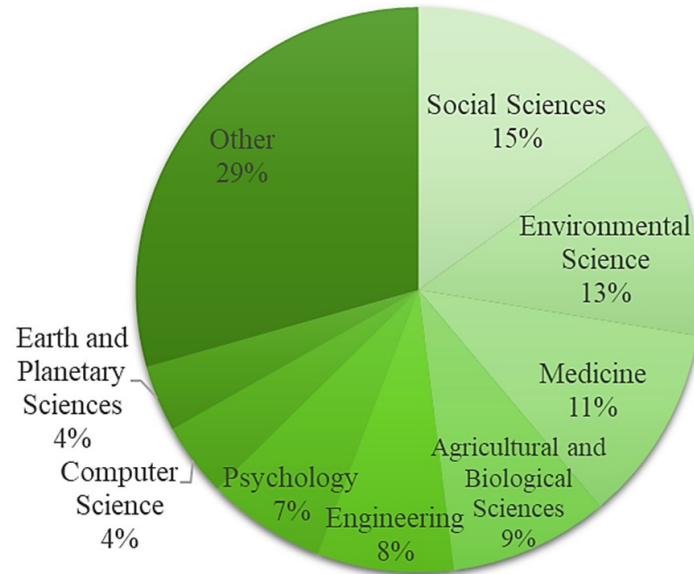
Source: Author's elaboration based on Scopus database

2.2.1.1 Resilience

In order to verify the current state of resilience in scientific literature, a survey was carried out with the refinement described at the beginning of the section. All the published papers in Scopus database containing either "resilience" or "resiliency" in their title, abstract or keywords were listed and analyzed. The total amount found by this research was 89,713 works, which is a significant number. As it can be seen in Figure 15, resilience is mostly related to social sciences, environmental sciences and medicine, reiterating the adaptation of this term by several fields. Only 8% of the published works are associated with engineering, while energy field is not even within the greatest areas.

Regardless the subjected area, the interest in resilience within the scientific literature is hardly increasing in last decades, as depicted by Figure 16. For instance, comparing only 2020 to 2021, the published papers increased from 11938 to 16447, a 38% growth, which indicates that this topic is currently receiving a high amount of attention. In addition, the beginning of the exponential growth in the mid 2000s points to a recent interest in resilience, implying a high number of scientific gaps yet to be explored.

In Figure 17, the most mentioned keywords in the 2000 most relevant articles according to Scopus are exhibited and connected. Keywords related to social sciences and some psychology derivatives have the higher frequency in the whole network, which indicates that clinical studies are currently the most relevant regarding resilience concept, with high interest in resilience of communities and individuals. In addition, there is a relevant space in other fields to deeper explore this theme.

By refining the survey to engineering field, 12,337 papers were found. In the 2000 most relevant works, classified by Scopus, the main keywords are represented in Figure 18. Terms as "decision making", "risk management", "disaster management", "recovery", "restoration" point to the features being studied by the works, while "supply chains", "electric power transmission network", and "critical infrastructure" stand out as the systems addressed by the researches. The threats are generically cited as "hazards" and "disasters", but "earthquakes" emerge as the most studied one. Both words "resilience"

Figure 16 – Number of published papers related to resilience

Source: Author's elaboration based on Scopus database

Figure 17 – Frequency of keywords related to resilience

Source: Author's elaboration based on Scopus database

Figure 18 – Frequency of keywords related to resilience in engineering field
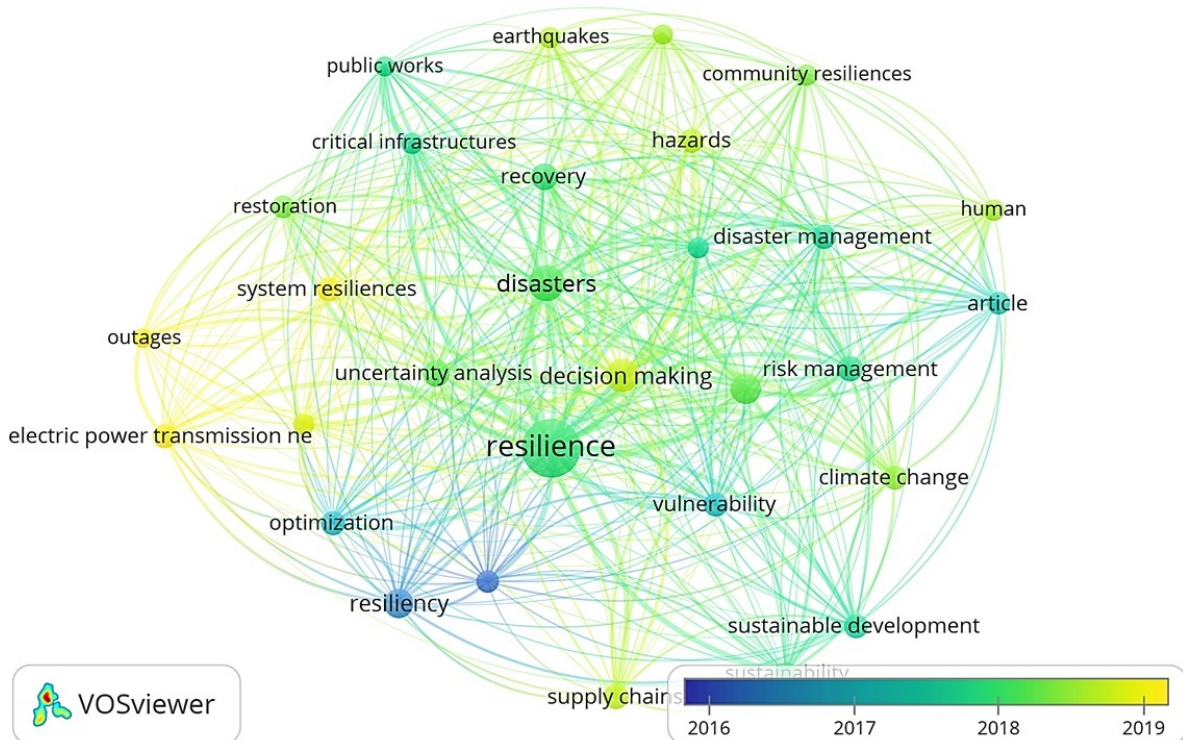
Source: Author's elaboration based on Scopus database

and "resiliency" appear as possibilities to refer to this concept. The division by colors points to "electric power transmission networks" as one of the recent addressed subjects. In a nutshell, the analysis of these keywords point to researches declaring natural disasters as threats to a high variety of engineering systems and proposing different resilience approaches to support the risk management.

2.2.1.2 Resilience in energy field

The energy field is not contemplated by the most relevant works in engineering, as pointed by the above presented keywords network, being the only exception the term "electric power transmission network". In order to verify the concept of resilience in the context of energy, the survey with the words ("resilience" or "resiliency") was refined to show results only covering this field. The detailed refinement is described at the beginning of the section. This research found 3,781 published papers.

The yearly number of publications is depicted in Figure 19. It is clear that resilience becomes an important subject of analysis in energy in past years, mainly from 2012, when the number of published papers increased substantially. In the same period, important journals in energy field started to publish investigations on this subject, especially "Sustainability", which itself alone published 441 papers regarding resilience only in 2021, almost 41% of the total amount. The Sustainability is an open access journal that aims to cover sustainable development of multiple areas, as environmental, cultural, economic and social. Giving the recent considerable growth and the several areas that energy encompasses, and considering the wide number of journals yet to address this subject, resilience still needs development and has gaps to be investigated.

In Figure 20, the most cited keywords of the 2,000 most relevant among the 3,781 published papers

Figure 19 – Number of published papers related to resilience and energy system
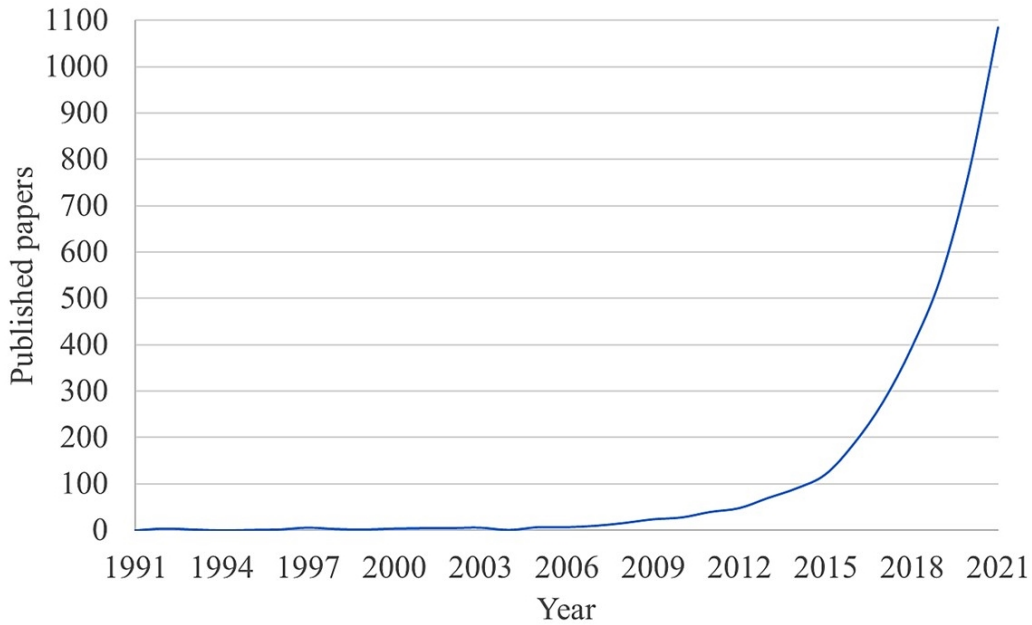
Source: Author's elaboration based on Scopus database

in this survey are represented. It is possible to see two different chains divided by color. The red one contains works focus on urban areas, as the terms "urban resilience", "urban area", and "urban planning" can be found. Even "covid-19" is represented, which points to a subject diversity. The green network presents "electric power transmission network" and "microgrids" as the main addressed systems, while "restoration" indicates which feature is the most covered by the researches within this chain. Among all the represented terms, there is no mention to energy generation systems, indicating an interesting area yet to be explored.

2.2.1.3 Resilience in energy generation systems

As the energy field contains several ramifications, as demonstrated in previous section, the survey was refined in order to take into account only the energy generation systems, which are the focus of this work. The search considering the terms ("resilience" or "resiliency") and ("power plant" or "energy generation" or "cogeneration" or "power system" or "power generation") found 1,158 published articles. However, within these works, several keywords were found to be unrelated with energy generation systems, such as "electric power transmission network" (322 occurrences), "microgrids" (121), "electric power system control" (111), "smart power grids" (97), "energy storage" (72), among others. Therefore, another refinement was done by limiting the survey to the works addressing the following keywords: "power generation", "power plant", "electric power generation", "power system(s)", and "electric power plant". Giving the results with a residual topic of transmission lines, the keyword "electric power transmission networks" was excluded. The total number of works found after this process was 187.

The yearly number of publications is shown in Figure 21. It can be noted a recent interest in this topic since 2016, giving the notable substantial growth. The amount of published papers in 2021, 43, represents 23% of the full amount found by this survey. This points resilience as an emerging theme

Figure 20 – Frequency of keywords related to resilience and energy system
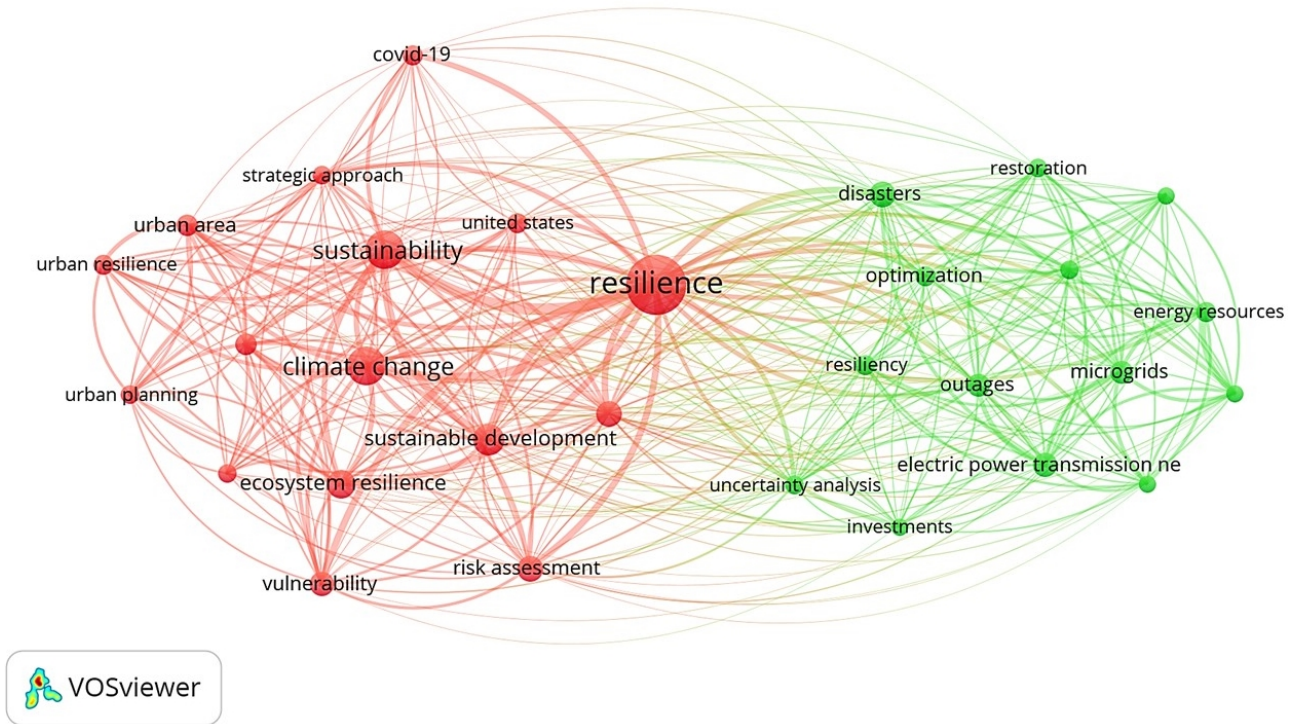
Source: Author's elaboration based on Scopus database

Figure 21 – Number of published papers related to resilience and energy generation system
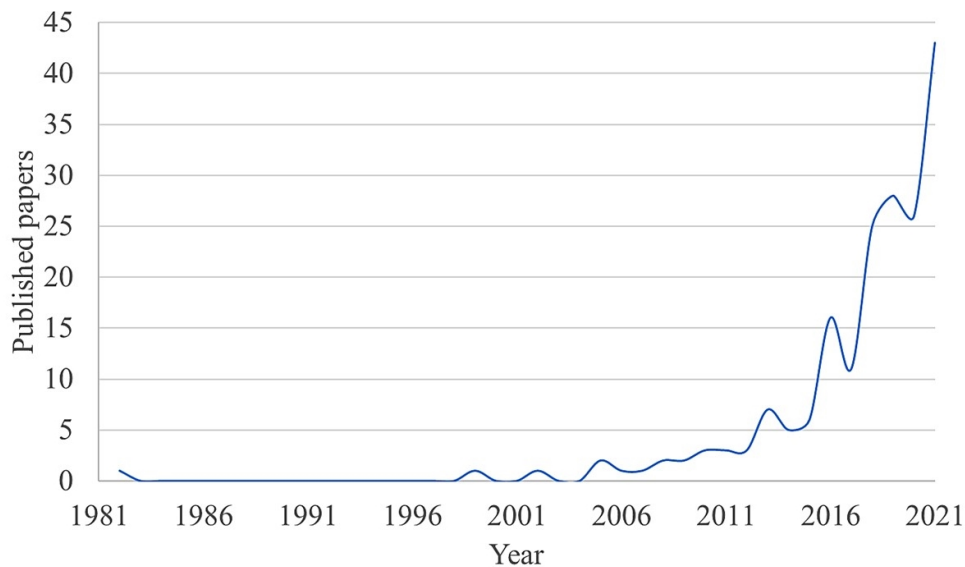
Source: Author's elaboration based on Scopus database

within energy generation systems, with much to be explored and with recent findings to be improved.

In Figure 22, the number of publications divided by source is presented. As it can be seem, important journals recently started to publish papers related to resilience of energy generation systems. in 2021, the journal "Energy", along with "Sustainability", were the ones with highest amount of publications. "Energy" aims to cover mechanical engineering and thermal sciences articles, specifically considering energy analysis, modelling, planning and management. It is also possible to note that until 2017 the highest amount of publications in a year was 2.

Figure 22 – Number of published papers related to resilience and energy generation system by source
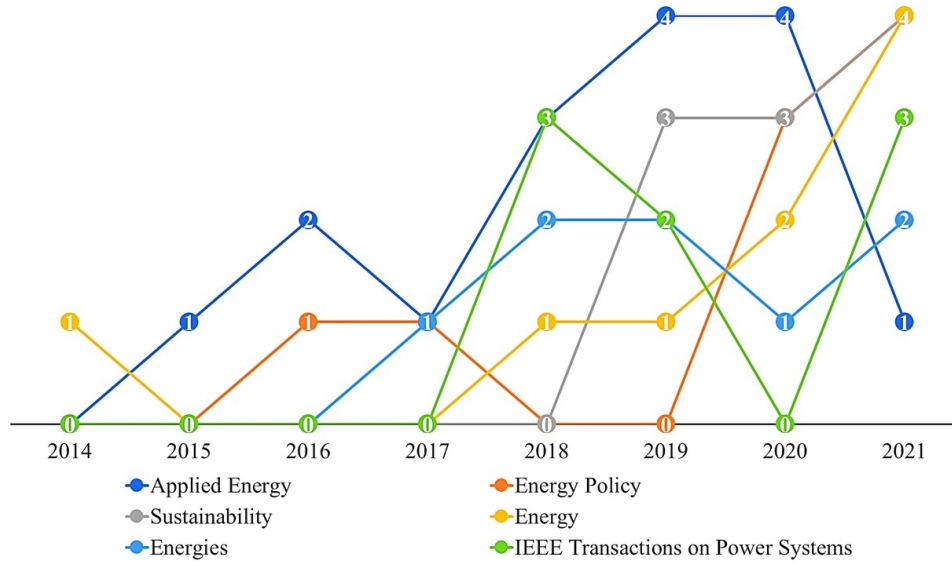
Source: Author's elaboration based on Scopus database

Figure 23 – Subjected areas of published papers related to resilience and energy generation system
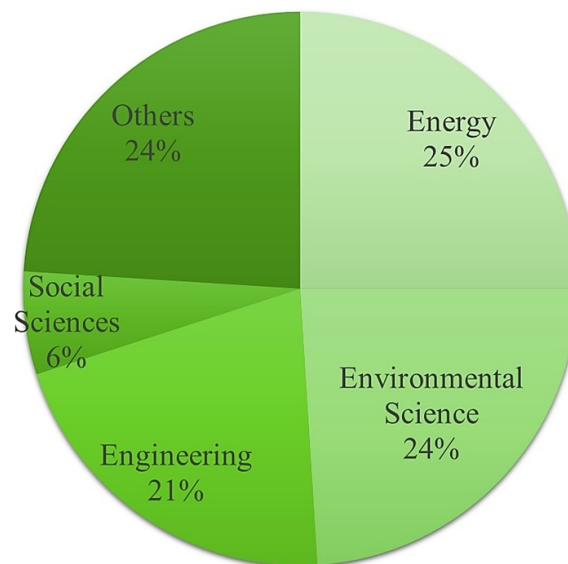
Source: Author's elaboration based on Scopus database

The most covered subjected areas are exhibited in Figure 23. Energy is the field related the most by the papers, following by environmental science and engineering. All the areas are related, since environmental issues lead to unexpected situations in energy systems, inducing the resilience investigation. The keywords in Figure 24 restate this condition, since "disasters" and "climate change" are two of the most frequent ones within these papers. In this figure, "photovoltaic system" and "hydroelectric power" stand out as two of the addressed systems, while "natural gas" seems to be feed the other types of systems. Even with the refinements, "microgrids" and "energy storage" still appears as two of the most mentioned topics. It is interesting that the term "economic analysis" can be found, possibly indicating attempts to relate resilience and costs.

The contributions by country is depicted by Figure 25, in which it is possible to notice that United

Figure 24 – Frequency of keywords related to resilience and energy generation system
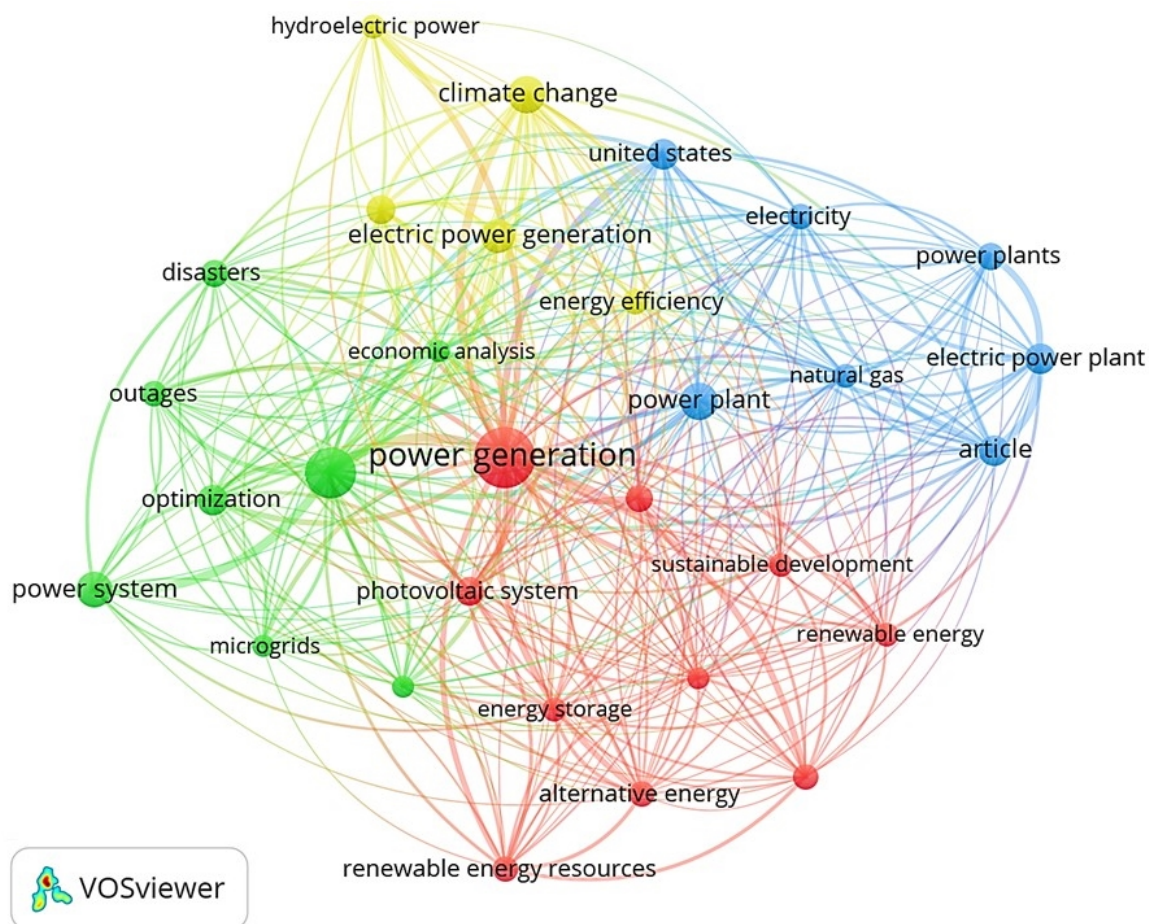
Source: Author's elaboration based on Scopus database

States is the one with the highest number of published papers, with 42% of the total. Although it is a still a modest number, its amount of articles is almost three times higher than the second one, China. Except for these two countries, the others listed have no more than 20 publications. This fact demonstrates the still preliminary stage of such theme in scientific literature.

Another evidence of this preliminary stage is the authors network, exhibited in Figure 26. As it can be seen, the papers have few connections between them, which indicates that there are small groups working on these subjects, with no strong relation and consensus. In order to understand better the published papers and their contents, the thirty most cited works are listed in Table 6 in decreasing order of citation. The relevance of the journal is identified by the SCImago Journal Rank (SJR), which is an indicator proposed by Bote and Anegón [176]. 63% of the listed papers are published in journals classified with a SJR higher than 1.5, which is a considerable rate. "Energy and Environmental Science" is by far the best rated journal among the ones mentioned in the table, with SJR of 14.486. This journal aims to cover works over energy security giving actual global and societal challenges. The rate of citations per year can indicate the papers with higher potential of citations, since some works are recent and their position at the table can wrongly induce the perception that they are low disseminated.

Figure 25 – Countries with the highest number of contributions on resilience and energy generation system
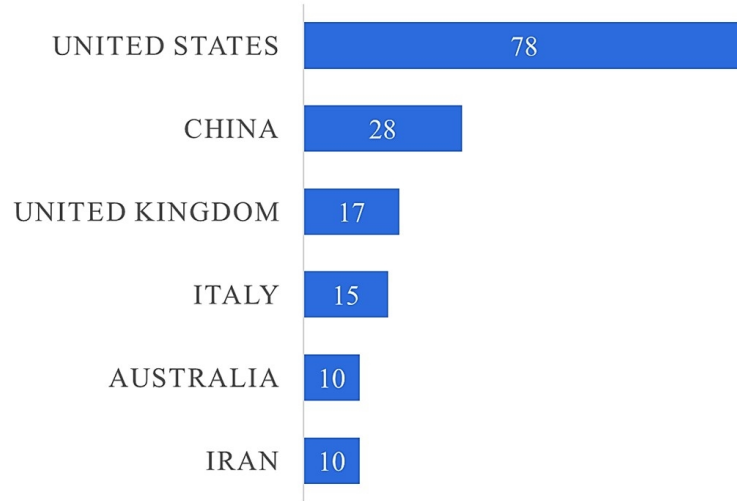
Source: Author's elaboration based on Scopus database

Figure 26 – Network of the authors with published papers on resilience and energy generation system
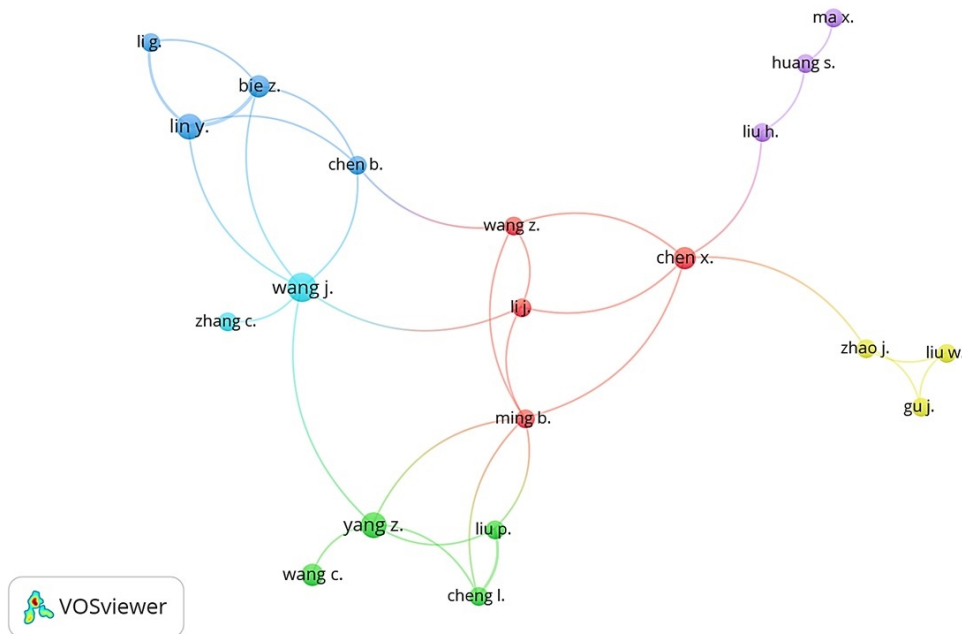
Source: Author's elaboration based on Scopus database

Table 6 – Published papers on resilience and energy generation system

#	Title	Authors	Journal (SJR 2020)	Citation	Year	Citations per year
1	Modeling cascading failures in the North American power grid	Kinney, R., Crucitti, P., Albert, R., Latora, V.	European Physical Journal B (0.451)	550	2005	32.4
2	A three-stage resilience analysis framework for urban infrastructure systems	Ouyang, M., Dueñas-Osorio, L., Min, X.	Structural Safety (1.644)	453	2012	45.3
3	Battling the Extreme: A Study on the Power System Resilience	Bie, Z., Lin, Y., Li, G., Li, F.	Proceedings of the IEEE (2.383)	260	2017	52.0
4	The wide world of wide-area measurement	Phadke, A.G.	IEEE Power and Energy Magazine (1.482)	257	2008	11.2
5	Modeling and evaluating the resilience of critical electrical power infrastructure to extreme weather events	Panteli, M., Mancarella, P.	IEEE Systems Journal (0.864)	215	2017	43.0
6	Resilience enhancement strategy for distribution systems under extreme weather events	Ma, S., Chen, B., Wang, Z.	IEEE Transactions on Smart Grid (3.571)	175	2018	43.8
7	Reservoir performance under uncertainty in hydrologic impacts of climate change	Raje, D., Mujumdar, P.P.	Advances in Water Resources (1.314)	161	2010	13.4
8	Business interruption impacts of a terrorist attack on the electric power system of Los Angeles: Customer resilience to a total blackout	Rose, A., Oladosu, G., Liao, S.-Y.	Risk Analysis (0.972)	127	2007	8.5
9	Defining and Enabling Resiliency of Electric Distribution Systems with Multiple Microgrids	Chanda, S., Srivastava, A.K.	IEEE Transactions on Smart Grid (3.571)	121	2016	20.2

10	Sweat-based wearable energy harvesting-storage hybrid textile devices	Lv, J., Jeerapan, I., Tehrani, F., Yin, L., Lopez, C.A.S., Jang, J.H., Joshuia, D., Shah, R., Liang, Y., Xie, L., Soto, F., Chen, C.	Energy and Environmental Science (14.486)	113	2018	28.3
11	Microgrid to enable optimal distributed energy retail and end-user demand response	Jin, M., Feng, W., Marnay, C., Spanos, C.	Applied Energy (3.035)	112	2018	28.0
12	Understanding resilience in industrial symbiosis networks: Insights from network analysis	Chopra, S.S., Khanna, V.	Journal of Environmental Management (1.441)	112	2014	14.0
13	Renewable rural electrification: Sustainability assessment of mini-hybrid off-grid technological systems in the African context	Brent, A.C., Rogers, D.E.	Renewable Energy (1.825)	103	2010	8.6
14	Impacts of future weather data typology on building energy performance – Investigating long-term patterns of climate change and extreme weather conditions	Moazami, A., Nik, V.M., Carlucci, S., Geving, S.	Applied Energy (3.035)	96	2019	32.0
15	Agrivoltaic systems to optimise land use for electric energy production	Amaducci, S., Yin, X., Colauzzi, M.	Applied Energy (3.035)	85	2018	21.3
16	Optimal Allocation of PV Generation and Battery Storage for Enhanced Resilience	Zhang, B., Dehghanian, P., Kezunovic, M.	IEEE Transactions on Smart Grid (3.571)	82	2019	27.3
17	Drought and the water-energy nexus in Texas	Scanlon, B.R., Duncan, I., Reedy, R.C.	Environmental Research Letters (2.370)	75	2013	8.3
18	Factors in the resilience of electrical power distribution infrastructures	Maliszewski, P.J., Perrings, C.	Applied Geography (1.165)	63	2012	6.3

19	Optimized reservoir operation model of regional wind and hydro power integration case study: Zambezi basin and South Africa	Gebretsadik, Y., Fant, C., Strzepek, K., Arndt, C.	Applied Energy (3.035)	52	2016	8.7
20	Vulnerabilities and resilience of European power generation to 1.5 °c, 2 °c and 3 °c warming	Tobin, I., Greuell, W., Jerez, S., Ludwig, F., Vautard, R., Van Vliet, M.T.H., Breón, F.M.	Environmental Research Letters (2.370)	50	2018	12.5
21	The energy metabolism of megacities	Facchini, A., Kennedy, C., Stewart, I., Mele, R.	Applied Energy (3.035)	50	2017	10.0
22	Twelve Principles for Green Energy Storage in Grid Applications	Arbabzadeh, M., Johnson, J.X., Keoleian, G.A., Rasmussen, P.G., Thompson, L.T.	Environmental Science and Technology (2.851)	50	2016	8.3
23	Micro-tubular flame-assisted fuel cells for micro-combined heat and power systems	Milcarek, R.J., Wang, K., Falkenstein-Smith, R.L., Ahn, J.	Journal of Power Sources (2.139)	49	2016	8.2
24	Analysis of safety functions and barriers in accidents	Harms-Ringdahl, L.	Safety Science (1.178)	49	2009	3.8
25	Hybrid renewable energy systems for renewable integration in microgrids: Influence of sizing on performance	Bartolucci, L., Cordiner, S., Mulone, V., Rocco, V., Rossi, J.L.	Energy (1.961)	46	2018	11.5
26	Resilience of roof-top Plant-Microbial Fuel Cells during Dutch winter	Helder, M., Strik, D.P.B.T.B., Timmers, R.A., Raes, S.M.T., Hamelers, H.V.M., Buisman, C.J.N.	Biomass and Bioenergy (1.037)	46	2013	5.1
27	Losing the roadmap: Renewable energy paralysis in Spain and its implications for the EU low carbon economy	Alonso, P.M., Hewitt, R., Pacheco, J.D., Bermejo, L.R., Jiménez, V.H., Guillén, J.V., Bressers, H., Boer, C.	Renewable Energy (1.825)	41	2016	6.8

28	Techno-economic analysis of solar inte-grated hydrothermal liquefaction of mi-croalgae	Pearce, M., Shemfe, M., San-som, C.	Applied Energy (3.035)	40	2016	6.7
29	Optimization of Exclusive Release Poli-cies for Hydropower Reservoir Opera-tion by Using Genetic Algorithm	Tayebiyan, A., Mohammed Ali, T.A., Ghazali, A.H., Malek, M.A.	Water Resources Management (0.941)	39	2016	6.5
30	The charcoal trap: Miombo forests and the energy needs of people	Kutsch, W.L., Merbold, L., Ziegler, W., Mukelabai, M.M., Muchinda, M., Kolle, O., Sc-holes, R.J.	Carbon Balance and Management (1.148)	39	2011	3.5

Source: Author's elaboration based on Scopus database

The abstract of the thirty listed papers were carefully read and only the five following works are selected, once they could potentially provide aspects of resilience evaluation for energy generation systems: #5, #7, #17, #20, and #26. It is interesting to point that even excluding the keyword relating the papers to other systems, it is notable that some works address grids and transmission networks in their titles, which demonstrates the importance of selecting properly keywords and title.

Panteli and Mancarella [27] (#5) proposed a Monte Carlo-based simulation considering the component failure probability as dependent on the weather condition, obtaining its value according to empirical statistical climatic data. The authors used transmission lines as case study and applied the proposed method.

Raje and Mujumdar [177] (#7) studied the effects of climate changes on the hydropower generation, being resilience one of the proposed indicators. The authors calculated this parameter by dividing the total number of system transitions from a collapsed functional state to a satisfactory one by the total number of failures.

In their work, Scanlon *et al.* [178] (#17) discussed some plant features over the drought resilience, regarding to water availability for the system to keep its operation. In addition, they related the use of natural gas to this parameter and proposed some actions to enhance the plant drought resilience.

By simulating global warming conditions, Tobin *et al.* [179] (#20) investigated the effect of 1.5, 2, and 3 ℃ warming on different power plants, then discussing the most vulnerable systems to these scenarios. The authors proposed some strategies to attenuate the consequences.

Helder *et al.* [180] (#26) tested several plant-microbial fuel cells under different ambient conditions for 221 days. The authors called resilience the ability of the fuel cells to recover from a frost period and keep operating, limiting the concept to cold weathers.

A critical analysis of the works above described can elucidate important points over resilience of energy generation systems. It can be seen that the analyzed papers provided plant features under specific weather scenarios, being temperature and water availability addressed. None of them proposed generic methods to resilience evaluation. Another relevant aspect is that their subjects were mostly limited to one type of system, being paper #26 the only exception, although the authors did not develop an evaluation method.

The content of the listed papers, along with the network of the authors presented above in Figure 26, points to the lack of consensus in both resilience definition and strategies of evaluation. It seems that some ramifications are being developed in some research groups, still with no unification. Therefore, there is still gap not only for resilience evaluation (as confirmed by [169, 181]), but also to its definition (confirmed by [182, 183]). This analysis is also corroborated by the recent growth of the publications shown in Figure 21.

It can also be noted that only few works focused on energy generation systems, even with the refinements. Some previous reviews ([35, 184]) confirmed that analysis by verifying that transmission and distribution systems are the most covered by resilient researches. In addition, still those that investigated energy generation systems selected a specific one. In other words, there is no generic method to evaluate resilience that can suit an analysis during the system design phase, especially those responsible for generation.

An important verification is that the articles covered mostly meteorological and climatological disasters, which indicates that other hazards, including man-made ones, still need further development. This fact also contributes to the necessity of a method capable of evaluate resilience in a general way, once the system is susceptible of many types of catastrophic events.

The interest in resilience in energy context is relatively recent, and therefore there are still some important hindrances. The definition of the concept and both development and generalization of an evaluation method are within the great challenges in this field. This work then fills these gaps by proposing an evaluation method for resilience in energy generation systems.

3 MATERIAL AND METHOD

In this chapter, the developed methods for objective resilience evaluation in energy systems are described, along with their application in a case study.

3.1 SIMULATION FRAMEWORK

The development of a simulation framework is based on Monte Carlo approach. This method is an unbiased estimation of one or more values giving a sufficient amount of samples, which converges regardless the dimensionality of the problem [185]. The higher the number of samples, combined with lower variance values, the smaller the estimation error [186]. The basic idea of the proposed simulation is to repeatedly reproduce the operation of an energy system, in a way that it is possible to verify its behavior under failure scenarios. The code was designed in PyCharm IDE [187], using Python programming language to describe an energy system composed of fully operational components.

Two distinct simulation methods were developed, based on the same initial steps. The first one, explained in section 3.1.1 and detailed and published in [188], is responsible for providing the time counters, which are analyzed to suit the proposed quantitative metrics. The other one, presented in section 3.1.2 and shown in details in Appendix A (written in portuguese), carries as the output the information needed to the graphical analysis. The Python packages used in the codes are the csv [189], numpy [190], os [191], time [192], and winsound [193]. The scheme exhibited in Figure 27 shows both the shared initial steps and the divergent paths during the simulation.

It is important to highlight that the simulation conditions and further metrics were designed only considering stochastic failures, i.e., excluding the expected failures and conditions due to normal operation. It is built, therefore, specific scenarios for resilience analysis only.

3.1.1 Time counters simulation

The simulation that aims to yield the time counters proceeds as shown by the following steps [194]:

1. Failure verification

   a) Random choice of a functional component i;

   b) Failure probability p_b is randomly assigned to component i;

   c) Comparison of p_b with a pre-established probability of component normal operation p_i;

   d) If $p_b > p_i$, the component fails and the failure propagation check represented in Figure 28 immediately starts for all the components, and restart in case of any failure by propagation; if $p_b < p_i$, the component remains functional and the simulation continues;

   e) If component i failed in previous step, the repair verification starts.

2. Repair verification

Figure 27 – Steps of each simulation developed herein
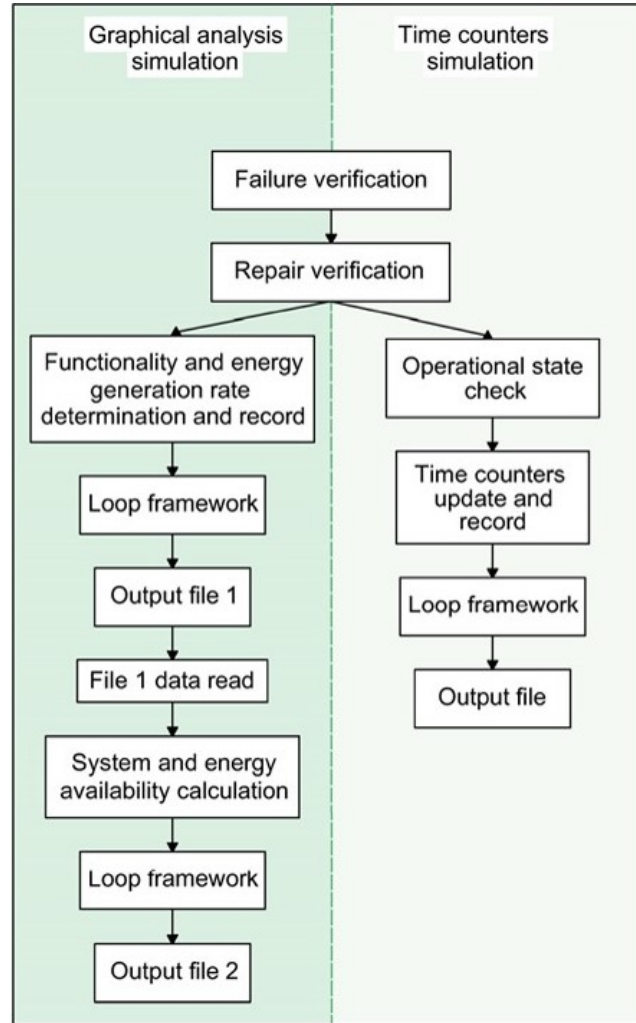
Source: Author's elaboration

a) A repair probability p_{cr} is randomly assigned to component i;

b) Comparison of p_{cr} with a pre-established unsuccessful repair probability p_{cnr};

c) If $p_{cr} > p_{cnr}$, the component immediately starts a repair process, schematized in Figure 29, and dependent on time spent in repair st and a pre-established repair time rt; if $p_{cr} < p_{cnr}$, the component remains failed until the end of current simulation round.

3. Based on the still-functional components, the system operational state is checked

4. Update of the respective time counters as represented by Table 7

5. Loop framework

a) If simulation time t did not reach the pre-established system lifetime T and the system did not fail, another hour of simulation starts from step 1; if $t = T$ or if the system fails, this simulation round stops and the final simulation time t, resilient time r and downtime d are recorded;

b) If the round counter c did not reach the pre-established number of simulations N, another round starts; if $c = N$, the simulation stops.

6. Output file

    a) The simulation generates an excel file containing the values of final t, r and d of every round.

Figure 28 – Process of propagation check
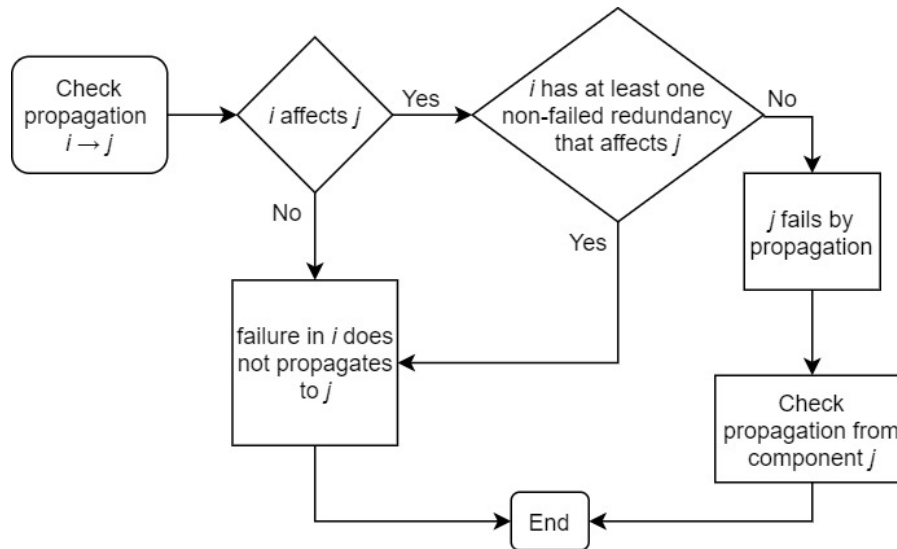
Source: Author's elaboration

Figure 29 – Repair process
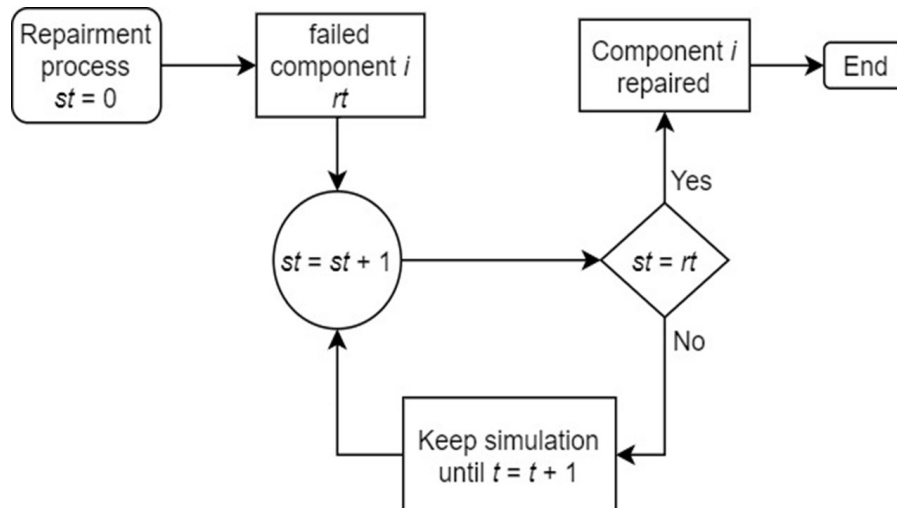
Source: Author's elaboration

In addition to represent disruptions as a consequence of unexpected events, then expressing the uncertainty of the possible failure sources, the randomly attribution of failure probability also allows the manipulation of p_i value, which can indicate the influence of this variable in the simulation results. The variable manipulation is also the aim of the random repair probability, besides the reproduction of several failure scenarios. As it is not possible to anticipate both nature and severity of an eventual unpredictable failure, assuming a random behavior for repair probability is also conceptually acceptable.

Table 7 – System operational states and respective time counters

System operational state	Description	Time counters
Normal	There are no failed components and the system generates demanded power and chilled water loads completely	t, n
Resilient	There are failed components, but the system keeps operating and generating demanded power and chilled water loads completely or partially	t, r
Stagnant	There is no generation of the requested energy due to failure (original or propagated) of the components responsible for it. However, some components are under repair, which can lead the system back to normal or resilient operation after the repair process	t, d
Failed	The system no longer generates the demand energy and there are no components under repair	-

Source: Author's elaboration

3.1.2 Graphical analysis simulation

The steps of the framework developed to obtain the data to be plotted are enumerated below. The first two steps are the same as the previous simulation, and therefore they are not described in details. The main difference between the two frameworks is that the graphical analysis simulation calculates the requested parameters, while the time counters simulation output requires further mathematical manipulation, explained in next sections.

1. Failure verification

2. Repair verification

3. Parameters obtaining and recording

    a) The number of functional components responsible for either thermal or electrical generation is counted;

    b) If there are no functional components for energy generation left, the system functionality F is equal to 0; otherwise $F = 1$;

    c) The energy generation rate EGR for each simulation round c and time t is obtained by dividing the momentary total generated energy $E_g(c,t)$, and the system rated capacity E_{rc}, as exhibited in equation 1;

$$EGR(c,t) = \frac{E_g(c,t)}{E_{rc}} \tag{1}$$

d) The instantaneous simulation time t, the round counter c, the system functionality F, and the energy generation rate EGR are recorded.

4. Loop framework

   a) A simulation round continues until $t = T$, being both F and EGR equal to 0 when there are no generation left;

   b) This part of the simulation stops when $c = N$.

5. First output file

   a) The simulation generates an output file with values of F and EGR for each hour of simulation and each c, i.e., each file contains an amount of $N \cdot T$ lines.

6. In a second moment, the first files are opened and read by the simulation

7. System availability determination

   a) Passing through each c of all the N simulations, the values of system functionality F are grouped by each hour, their amount are summed, and then divided by the total number of simulations N, as expressed in equation 2, so that the system availability a can be calculated for each time t.

   $$a(t) = \frac{\sum_{c=1}^{N} F(t)}{N} \tag{2}$$

8. Energy availability determination

   a) Within the N simulations, the values of EGR for each hour are summed and divided by the total number of simulations N, in a way to calculate the energy availability a_e, exhibited by the equation 3.

   $$a_e(t) = \frac{\sum_{c=1}^{N} EGR(t)}{N} \tag{3}$$

9. Loop framework

   a) The simulation continues until the lifetime of all the N simulations are covered.

10. Second file output

    a) The second file output contains the values of t (passing through each hour of simulation), a and a_e;

    b) As soon as this file is saved, the first one is deleted.

As described above, the desired parameters are the system availability a and the energy availability a_e. The former is an average of the functionality in a certain time and it can be interpreted as the probability of the system to functionally operate, under a specific operational environment, at a certain moment; while the latter represents the mean generated energy, also considered as the generation rate at a specific moment.

3.2   QUANTITATIVE METRICS FOR RESILIENCE EVALUATION

The data obtained by the time counters simulation composed seven metrics associated with resilience evaluation, being five of them (i - v) introduced by Matelli and Goebel [130], and the other two (vi and vii) originally proposed by this work. As the approach of Matelli and Goebel considered a condition without repairing actions, thus not enabling system recovery, the development of a repairable scenario and the simulation of the previously proposed metrics under this condition are other contributions of this work.

i Probability of resilient operation (p_r): this metric represents the probability of the system to operate until its lifetime resiliently, in which failed components did not compromise the whole system functionality. It is a relation between the number of simulations k when $r_k > 0$ and $t_k = T$ (N_r) and the total number of simulations N. The closer p_r gets to the unity, the higher the number of resilient simulations.

$$p_r = \lim_{N \to \infty} \left(\frac{N_r}{N} \right) \tag{4}$$

ii Resilient operating time ($\bar{r}$): it is defined as the weighted average of the resilient operating time r for all the N_r simulations. This variable expresses the mean resilient time for each system.

$$\bar{r} = \frac{p_r}{N_r} \sum_{k=1}^{N_r} r_k \tag{5}$$

iii Time until failure ($\bar{f}$): this parameter indicates the period that the system can operate before its complete failure. Its value is calculated through the average time of k simulations in which $t_k < T$ (N_f). The higher $\bar{f}$, the more resilient is the system, since it can operate for longer periods.

$$\bar{f} = \frac{1}{N_f} \sum_{k=1}^{N_f} t_k \tag{6}$$

iv Probability of failure (p_f): it expresses the probability of the system to fail before lifetime. It is obtained by the ratio between N_f and N, and a resilient system tends to get this variable close to zero.

$$p_f = \lim_{N \to \infty} \left(\frac{N_f}{N} \right) \tag{7}$$

v Normalized resilience index (ρ): this variable denotes the percentage of lifetime that the system can operate under the simulation conditions, and therefore the closer it gets to the unity, the higher the system resilience. It is obtained through a relation between the average operating time $\bar{t}$ and the system expected lifetime T. The value of $\bar{t}$ is an average of the total operating time of the system for all the N simulations, as represented in Equation 8.

$$\bar{t} = p_f \bar{f} + (1 - p_f)T \tag{8}$$

$$\rho = \frac{\bar{t}}{T} \tag{9}$$

vi <u>Probability of system recovery</u> (p_d): this metric represents the probability of the system to recover after it stops its energy generation, being in a stagnant condition. It is the relation between the number of simulations k in which the system returned to operation and reached lifetime after becoming stagnant (N_d), i.e., when $t_k = T$ and $d_k > 0$, and the total number of simulations with stagnant conditions – even when the system became stagnant and did not recover – ($N_{d,T}$). The closer p_d gets to the unity, the higher the system recovering efficiency, and the higher its resilience.

$$p_d = \lim_{N \to \infty} \left(\frac{N_d}{N_{d,t}} \right) \tag{10}$$

vii <u>Resilient-stagnant ratio</u> (θ): this metric considers specifically the moment after a component fails without causing the system collapse. In this situation, the system can become either resilient or stagnant. The aim of this parameter is to compare the time counters associated with these two operational states in simulations when the system reaches lifetime. θ is then defined as a ratio between the average resilient time $\bar{r}$ and the average system downtime $\bar{D}$. With this metric, it is possible to analyze the tendency of the system to keep resiliently operating after a component failure, rather than becoming stagnant. The higher its value, the higher the resilience.

The average downtime $\bar{D}$ is calculated as in Equation 12. This variable is a weighted average of the downtime d for all the simulations when $t_k = T$ and $d_k > 0$ (N_d). It also considers the probability of the system to recover and reach lifetime $p_{d,T}$, which is represented in Equation 11. An analysis of $\bar{D}$ does not provide accurate information about resilience, since by considering only the cases in which system reached lifetime, it discards the situations when the system recovered, but collapsed ($t < T$). Therefore, as the variable $\bar{D}$ does not include all the possible recovering scenarios, it can not alone be an indicator.

$$p_{d,T} = \lim_{N \to \infty} \left(\frac{N_d}{N} \right) \tag{11}$$

$$\bar{D} = \frac{p_{d,T}}{N_d} \sum_{k=1}^{N_d} d_k \tag{12}$$

$$\theta = \frac{\bar{r}}{\bar{D}} \tag{13}$$

It is important to state that among the proposed metrics, metric v is the most generalist one and the most valuable in a preliminary evaluation, since it verifies the total amount of time that the system is able to operate compared to its lifetime under specific operational conditions, passing through all the phases after the failures. On the other hand, it is not possible to assess some specific features of the system through its value. Metrics i, ii, iii, and iv, for instance, have important information over the withstanding phase, being the first two related to system operation with failed components, while the last two refer to withstanding failures until it collapses. Metrics vi and vii point to recovery and absorption phases, respectively.

3.3 INFLUENCE OF REPAIRING ACTIONS

Within the scientific literature for systems with multiple connected components, researchers consider basically three repair models: perfect, imperfect and minimal [195]. Perfect repair is equivalent to replace the failed component for a new one (good-as-new condition), imperfect repair leaves the equipment with a performance between the good-as-new and the one before it failed (bad-as-old condition), and the minimal repair restores the component to the bad-as-old status. In this work, as no partial operation is assumed for the components (see section 3.4.2), the perfect repair is considered.

A repair process, as described in section 3.1, stars when $p_{cr} > p_{cnr}$. The simulation code receives the component unsuccessful repair probability p_{cnr} as the input parameter. However, for the purpose of better understanding, its complement – repair probability p_{cr} – will be adopted as the manipulable variable hereafter.

Although some studies focus on this theme, the estimation of repair probability is not precise, and therefore considering its behavior as random is an acceptable approach [196, 197]. In practice, it is possible to improve this parameter by adopting some strategies, such as proactive management aiming the development of integrated repair plans [198, 199], storage of new or repaired components for instantaneous replacement of failed ones [200], and availability of repair technical groups [201]. However, giving both the necessity of considering the local context of the system operational conditions to stipulate such strategies and the lack of information during the conceptual phase of the system design, planning the repair is neither simple nor generalizable. Therefore, it is out of the scope of this work to discuss the practical actions to improve repair probability.

The impact of repairing actions to system resilience is evaluated through the manipulation of the repair probability during the simulations, including the condition when no repair actions are taken, i.e., with $p_{cr} = 0$. In order to objectively quantify the number of simulations that avoided interruptions during system operation with the addition or increase of repair probability, the Equation 14 is proposed. This equation calculates the difference between two types of simulation: the ones that failed with no repair actions and the ones that were potential candidates to fail in a repairable environment.

$$NFx = N_f\left(p_{cr} = 0\right) - \left[N_f\left(p_{cr} = x\right) + N_d\left(p_{cr} = x\right)\right] \tag{14}$$

Based on the simulation inputs presented in section 3.4.2, the admitted values of x are 50% or 75%. The variable N_f represents the number of simulations that failed completely, while N_d is the ones that would fail, but were able to recover due to the repair consideration. Therefore, NFx represents the number of simulations that were able to operate until lifetime without interruptions due to the consideration of a repair probability of x, but that would collapse under a condition with no repair. As x assumes two different values herein, they are compared by the Equation 15, in which $IP_{x_1-x_2}$ represents the percentage of interruption prevention during the operation due to repair probability raise from x_1 to x_2. The comparison of IP for different systems quantifies which one can avoid operational interruptions the most, after an increase in repair probability. The higher the value of IP, the higher the impact of repairing actions in the resilience.

$$IP_{50-75} = \frac{NF75 - NF50}{NF50} \qquad (15)$$

3.4 CASE STUDY

3.4.1 Systems description

Focusing on validating the described method in energy generation systems, it is applied in four cogeneration plants with different configurations. The consideration of four different systems enable the comparison of the results based on their initial arrangement. These plants are previously introduced by Matelli and Goebel [130], and were designed by a knowledge-based system developed by Silva *et al.* [202], a program comprising data based on real components. The required inputs to systems design are shown in Table 8.

Table 8 – Input parameters for systems design

Parameter	Value
Local average temperature	18 °C
Local altitude	670 m
Maximum power demand	1500 kW
Minimum power demand	900 kW
Electrical energy consumption	28 MWh
Chilled water demand	1407 kW
Daily operation	24 h/day
Weekly operation	7 days/week
Electric connection scheme	Tied to the grid
Chilled water storage	no

Source: [130]

The cogeneration systems are illustrated by Figure 30 - Figure 33. They are designed for generation of electricity and chilled water, which are the energy demands of the initial project. The four configurations operate with the same principles, being the number of prime movers the capital difference between them. The purpose was to verify the influence of redundancy, an aspect that Matelli and Goebel [130] concluded to be important for system resilience.

Systems S#1 (Figure 30) and S#2 (Figure 31) operate based on internal combustion engines (E), each coupled with an associated generator (G) that generates electrical energy, which is distributed by a bus bar connected to the external grid, providing the requested power load. The heat from the jacket water is used by heat exchangers (HEX) to produce hot water, feeding a single effect absorption chiller (HWAC) that produces the demanded chilled water through a attached pump (CWP). The HWAC is also connected to a pump (ACP), which also feeds the HEX with water. In cases when the HWAC is off, a radiator (R) maintains the functionality of the engine and a mechanical-driven chiller (MDC) suits as a backup. The residual heat from the chillers is rejected by the cooling tower (CT).

The operation of systems S#3 (Figure 32) and S#4 (Figure 33) is similar. Gas turbines (GT) are coupled to generators (G) that generate electrical energy, which is distributed by a bus bar in conjunction with the external grid, meeting the demanded power load. The steam flow that feeds the

Figure 30 – S#1: system based on one internal combustion engine
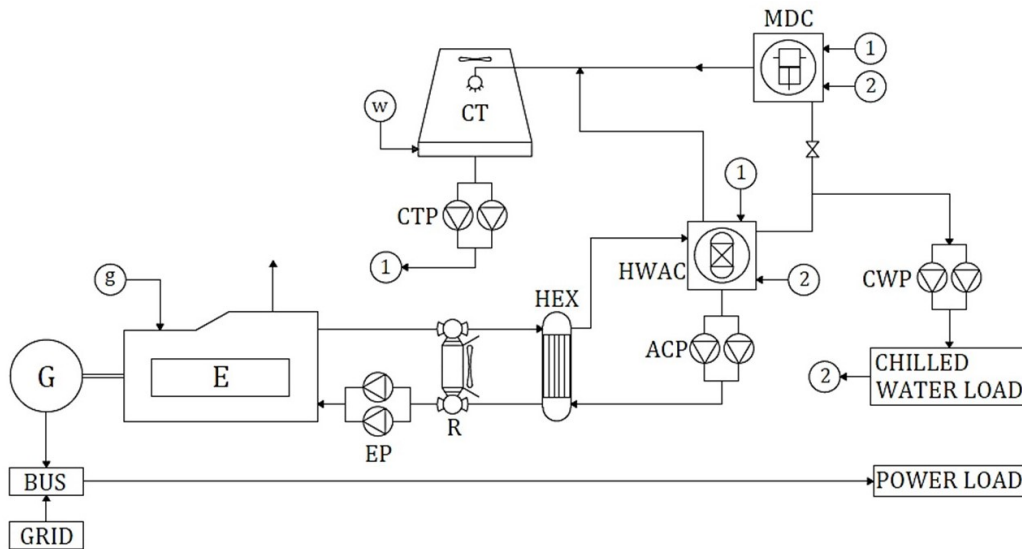
Source: adapted from [130]

Figure 31 – S#2: system based on two internal combustion engines
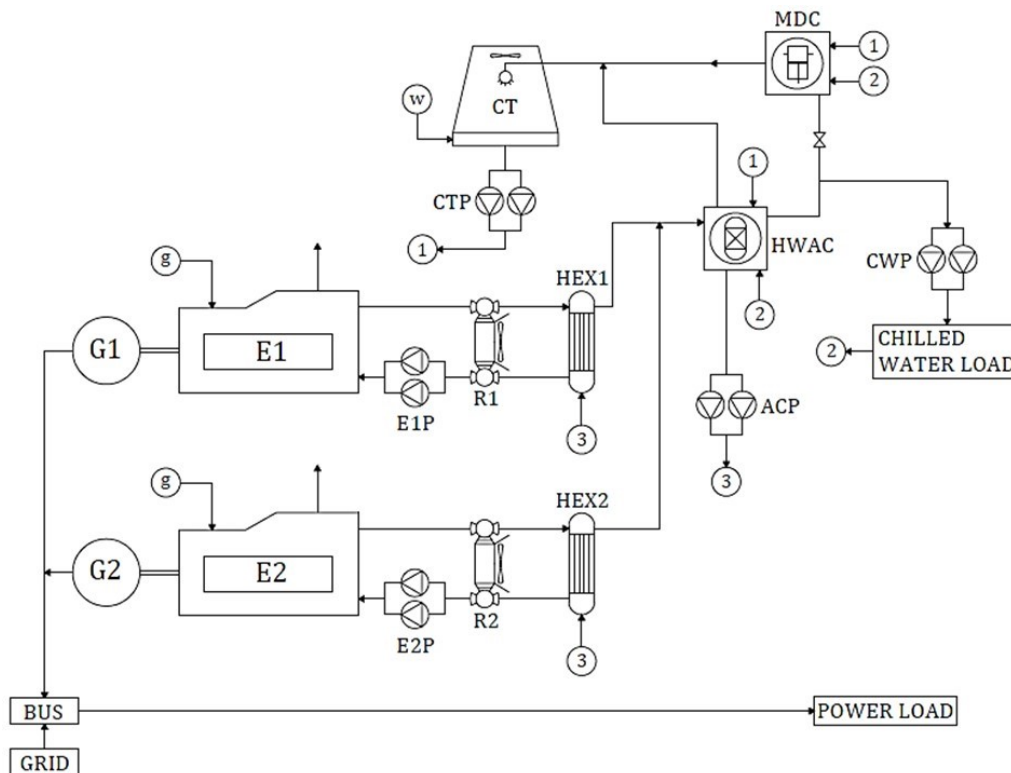
Source: adapted from [130]

double effect absorption chiller (SAC) is produced by the heat recovery steam generator (HRSG), which uses the exhaust gases from the gas turbine. The SAC holds an output that feeds a tank (CDT) with condensate before a pump (CDP) pressurizes this flow back to the HRSG, in addition to another output that contains the demanded chilled water load, which is also pumped by the chilled water pump (CWP). A mechanical-driven chiller (MDC) is used as backup. The cooling tower (CT) is responsible for rejecting the residual heat from the chillers.

The technical parameters of the four cogeneration systems are shown in Table 9. In this table, the

Figure 32 – S#3: system based on one gas turbine
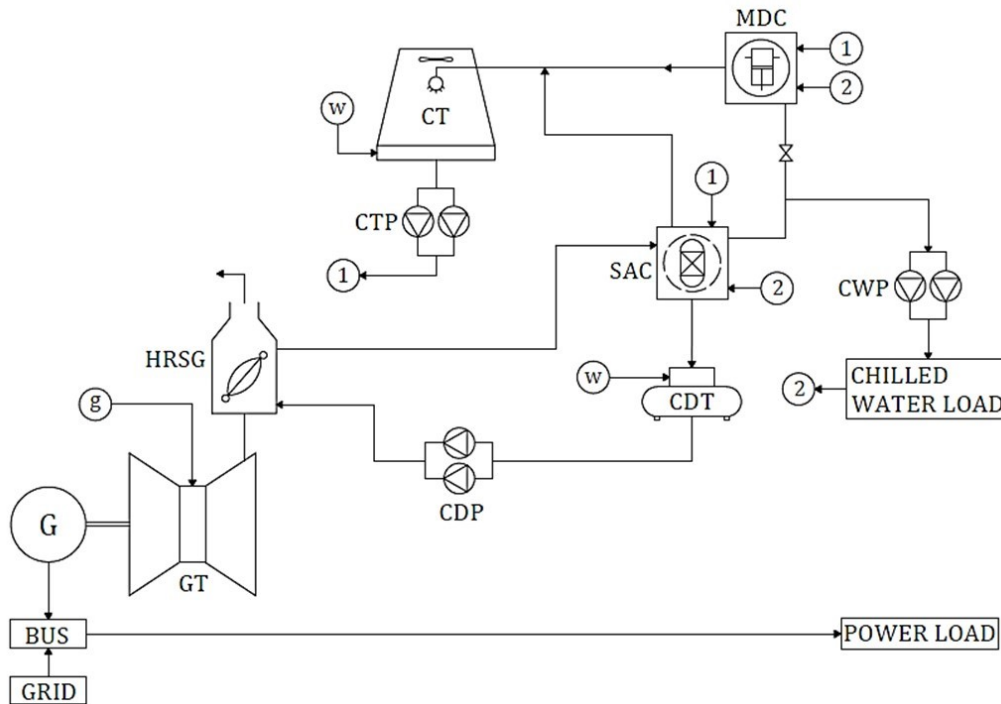
Source: adapted from [130]

term PER refers to primary energy rate, an indicator of the efficiency of the system to convert the energy of the fuel to both electrical and thermal energies, as shown in equation 16. An analysis of the PER value for each system points to S#1 as the one with best thermal performance, followed by S#2, S#3 and S#4. Therefore, if thermal analysis was the only one considered at the initial phase of the project, S#1 should be selected.

$$PER = \frac{W + Q}{m_f \cdot LHV} \tag{16}$$

3.4.2 Simulation inputs

Each system is defined by the corresponding component set, which also has its own features. The default initial information given as input to the Python program are specified in Table 10. Besides the parameters presented in this table, the program request for the system the three different number of components: the total one, the ones that generate electricity and those responsible for chilled water production. For the graphical analysis simulation, the rated capacity, previously presented in Table 9, is also required. The components specifications are the type, function (electricity, thermal or none), repair time and three different lists: one of the components affected by the specified one, another one indicating the redundant components, and a third one enumerating the components that affect the specified one. The codes responsible for graphical analysis also receive the energy output of each component.

In order to configure the simulation conditions, the following assumptions are made:

- Each year considered in lifetime is equal to 8760 hours, which represents uninterruptedly

Figure 33 – S#4: system based on two gas turbines
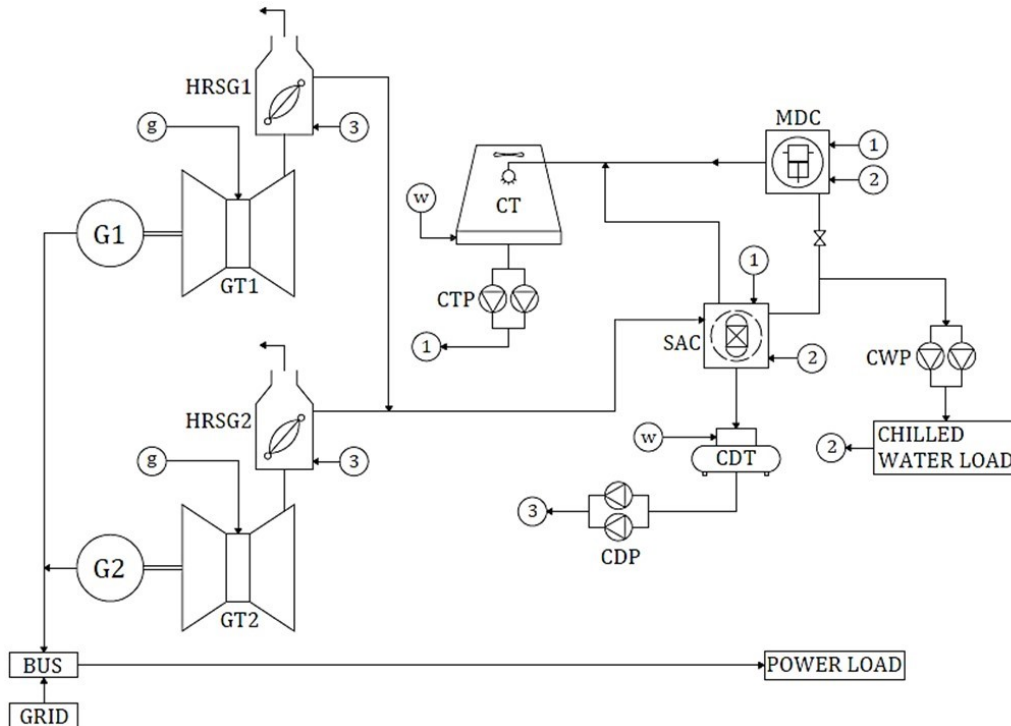
Source: adapted from [130]

operation over a year;

- The probabilities p_i and p_{cnr} assigned to all the components are constants over time;

- The operational state of the components can only assume failed or normal values;

- The failure propagation occurs for every components affected by the originally failed one, regardless the nature of connection;

- Component repair time is treated as a normal distribution;

- Component repair process starts immediately after the repair probability is verified and accomplished.

The constant behavior of p_i and p_{cnr} aims to stablish neutral conditions of simulation, as well as satisfy the premise that the only difference between the systems is their configurations. Therefore, these variables are arbitrary, and their manipulation aims specifically to analyze their influence in systems resilience. This assumption allows the comparison of the results and the indication of the best configuration from resilience point of view at the design phase, when precise information about the systems and their operation are usually not available. Although it is not a realistic supposition – as it supposed to be, since one of the features of the developed environment is the unpredictability, and therefore any input suits only a conceptual purpose–, it becomes acceptable for the intention of this work.

The initial fixed value for p_i is 0.9970, while for p_{cnr} are 0.25, 0.50 and 1, with consequent complement – repair probability – established as 0 (with no repairing actions), 0.50 and 0.75. This

Table 9 – Technical parameters of the cogeneration systems

Parameter	S#1	S#2	S#3	S#4
Machine models				
Prime mover	1x Waukesha 12V-AT27GL	2x Waukesha 8L-AT27GL	1x Solar Centaur 40	2x Solar Saturn 20
Absorption chiller	1x LG B160AL	1x LG B190AL	1x LG LSH-G050	1x LG LSH-G110
Mechanical-driven chiller	1x LG LTP-040	1x LG LTP-040	1x LG LTP-040	1x LG LTP-040
Rated capacity (kW)				
Power	2100.0	2800.0	3515.0	2420.0
Absorption refrigeration	567.7	668.2	1758.5	3868.7
Mechanical-driven refrigeration	1406.8	1406.8	1406.8	1406.8
Average output (kW)				
Power	1166.7	1166.7	1166.7	1166.7
Refrigeration	1406.8	1406.8	1406.8	1406.8
Efficiency[a]				
Prime mover[b]	0.3314	0.3181	0.1808	0.1806
Absoprtion chiller	0.702	0.7015	1.219	1.22
Mechanical-driven chiller	5.024	5.024	5.024	5.024
System parameters				
Fuel consumption[c] (kg/s)	0.07491	0.07803	0.13730	0.13760
Imported power (kW)	176.8	155.6	0.0	0.0
PER	0.6959	0.6731	0.3988	0.398

Source: [130]

[a] COP for chillers.

[b] The efficiency of prime movers is set according to ambient conditions.

[c] Considering a LHV of 47 MJ/kg.

variation allows the analysis of the impact of repair probability in system resilience. The number of simulations, which depends on the coefficient of variation, is explained and set in section 4.1.

According to Watson *et al.* [203], a disaster scenario may lead to numerous sources of uncertainty, then being impossible to foresee a precise value of the repair time of a specific component. In addition, during the conceptual phase of system design there is no proper information about the components. In order to cover these uncertainties, the repair time can be assumed to follow as a normal distribution [203]. The mean repair time of the components, associated with their function and complexity (Table 11), and a standard deviation of 20% are assumed herein, mainly due to the lack of precise information within scientific literature. It is adequate to inform that simulations with constant repair time were run before the consideration of normal distribution behavior, and there were no significant variations between the results. The latter was then selected to continue further investigation, once it represents

Table 10 – Default information for simulation

Parameter	Input
System	
Operational state	Normal
Failed components	0
Repairing components	0
Components	
Operational state	Normal
Repairing	No
Time spent in repair	0

Source: Author's elaboration

more accurately different natures of failure.

Table 11 – Components repairing time

Function	Mean repairing time (h)	Component
Shaft work generation	100	Turbine Engine
Power generation	80	Generator
Heat exchanger	60	Hot water absorption chiller Mechanical chiller Heat exchanger Steam absorption chiller Heat recovery steam generator Cooling tower Radiator
Feeding	40	Chilled water pump Hot water chiller pump Jacket water pump Cooling tower pump Condensate pump
Structural	40	Grid Bus Power load Chilled water load Gas line Water line
Storage	30	Condensate tank

Source: Author's elaboration

4 RESULTS AND DISCUSSION

4.1 NUMBER OF SIMULATIONS

The standard number of simulations needs to cover an amount of samples enough to find a system behavior pattern. This condition, which is the basis of the Monte Carlo approach, happens when the coefficient of variation of a particular variable stabilizes, presenting convergence due to a smaller error situation [204].

The coefficient of variation, c_v, indicates the degree of dispersion of a particular value estimation. It is obtained by the division of the standard variation and the average of the estimate – in the case of this work, resilient time is selected, as represented by Equation 17. For the purpose of analyzing in which range of N this coefficient stabilizes, it is calculated with the following number of simulations: 50, 100, 500, 1000, 3000, 5000, 10000, 20000, 50000, 70000, and 100000. The condition of the simulation was admitted to be $p_i = 0.997$, $p_{cr} = 0$, and $T = 1$ year. The results for each system is shown in Figure 34, being a logarithmic basis applied on the x axis. It can be seen that c_v primarily achieves the steady value at $N = 500$, thus maintaining its stabilization for further number of simulations. To assure a high amount of samples and converge with the number expressed in [130], N was assumed to be 3000 for the conditions hereafter.

$$c_v = \frac{\bar{\sigma}}{\bar{r}} \tag{17}$$

Figure 34 – Coefficient of variation of resilient time for different values of N
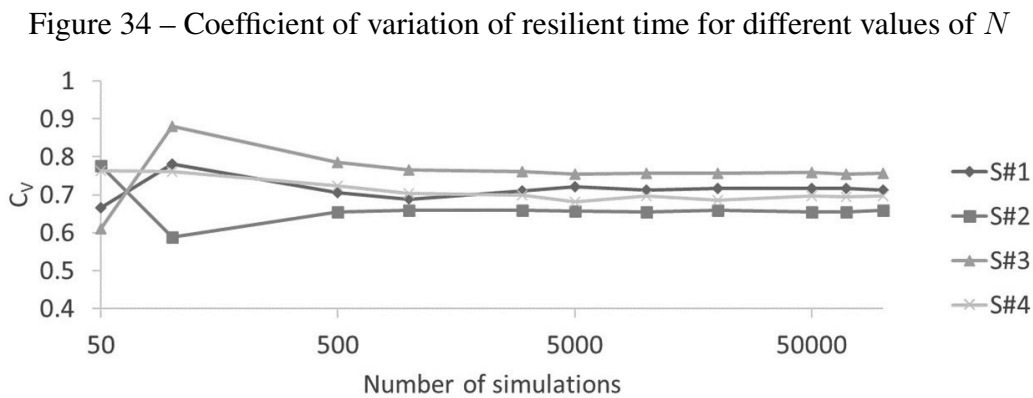
Source: Author's elaboration

4.2 PROPOSED METRICS

The initial analysis consisted of the four cogeneration systems operating for one year (8760 hours), with $p_i = 0.9970$, p_{cr} varying within 0, 0.50 and 0.75, and $N = 3000$ simulations. The aim of the first condition is to compare the seven metrics for the four different configurations. The results of each metric are shown in Figure 35 - Figure 41.

All the metrics point to both S#2 as the most resilient system and S#3 as the least resilient one. System S#1 is pointed as more resilient than S#4 by the metrics i, ii, iv, vi, and vii, while the contrary

Figure 35 – Probability of resilient operation for different p_{cr} values

$$p_r$$

■ 0 ■ 0.5 ■ 0.75
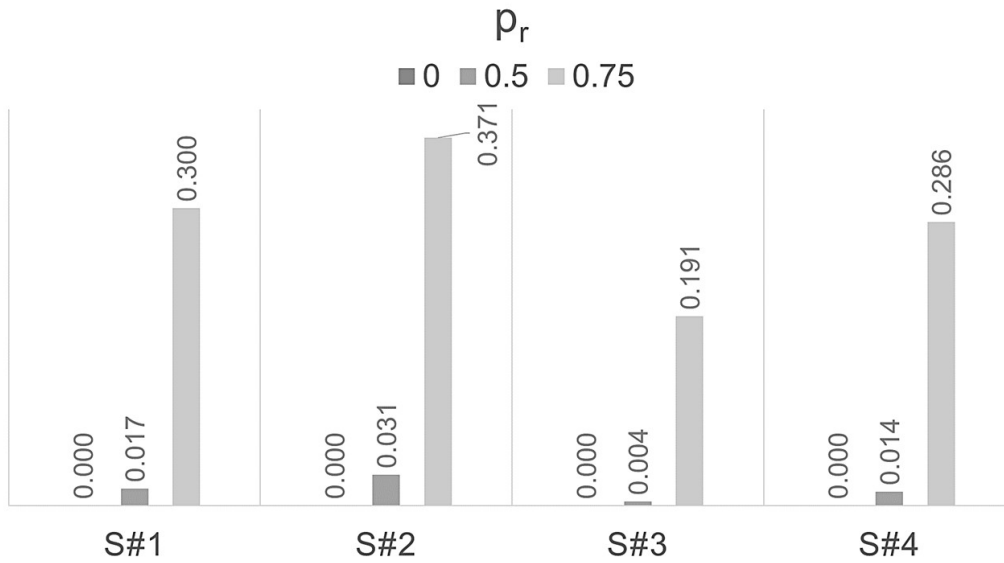
Source: Author's elaboration

Figure 36 – Resilient operating time for different p_{cr} values

$$\overline{r}$$

■ 0 ■ 0.5 ■ 0.75
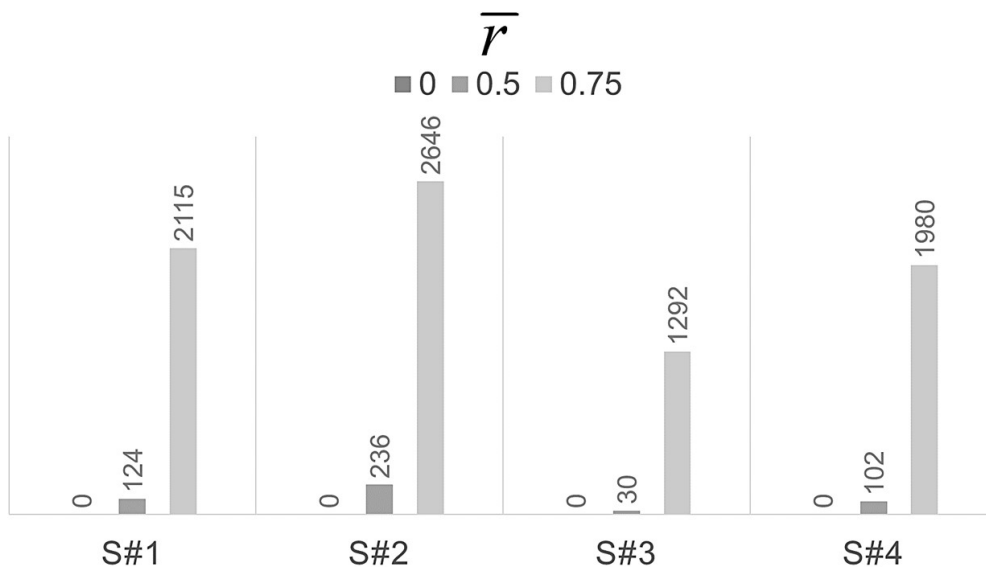
Source: Author's elaboration

is seen in metrics iii and v. This interesting fact can be explained by the description of each metric presented in section 3.2. The parameter ρ, the most generalist one, indicates a higher operation time of S#4. However, S#1 seems to have a higher probability to reach its lifetime with failed components (metric i), resiliently operate for longer (metric ii), and better respond to a component failure, presenting more probability of entering in a resilient operation rather than stagnate (metric vii). In addition, S#1 is less destined to fail (metric iv) and exhibits a better recovery (metric vi). By analyzing all the metrics, it can be concluded that S#4 can operate for longer periods compared to S#1, but only considering simulations in which the systems fail completely. When S#1 collapses, it happens quicker than in S#4. S#1, however, seems to better respond to failures under the simulated scenario.

The initial condition of p_i = 0.9970, which represents a failure probability of 0.3%, indicates a

Figure 37 – Time until failure (metric i) for different p_{cr} values

$$\overline{f}$$

■ 0 ■ 0.5 ■ 0.75

Source: Author's elaboration
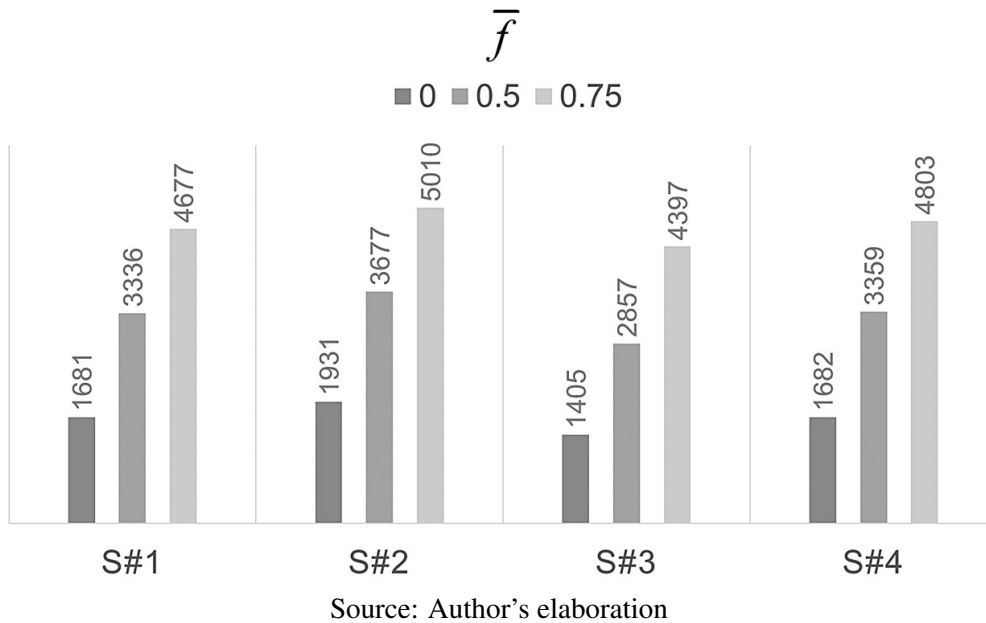
Figure 38 – Probability of failure (metric ii) for different p_{cr} values

$$p_f$$

■ 0 ■ 0.5 ■ 0.75

Source: Author's elaboration
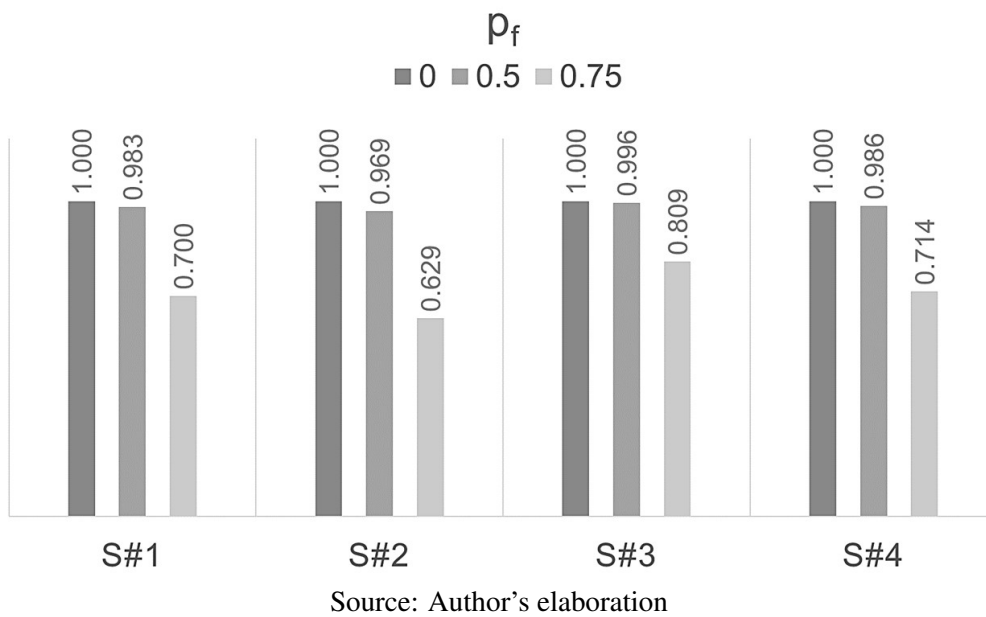
significant adverse operational environment. Not even S#2, the most resilient system, were able to avoid total failed simulations with no repair, and no significant improvement can be seen until the repair probability reaches 0.75, when S#2 collapsed in 62.9% of the simulations. These results point to the real importance of the consideration of resilience at the design phase, since not even a repair probability of 0.75 and only a 1-year operation were enough for the system to satisfactorily operate considering an environment with stochastic failure. The real increasing threat of disasters can lead to a serious detrimental operational condition.

As the metrics point to a significant adverse condition even with $p_{cr} = 0.75$, it can be stated that investment in repair seems to be not enough to improve the operational stability until an acceptable performance under such scenarios. However, it is clear that the increase in p_{cr} supported an enhancement

Figure 39 – Normalized resilience index (metric iii) for different p_{cr} values

ρ

■ 0 ■ 0.5 ■ 0.75

Source: Author's elaboration
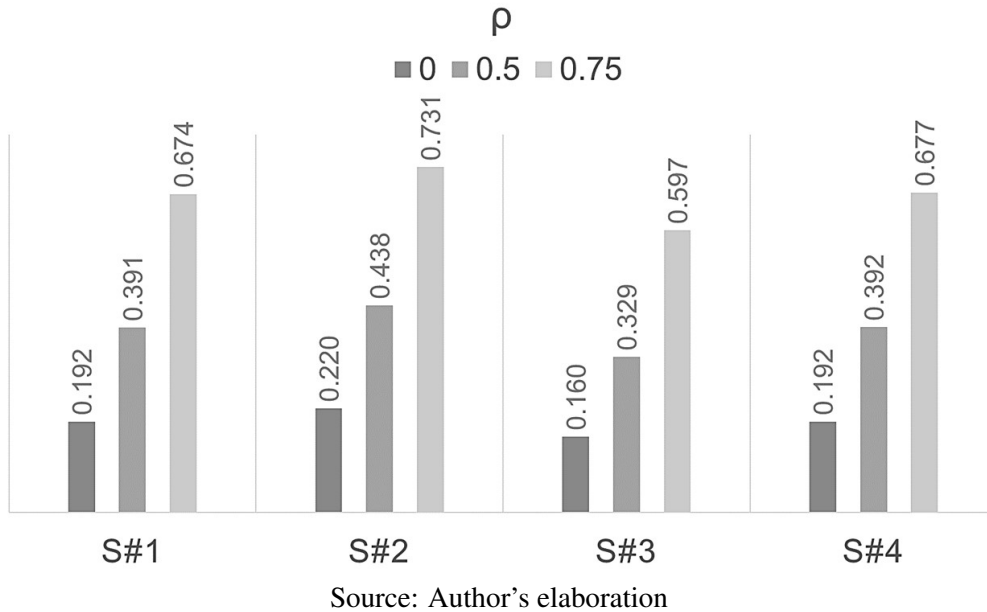
Figure 40 – Probability of system recovery (metric iv) for different p_{cr} values

p_d

■ 0.5   ■ 0.75

Source: Author's elaboration
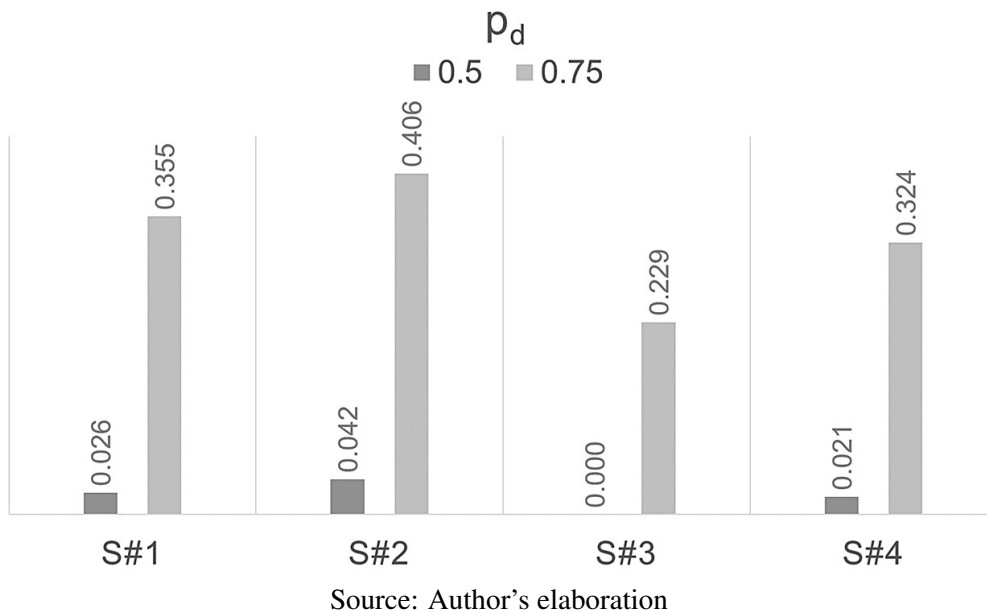
in all the metrics for the four systems. To clarify this effect, the quantitative analysis of the influence of repairing actions is shown in Table 12.

S#3, the least resilient one, is the most affected by the increment of p_{cr} from 0.50 to 0.75, being able to avoid a considerable number of 1750% more interruptions during its operation. S#4, S#1 and S#2, in this order, compose the sequence of the most affected systems. The investment in repairing actions proved to be more beneficial to the systems with lower initial resilience, and therefore can be a great and cheaper alternative for those systems in operation, rather than change their configuration.

Figure 41 – Resilient-stagnant ratio (metric v) for different p_{cr} values
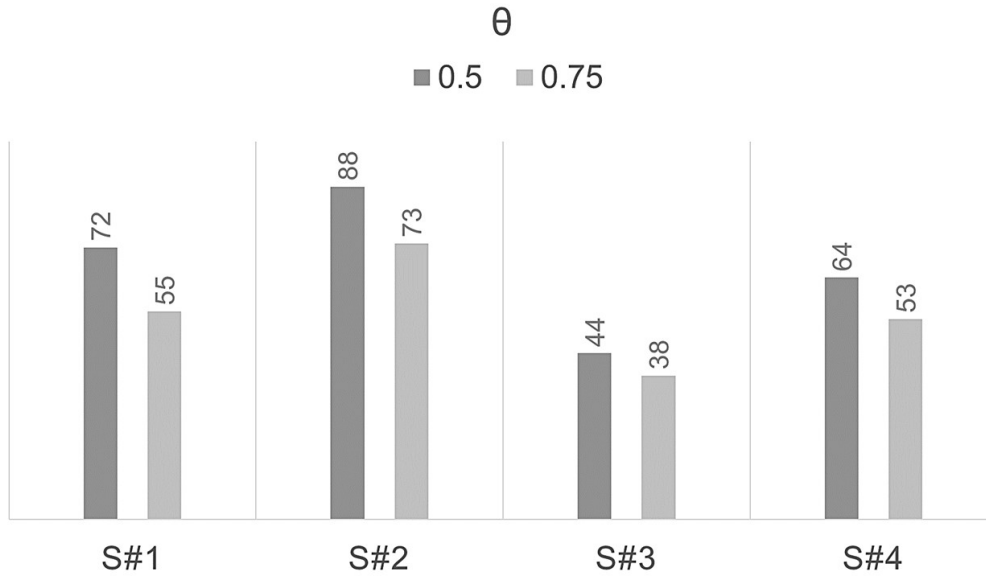
Source: Author's elaboration

Table 12 – Interruptions prevention IP in percentage

	1 year		
	NF50	**NF75**	**IP[%]**
S#1	8	103	1188
S#2	25	226	804
S#3	2	37	1750
S#4	7	111	1486

Source: Author's elaboration

4.3 VARIATION OF INPUT PARAMETERS

The variation of p_i and T was investigated, in order to analyze their influence on resilience. While the former assumed values from 0.9970 to 0.9995, the lifetime was extended up to 20 years (175200 h). The results are shown in Tables 13-21. In these tables, the values with the darkest highlighted green are those with greatest resilience. These highlights are distributed throughout the whole table, except for Table 21, because as θ can not be normalized, the positions delimited for highlights are the p_i lines. The variables $\bar{r}$ and $\bar{f}$ represent amounts of time, and therefore they are normalized by dividing their value by the plant expected lifetime T, in hours.

Table 13 refers to the variation of p_r under different p_i and T. It is clear a region of concentration of higher resilience (darker green tones) in left (lower T) and down (higher p_i) parts of the table. This is a behavioral pattern present in the tables hereafter, and it indicates that the system expected lifetime is directly connected to the evaluation of resilience during design phase, i.e., the lower the projected lifetime, the higher the associated resilience.

Table 13 – Variation of p_r with different p_i and T

p_i	p_{cr}	1 year				2 years				5 years				10 years				15 years				20 years			
		S#1	S#2	S#3	S#4	S#1	S#2	S#3	S#4	S#1	S#2	S#3	S#4	S#1	S#2	S#3	S#4	S#1	S#2	S#3	S#4	S#1	S#2	S#3	S#4
	0	0	0	0	0	0	0	0	0	0	0	0	0	0	0	0	0	0	0	0	0	0	0	0	0
0.9970	**0.50**	0.017	0.031	0.004	0.014	0	0	0	0	0	0	0	0	0	0	0	0	0	0	0	0	0	0	0	0
	0.75	0.300	0.371	0.191	0.286	0.016	0.021	0.011	0.015	0	0	0	0	0	0	0	0	0	0	0	0	0	0	0	0
	0	0.001	0.002	0	0.001	0	0	0	0	0	0	0	0	0	0	0	0	0	0	0	0	0	0	0	0
0.9980	**0.50**	0.127	0.186	0.066	0.124	0.002	0.003	0	0.001	0	0	0	0	0	0	0	0	0	0	0	0	0	0	0	0
	0.75	0.533	0.642	0.417	0.523	0.131	0.178	0.063	0.118	0	0	0	0	0	0	0	0	0	0	0	0	0	0	0	0
	0	0.125	0.192	0.069	0.113	0.001	0.002	0	0.001	0	0	0	0	0	0	0	0	0	0	0	0	0	0	0	0
0.9990	**0.50**	0.547	0.620	0.424	0.537	0.137	0.183	0.056	0.114	0	0	0	0	0	0	0	0	0	0	0	0	0	0	0	0
	0.75	0.813	0.867	0.761	0.833	0.550	0.623	0.427	0.554	0.507	0.076	0.023	0.052	0	0	0	0	0	0	0	0	0	0	0	0
	0	0.523	0.604	0.415	0.526	0.127	0.181	0.060	0.106	0	0	0	0	0	0	0	0	0	0	0	0	0	0	0	0
0.9995	**0.50**	0.807	0.835	0.750	0.821	0.524	0.632	0.416	0.548	0.045	0.070	0.018	0.046	0	0	0	0	0	0	0	0	0	0	0	0
	0.75	0.908	0.934	0.895	0.921	0.820	0.867	0.764	0.819	0.401	0.490	0.297	0.395	0.043	0.074	0.022	0.042	0.005	0.006	0.001	0.003	0	0.001	0	0

Note[1]: Green is highlighted throughout the whole table.
Note[2]: Subtitle:

Higher p_r Lower p_r

Source: Author's elaboration

Table 14 – Variation of calculated $\bar{r}$ with different p_i and T

p_i	p_{cr}	1 year				2 years				5 years				10 years				15 years				20 years			
		S#1	S#2	S#3	S#4	S#1	S#2	S#3	S#4	S#1	S#2	S#3	S#4	S#1	S#2	S#3	S#4	S#1	S#2	S#3	S#4	S#1	S#2	S#3	S#4
	0	0	0	0	0	0	0	0	0	0	0	0	0	0	0	0	0	0	0	0	0	0	0	0	0
0.9970	**0.50**	124	236	30	102	0	0	0	0	0	0	0	0	0	0	0	0	0	0	0	0	0	0	0	0
	0.75	2115	2646	1292	1980	244	312	155	215	0	0	0	0	0	0	0	0	0	0	0	0	0	0	0	0
	0	5	16	0	8	0	0	0	0	0	0	0	0	0	0	0	0	0	0	0	0	0	0	0	0
0.9980	**0.50**	915	1349	460	889	26	46	0	11	0	0	0	0	0	0	0	0	0	0	0	0	0	0	0	0
	0.75	3425	4228	2561	3372	1878	2617	890	1719	0	0	0	0	0	0	0	0	0	0	0	0	0	0	0	0
	0	892	1415	486	802	21	35	0	16	0	0	0	0	0	0	0	0	0	0	0	0	0	0	0	0
0.9990	**0.50**	3511	4062	2626	3407	2000	2650	759	1644	0	0	0	0	0	0	0	0	0	0	0	0	0	0	0	0
	0.75	4117	4484	3682	4281	7068	8080	5156	7059	1855	2832	825	1843	0	0	0	0	0	0	0	0	0	0	0	0
	0	3356	4010	2607	3453	1816	2605	848	1519	0	0	0	0	0	0	0	0	0	0	0	0	0	0	0	0
0.9995	**0.50**	4086	4210	3736	4227	6743	8163	5055	6960	1649	2611	618	1696	0	17	0	0	0	0	0	0	0	0	0	0
	0.75	3037	3218	3086	3145	8071	8710	7504	8096	13409	16781	9784	13221	3169	5535	1589	3161	588	701	105	332	0	95	0	0

Note[1]: $\bar{r}$ is nominally expressed, regardless the value of T.
Note[2]: Green is highlighted throughout the whole table.
Note[3]: Subtitle:

Higher $\bar{r}$ Lower $\bar{r}$

Source: Author's elaboration

Table 15 – Variation of normalized $\bar{r}$ with different p_i and T

p_i	p_{cr}	1 year				2 years				5 years				10 years				15 years				20 years			
		S#1	S#2	S#3	S#4	S#1	S#2	S#3	S#4	S#1	S#2	S#3	S#4	S#1	S#2	S#3	S#4	S#1	S#2	S#3	S#4	S#1	S#2	S#3	S#4
	0	0	0	0	0	0	0	0	0	0	0	0	0	0	0	0	0	0	0	0	0	0	0	0	0
0.9970	**0.50**	0.014	0.027	0.003	0.012	0	0	0	0	0	0	0	0	0	0	0	0	0	0	0	0	0	0	0	0
	0.75	0.241	0.302	0.147	0.226	0.014	0.018	0.009	0.012	0	0	0	0	0	0	0	0	0	0	0	0	0	0	0	0
	0	0.001	0.002	0	0.001	0	0	0	0	0	0	0	0	0	0	0	0	0	0	0	0	0	0	0	0
0.9980	**0.50**	0.104	0.154	0.053	0.101	0.001	0.003	0	0.001	0	0	0	0	0	0	0	0	0	0	0	0	0	0	0	0
	0.75	0.391	0.483	0.292	0.385	0.107	0.149	0.051	0.098	0	0	0	0	0	0	0	0	0	0	0	0	0	0	0	0
	0	0.102	0.162	0.055	0.092	0.001	0.002	0	0.001	0	0	0	0	0	0	0	0	0	0	0	0	0	0	0	0
0.9990	**0.50**	0.401	0.464	0.300	0.389	0.114	0.151	0.043	0.094	0	0	0	0	0	0	0	0	0	0	0	0	0	0	0	0
	0.75	0.470	0.512	0.420	0.489	0.403	0.461	0.294	0.403	0.042	0.065	0.019	0.042	0	0	0	0	0	0	0	0	0	0	0	0
	0	0.383	0.458	0.298	0.394	0.104	0.149	0.048	0.087	0	0	0	0	0	0	0	0	0	0	0	0	0	0	0	0
0.9995	**0.50**	0.466	0.481	0.426	0.483	0.385	0.466	0.289	0.397	0.038	0.060	0.014	0.039	0	0.000	0	0	0	0	0	0	0	0	0	0
	0.75	0.347	0.367	0.352	0.359	0.461	0.497	0.428	0.462	0.306	0.383	0.223	0.302	0.036	0.063	0.018	0.036	0.004	0.005	0.001	0.003	0	0.001	0	0

Note[1]: Normalized values are divided by the associated T
Note[2]: Green is highlighted throughout the whole table.
Note[3]: Subtitle:

Higher normalized $\bar{r}$ Lower normalized $\bar{r}$

Source: Author's elaboration

The values of p_r present in Table 13 raise interesting points. When $p_i = 0.9995$ and $p_{cr} = 0$ – the same environment analyzed by Matelli and Goebel [130] –, the sequence of the most resilient systems is S#2 → S#4 → S#1 → S#3, which matches their results. However, under more adverse scenarios (higher T and lower p_i), S#1 presents higher p_r than S#4. It points to a slower degradation of S#1 under detrimental operational condition, when compared to S#4. Redundancy, a feature present in S#4 and absent in S#1, was able to support a higher p_r for S#4 only in favorable situations, not being enough to maintain this configuration as the second most resilient one in disturbing circumstances. By this metric, S#1 presents higher probability to resiliently operate during its lifetime than S#4, except for positive scenarios.

The values of $\bar{r}$ in Table 14 reveal a possibility of higher resilient time until 5 years for $p_i = 0.9995$ and $p_{cr} = 0.75$, and until 2 years for $p_i = 0.9990$. To clarify the interpretation of this parameter, it was normalized in Table 15. The normalized values indicate a saturation of resilient time when the condition is highly beneficial. When $p_i = 0.9995$, normalized $\bar{r}$ diminish its value for all systems when p_{cr} increases from 0.50 to 0.75. In this case, the normal operating time – when there are no failed component – increased, reducing the associated $\bar{r}$. This metric seems to serve better under detrimental situations, once the higher normal operating times can lead to a misinterpretation.

Table 16 – Variation of calculated $\bar{f}$ with different p_i and T

p_i	p_{cr}	1 year				2 years				5 years				10 years				15 years				20 years			
		S#1	S#2	S#3	S#4	S#1	S#2	S#3	S#4	S#1	S#2	S#3	S#4	S#1	S#2	S#3	S#4	S#1	S#2	S#3	S#4	S#1	S#2	S#3	S#4
	0	1681	1931	1405	1682	1701	1936	1426	1666	1705	1950	1453	1675	1688	1946	1405	1704	1675	1932	1428	1695	1690	1926	1450	1697
0.9970	0.50	3336	3677	2857	3359	3398	3850	2840	3374	3368	3832	2854	3360	3460	3880	2925	3464	3450	3938	2932	3368	3426	3824	2918	3378
	0.75	4677	5010	4397	4803	6641	7333	5642	6667	6769	7664	5793	6789	6707	7660	5840	6857	6881	7759	5641	6871	6752	7715	5755	6848
	0	2539	2893	2115	2561	2580	2907	2075	2581	2524	2902	2112	2566	2622	2880	2123	2505	2481	2907	2127	2581	2540	2872	2122	2505
0.9980	0.50	4202	4685	3862	4334	5059	5733	4241	5151	5027	5870	4349	5115	5103	5781	4318	5066	5087	5926	4326	5037	5135	5770	4320	5145
	0.75	5036	5229	4793	5128	8446	9512	7627	8630	10089	11509	8563	10184	10323	11691	8605	10383	10139	11824	8670	10229	10193	11607	8545	10248
	0	4189	4683	3853	4354	5055	5815	4394	5078	5101	5910	4294	5025	5159	5821	4262	5169	5047	5882	4295	5134	5066	5736	4226	5070
0.9990	0.50	4913	5282	4857	5082	8542	9105	7745	8662	10223	11727	8607	10220	10114	11601	8671	10104	10244	11414	8472	10231	10211	11717	8738	10153
	0.75	5079	5195	5101	5139	10046	10609	9699	10122	18846	20678	16641	18877	20562	23408	17525	20376	20520	23352	17002	20367	20237	23328	16816	20711
	0	5045	5333	5007	5077	8379	9431	7707	8529	10458	11519	8597	10033	10153	11607	8494	10265	10192	11615	8567	10309	10248	11617	8555	9869
0.9995	0.50	4867	5195	4996	5224	9837	10338	9763	10143	18715	20795	16212	18848	20451	23045	17083	20534	19988	23310	17052	20187	20273	23212	17401	20107
	0.75	4592	4661	4816	4823	10296	10214	10171	10170	24077	25898	23661	24640	37749	42201	32673	38155	41008	45552	34571	40247	40837	46124	34564	40435

Note[1]: $\bar{f}$ is nominally expressed, regardless the value of T.
Note[2]: Null values to the left and below in the table represent conditions with no collapse during the operation.
Note[3]: Green is highlighted throughout the whole table.
Note[4]: Subtitle:

Higher $\bar{f}$ Lower $\bar{f}$

Source: Author's elaboration

Table 17 – Variation of normalized $\bar{f}$ with different p_i and T

p_i	p_{cr}	1 year				2 years				5 years				10 years				15 years				20 years			
		S#1	S#2	S#3	S#4	S#1	S#2	S#3	S#4	S#1	S#2	S#3	S#4	S#1	S#2	S#3	S#4	S#1	S#2	S#3	S#4	S#1	S#2	S#3	S#4
	0	0.192	0.220	0.160	0.192	0.097	0.111	0.081	0.095	0.039	0.045	0.033	0.038	0.019	0.022	0.016	0.019	0.013	0.015	0.011	0.013	0.010	0.011	0.008	0.010
0.9970	0.50	0.381	0.420	0.326	0.383	0.194	0.220	0.162	0.193	0.077	0.087	0.065	0.077	0.039	0.044	0.033	0.040	0.026	0.030	0.022	0.026	0.020	0.022	0.017	0.019
	0.75	0.534	0.572	0.502	0.548	0.379	0.419	0.322	0.381	0.155	0.175	0.132	0.155	0.077	0.087	0.067	0.078	0.052	0.059	0.043	0.052	0.039	0.044	0.033	0.039
	0	0.290	0.330	0.241	0.292	0.147	0.166	0.118	0.147	0.058	0.066	0.048	0.059	0.030	0.033	0.024	0.029	0.019	0.022	0.016	0.020	0.014	0.016	0.012	0.014
0.9980	0.50	0.480	0.535	0.441	0.495	0.289	0.327	0.242	0.294	0.115	0.134	0.099	0.117	0.058	0.066	0.049	0.058	0.039	0.045	0.033	0.038	0.029	0.033	0.025	0.029
	0.75	0.575	0.597	0.547	0.585	0.482	0.543	0.435	0.493	0.230	0.263	0.196	0.233	0.118	0.133	0.098	0.119	0.077	0.090	0.066	0.078	0.058	0.066	0.049	0.058
	0	0.478	0.535	0.440	0.497	0.289	0.332	0.251	0.290	0.116	0.135	0.098	0.115	0.059	0.066	0.049	0.059	0.038	0.045	0.033	0.039	0.029	0.033	0.024	0.029
0.9990	0.50	0.561	0.603	0.554	0.580	0.488	0.520	0.442	0.494	0.233	0.268	0.197	0.233	0.115	0.132	0.099	0.115	0.078	0.087	0.064	0.078	0.058	0.067	0.050	0.058
	0.75	0.580	0.593	0.582	0.587	0.573	0.606	0.554	0.578	0.430	0.472	0.380	0.431	0.235	0.267	0.200	0.233	0.156	0.178	0.129	0.155	0.116	0.133	0.096	0.118
	0	0.576	0.609	0.572	0.580	0.478	0.538	0.440	0.487	0.239	0.263	0.196	0.229	0.116	0.133	0.097	0.117	0.078	0.088	0.065	0.078	0.058	0.066	0.049	0.056
0.9995	0.50	0.556	0.593	0.570	0.596	0.561	0.590	0.557	0.579	0.427	0.475	0.370	0.430	0.233	0.263	0.195	0.234	0.152	0.177	0.130	0.154	0.116	0.132	0.099	0.115
	0.75	0.524	0.532	0.550	0.551	0.588	0.583	0.581	0.580	0.550	0.591	0.540	0.563	0.431	0.482	0.373	0.436	0.312	0.347	0.263	0.306	0.233	0.263	0.197	0.231

Note[1]: Normalized values are divided by the associated T
Note[2]: Null values to the left and below in the table represent conditions with no collapse during the operation.
Note[3]: Green is highlighted throughout the whole table.
Note[4]: Subtitle:

Higher normalized $\bar{f}$ Lower normalized $\bar{f}$

Source: Author's elaboration

The values in Table 16 points to a higher nominal value of $\bar{f}$ in situations with higher operating time, which is an expected behavior. However, the interpretation is cleared by the normalization of this variable, after which it can be seen a region of concentration of darker green tones, and therefore a higher associated resilience, concentrated in left (lower T) and down (higher p_i) parts of the table. As in $\bar{r}$, values in Table 17 under beneficial conditions can lead to a misinterpretation due to higher normal operating times. There is a major prevalence of the sequence S#2 $\rightarrow$ S#4 $\rightarrow$ S#1 $\rightarrow$ S#3, although S#1 presents greater values than S#4 in very detrimental scenarios, again indicating that this system tends to exhibit slower degradation than S#4, even with no redundancy. S#2 proved to be, in cases in which the system collapses, the one that can withstanding the most its operation, while S#3 is the most short-lived.

In Table 18, p_f almost reaches null values in the left and down parts of the table, but even the most favorable condition considered herein was not enough to prevent the systems to fail during the simulation, reiterating the detrimental scenario of stochastic failure. There is a prevalence of lower p_f to S#1 compared to S#4, but, as in other metrics, beneficial environments can induce S#4 as more resilient than S#1. A $p_f = 1$ indicates that none of the simulations reached the expected lifetime under the related scenarios. It can be seen that when $p_i = 0.9970$, the systems collapsed in almost all the simulations for a 2-year operation, regardless the repair probability. A better comprehension of p_f for longer operating times was only possible by modifying both p_{cr} and p_i, indicating that these parameters should be mutually considered at the design phase, since both are vital to system resilience.

Table 18 – Variation of p_f with different p_i and T

p_i	p_{cr}	1 year				2 years				5 years				10 years				15 years				20 years			
		S#1	S#2	S#3	S#4	S#1	S#2	S#3	S#4	S#1	S#2	S#3	S#4	S#1	S#2	S#3	S#4	S#1	S#2	S#3	S#4	S#1	S#2	S#3	S#4
	0	1	1	1	1	1	1	1	1	1	1	1	1	1	1	1	1	1	1	1	1	1	1	1	1
0.9970	0.50	0.983	0.969	0.996	0.986	1	1	1	1	1	1	1	1	1	1	1	1	1	1	1	1	1	1	1	1
	0.75	0.700	0.629	0.809	0.714	0.984	0.979	0.989	0.985	1	1	1	1	1	1	1	1	1	1	1	1	1	1	1	1
	0	0.999	0.998	1	0.999	1	1	1	1	1	1	1	1	1	1	1	1	1	1	1	1	1	1	1	1
0.9980	0.50	0.873	0.814	0.934	0.876	0.998	0.997	1	0.999	1	1	1	1	1	1	1	1	1	1	1	1	1	1	1	1
	0.75	0.467	0.358	0.583	0.477	0.869	0.822	0.937	0.882	1	1	1	1	1	1	1	1	1	1	1	1	1	1	1	1
	0	0.875	0.808	0.931	0.887	0.999	0.998	1	0.999	1	1	1	1	1	1	1	1	1	1	1	1	1	1	1	1
0.9990	0.50	0.453	0.380	0.576	0.463	0.863	0.817	0.994	0.886	1	1	1	1	1	1	1	1	1	1	1	1	1	1	1	1
	0.75	0.187	0.133	0.239	0.167	0.450	0.377	0.573	0.446	0.949	0.924	0.977	0.948	1	1	1	1	1	1	1	1	1	1	1	1
	0	0.462	0.380	0.571	0.457	0.873	0.819	0.940	0.894	1	1	1	1	1	1	1	1	1	1	1	1	1	1	1	1
0.9995	0.50	0.179	0.153	0.233	0.164	0.476	0.367	0.584	0.452	0.955	0.930	0.982	0.954	1	0.997	1	1	1	1	1	1	1	1	1	1
	0.75	0.078	0.051	0.091	0.062	0.180	0.133	0.236	0.181	0.599	0.510	0.803	0.605	0.957	0.926	0.978	0.958	0.995	0.994	0.999	0.997	1	0.999	1	1

Note[1]: Green is highlighted throughout the whole table.
Note[2]: Subtitle:

Lower p_f Higher p_f

Source: Author's elaboration

Table 19 – Variation of ρ with different p_i and T

p_i	p_{cr}	1 year				2 years				5 years				10 years				15 years				20 years			
		S#1	S#2	S#3	S#4	S#1	S#2	S#3	S#4	S#1	S#2	S#3	S#4	S#1	S#2	S#3	S#4	S#1	S#2	S#3	S#4	S#1	S#2	S#3	S#4
	0	0.192	0.220	0.160	0.192	0.097	0.111	0.081	0.095	0.039	0.045	0.033	0.038	0.019	0.022	0.016	0.020	0.013	0.015	0.011	0.013	0.010	0.011	0.008	0.010
0.9970	0.50	0.391	0.438	0.329	0.392	0.194	0.220	0.162	0.193	0.077	0.088	0.065	0.077	0.040	0.044	0.033	0.040	0.026	0.030	0.022	0.026	0.020	0.022	0.017	0.019
	0.75	0.674	0.731	0.597	0.677	0.389	0.431	0.329	0.390	0.155	0.175	0.132	0.155	0.077	0.087	0.067	0.078	0.052	0.059	0.043	0.052	0.039	0.044	0.033	0.039
	0	0.290	0.332	0.242	0.293	0.147	0.166	0.118	0.147	0.058	0.066	0.048	0.059	0.030	0.033	0.024	0.029	0.019	0.022	0.016	0.020	0.015	0.016	0.012	0.014
0.9980	0.50	0.546	0.622	0.478	0.557	0.290	0.329	0.242	0.295	0.115	0.134	0.099	0.117	0.058	0.066	0.049	0.058	0.039	0.045	0.033	0.038	0.029	0.033	0.025	0.029
	0.75	0.802	0.856	0.736	0.802	0.550	0.624	0.471	0.553	0.230	0.263	0.196	0.233	0.118	0.134	0.098	0.119	0.077	0.090	0.066	0.078	0.058	0.066	0.049	0.059
	0	0.544	0.624	0.479	0.554	0.290	0.333	0.251	0.291	0.117	0.135	0.098	0.115	0.059	0.066	0.049	0.059	0.038	0.045	0.033	0.039	0.029	0.033	0.024	0.029
0.9990	0.50	0.801	0.849	0.743	0.806	0.558	0.607	0.473	0.552	0.233	0.268	0.197	0.233	0.116	0.132	0.099	0.115	0.078	0.087	0.065	0.078	0.058	0.067	0.050	0.058
	0.75	0.921	0.946	0.900	0.931	0.808	0.851	0.744	0.812	0.459	0.512	0.394	0.461	0.235	0.267	0.200	0.233	0.156	0.178	0.129	0.155	0.116	0.133	0.096	0.118
	0	0.804	0.852	0.756	0.808	0.545	0.622	0.474	0.541	0.239	0.263	0.196	0.229	0.116	0.133	0.097	0.117	0.078	0.088	0.065	0.079	0.059	0.066	0.049	0.056
0.9995	0.50	0.920	0.938	0.900	0.934	0.791	0.850	0.742	0.810	0.453	0.511	0.382	0.457	0.234	0.263	0.195	0.234	0.152	0.177	0.130	0.154	0.116	0.133	0.099	0.115
	0.75	0.963	0.976	0.959	0.972	0.926	0.945	0.901	0.924	0.730	0.792	0.677	0.735	0.455	0.520	0.387	0.459	0.316	0.351	0.264	0.308	0.233	0.264	0.197	0.231

Note[1]: Green is highlighted throughout the whole table.
Note[2]: Subtitle:

Higher ρ Lower ρ

Source: Author's elaboration

The variation of the normalized resilience index shown in Table 19 converges to the same region of higher resilience as the previous tables, with higher both p_i and p_{cr} and lower T. For a scenario of 20-year operation with repair probability of 0.75 and probability of component normal operation of 0.9995, S#2, the most resilient system, was able to operate until only 26% of its lifetime in average, being a considerable low value. S#4 is mostly the system presenting the second highest ρ, although S#1 can take its place under more disturbing scenarios. This metric indicates that the S#2 is the system that operates for longer periods, considering all the operational aspects.

An analysis of the probability of system recovery p_d, exhibited in Table 20, allows the statement that the system with the highest capacity of recovery is S#2, followed by S#1, S#4 and S#3, respectively. Only in two occasions ($p_i = 0.9995$, and $p_i = 0.9990$, for $p_{cr} = 0.75$) the value of p_d for S#4 quickly increases, making this system the one with the highest probability of recovery. This is possibly due to the less necessity of recovery in these favorable conditions, reducing the number of simulations required as samples for the calculation and thus altering the values. A $p_d = 0$ indicates the cases when the simulations were not able to recover from a stagnant condition, even under a repairable environment. It shows that the repair probability is not the only parameter related to the probability of the system to recover from a stagnant condition, and it also depends on the failure probability and the expected lifetime. An energy system gradually sheds its ability of recovering from a failure as long as it operates. At $T = 20$ years, $p_i = 0.9995$ and $p_{cr} = 0.75$, none of the systems was able to recovery.

Table 20 – Variation of p_d with different p_i and T

p_i	p_{cr}	1 year				2 years				5 years				10 years				15 years				20 years			
		S#1	S#2	S#3	S#4	S#1	S#2	S#3	S#4	S#1	S#2	S#3	S#4	S#1	S#2	S#3	S#4	S#1	S#2	S#3	S#4	S#1	S#2	S#3	S#4
0.9970	**0.50**	0.026	0.042	0	0.021	0	0	0	0	0	0	0	0	0	0	0	0	0	0	0	0	0	0	0	0
	0.75	0.355	0.406	0.229	0.324	0.021	0.026	0.013	0.019	0	0	0	0	0	0	0	0	0	0	0	0	0	0	0	0
0.9980	**0.50**	0.167	0.236	0.091	0.166	0.003	0.006	0	0.001	0	0	0	0	0	0	0	0	0	0	0	0	0	0	0	0
	0.75	0.577	0.668	0.453	0.568	0.158	0.207	0.079	0.145	0	0	0	0	0	0	0	0	0	0	0	0	0	0	0	0
0.9990	**0.50**	0.594	0.613	0.484	0.579	0.191	0.214	0.082	0.160	0	0	0	0	0	0	0	0	0	0	0	0	0	0	0	0
	0.75	0.831	0.858	0.793	0.860	0.604	0.654	0.478	0.602	0.064	0.093	0.027	0.062	0	0	0	0	0	0	0	0	0	0	0	0
0.9995	**0.50**	0.844	0.855	0.802	0.862	0.599	0.635	0.478	0.579	0.070	0.099	0.029	0.072	0	0.001	0	0	0	0	0	0	0	0	0	0
	0.75	0.924	0.953	0.917	0.958	0.854	0.877	0.784	0.825	0.462	0.535	0.351	0.453	0.054	0.092	0.029	0.053	0.007	0.008	0.001	0.004	0	0.001	0	0

Note[1]: Green is highlighted throughout the whole table.
Note[2]: Subtitle:

Higher p_d Lower p_d

Source: Author's elaboration

Table 21 – Variation of θ with different p_i and T

p_i	p_{cr}	1 year				2 years				5 years				10 years				15 years				20 years			
		S#1	S#2	S#3	S#4	S#1	S#2	S#3	S#4	S#1	S#2	S#3	S#4	S#1	S#2	S#3	S#4	S#1	S#2	S#3	S#4	S#1	S#2	S#3	S#4
0.9970	0.50	72	88	44	64	-	-	-	-	-	-	-	-	-	-	-	-	-	-	-	-	-	-	-	-
	0.75	55	73	38	53	51	59	32	43	-	-	-	-	-	-	-	-	-	-	-	-	-	-	-	-
0.9980	0.50	117	148	104	113	112	109	-	68	-	-	-	-	-	-	-	-	-	-	-	-	-	-	-	-
	0.75	88	128	67	100	76	101	52	75	-	-	-	-	-	-	-	-	-	-	-	-	-	-	-	-
0.9990	0.50	282	437	208	307	228	331	174	225	-	-	-	-	-	-	-	-	-	-	-	-	-	-	-	-
	0.75	193	318	144	231	185	256	128	200	155	179	88	147	-	-	-	-	-	-	-	-	-	-	-	-
0.9995	0.50	578	902	456	692	540	834	401	569	458	564	407	419	-	229	-	-	-	-	-	-	-	-	-	-
	0.75	343	517	305	391	395	617	308	486	340	458	239	362	297	380	201	314	258	360	172	319	-	160	-	-

Note[1]: Green is highlighted along each p_i line.
Note[2]: Subtitle:

Higher θ Lower θ

Source: Author's elaboration

Table 21 presents valuable information about the systems behavior regarding operation interruption. Again, all cases point to S#2 as the system that can avoid interruptions the most, while S#3 is the one with the lowest number of avoidance. As pointed by previous results, the increment in p_{cr} decreased θ value, once the stagnant time increased proportionally more than the resilient operating time. For lower p_i values, S#1 presents higher θ than S#4, a scenario that changes as p_i increases. This situation does not refer to detrimental conditions, since even in longer lifetimes S#4 exhibited higher θ, but it seems to happen with lower p_i. In other words, a consideration of a greater failure probability induced S#1 to be more likely to operate resiliently rather than being stagnated after a component failure than S#4, even the latter containing redundancy. Apparently, the presence of redundancy is not so significant under environments with higher failure probabilities, and it does not assure that the system will avoid more interruptions in its energy delivery.

The metrics point to S#2 as the most resilient system and S#3 as the least one. Although the sequence of the most resilient systems for the condition previously investigated ($p_i = 0.9995$ and $p_{cr} = 0$, see [130]) remains the same, S#1 seems to stand out over S#4 in most cases. S#4 presents better results than S#1 in some special situations, mainly the most favorable ones. The only exception was θ (metric vii), which exhibited greater results for S#4 for longer lifetimes. It is clear that the variation of p_i and T, along with the introduction of p_{cr}, was important to verify the behavior of the metrics, even revealing that redundancy seems to be one of the important factors influencing resilience, but not the most impactful one. Somehow, the configuration containing the internal combustion engine proved to be more resilient than the ones based on gas turbine.

The tables also indicate the same resilience behavior with the variation of the input parameters. The highlighted green became darker in conditions of low T and high p_i, i.e., there is a visually identifiable concentration of better resilience results when they are located in left (lower T) and down (higher p_i) parts of the tables. It indicates that the system expected lifetime is an important factor to be considered in resilience design. Systems designed to operate in shorter periods do not need significant investment in resilience. On the other hand, those that supposed to work for longer periods require efforts in all aspects, including redundancy, repairing actions and system hardening strategies. A failure probability of 0.05% together with a repair probability of 75% was not enough to allow the most resilient system to operate in a acceptable way for 20 years, which means that, depending on the operational environment, allocating resources in isolated strategies may not be enough for a resiliently acceptable operation.

A practical interpretation of better conditions with higher p_i allows to state that defining strategies to reduce the failure probability of the components is important to induce the system to longer operation periods in a resilience point of view. Planning periodic maintenance [205] and observe some operational factors that can enhance the component susceptibility to fail [206] are two of the numerous possible actions. It is necessary to consider local aspects to manage this condition. It is appropriate to restate that proposing specific strategies for this purpose is out of the scope of this work.

Data on NFx variation is presented in Table 22. This table contains values of IP until $T = 5$ years, since both variables presented null values for higher T.

Values in Table 22 quantify the influence of repair on system resilience. By avoiding interruptions, the systems were able to operate for longer periods, withstanding disruptions and delivering their

Table 22 – IP variation with different T and p_i

	p_i = 0.9970								
	1 year			**2 years**			**5 years**		
	NF50	**NF75**	**IP[%]**	**NF50**	**NF75**	**IP[%]**	**NF50**	**NF75**	**IP[%]**
S#1	8	103	1188	-	-	-	-	-	-
S#2	25	226	804	-	-	-	-	-	-
S#3	2	37	1750	-	-	-	-	-	-
S#4	7	111	1486	-	-	-	-	-	-
	p_i = 0.9980								
	1 year			**2 years**			**5 years**		
	NF50	**NF75**	**IP[%]**	**NF50**	**NF75**	**IP[%]**	**NF50**	**NF75**	**IP[%]**
S#1	134	463	246	-	-	-	-	-	-
S#2	207	712	244	-	-	-	-	-	-
S#3	57	280	391	-	-	-	-	-	-
S#4	116	490	322	-	-	-	-	-	-
	p_i = 0.9990								
	1 year			**2 years**			**5 years**		
	NF50	**NF75**	**IP[%]**	**NF50**	**NF75**	**IP[%]**	**NF50**	**NF75**	**IP[%]**
S#1	665	1042	57	124	501	304	-	-	-
S#2	770	1227	59	241	744	209	-	-	-
S#3	495	974	97	42	280	567	-	-	-
S#4	708	1183	67	106	504	375	-	-	-
	p_i = 0.9995								
	1 year			**2 years**			**5 years**		
	NF50	**NF75**	**IP[%]**	**NF50**	**NF75**	**IP[%]**	**NF50**	**NF75**	**IP[%]**
S#1	416	604	45	604	1076	78	30	227	657
S#2	374	559	49	828	1284	55	65	433	566
S#3	555	858	55	510	1040	104	9	111	1133
S#4	475	656	38	751	1272	69	29	250	762

Source: Author's elaboration

energy services.

It is notable the influence of repairing actions on systems with lowest resilience. Simulations with higher p_{cr} were able to significantly avoid interruptions, mainly in more adverse conditions. For instance, for 5-year operation, S#3 – the less resilient one – avoided 1133% more interruptions with a 25% increment in p_{cr}. The same scenario provided 566% of increase in simulations with no interruption for S#2. Along the table, S#3 stands out as the most affected system by the p_{cr} improvement, followed by S#4, which reiterates that less resilient systems are the most impacted by repairing actions enhancement. Only the scenario with p_i = 0.9995, up to 2-years operation, pointed to S#1 being more influenced than S#4, corroborating to the results presented above.

Even for shorter operations, the IP values point to a condition in which it is necessary to invest in repairing actions. For 1-year operation and p_i = 0.9995, the increase in repair probability prevented 55% more interruptions in S#3 an expressive value. The other systems exhibited values close to S#3, increasing this difference with the variation of p_i and T. The decrease in IP when the scenario becomes more beneficial possibly implies an inflection point, after which the increase in repair probability causes no effect. A preliminary analysis is shown in Appendix B, but it needs further investigation.

4.4   GRAPHICAL ANALYSIS

With the data acquired from graphical analysis simulation, six graphics were plotted in Origin [207], covering the pre-established lifetimes of 1, 2, 5, 10, 15 and 20 years. The availability a and the energy availability a_e decay curves are represented from Figure 42 to Figure 47.

Figure 42 – a and a_e decay curves for T = 1 year
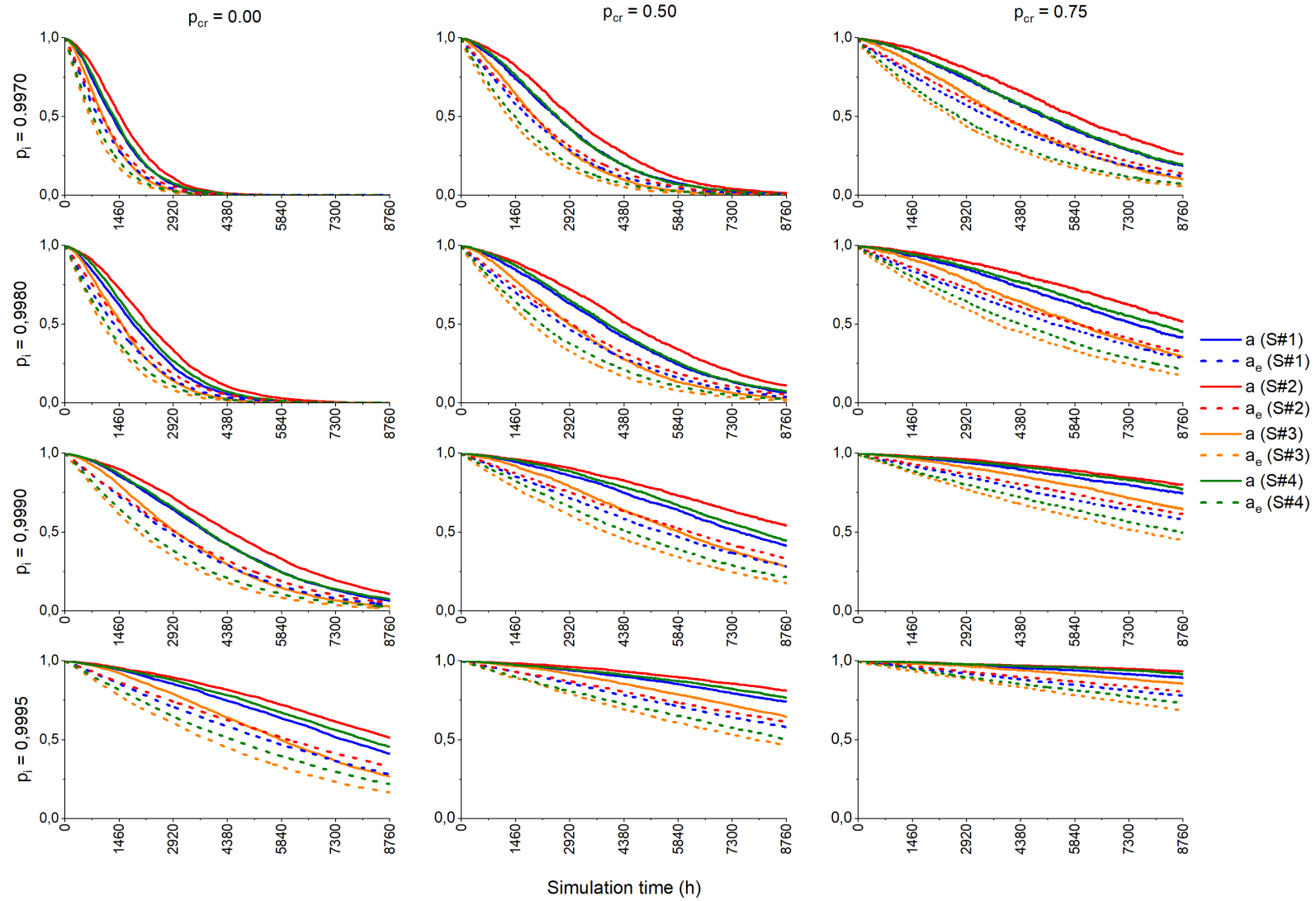
Source: Author's elaboration

Figure 43 – a and a_e decay curves for T = 2 year

Simulation time (h)
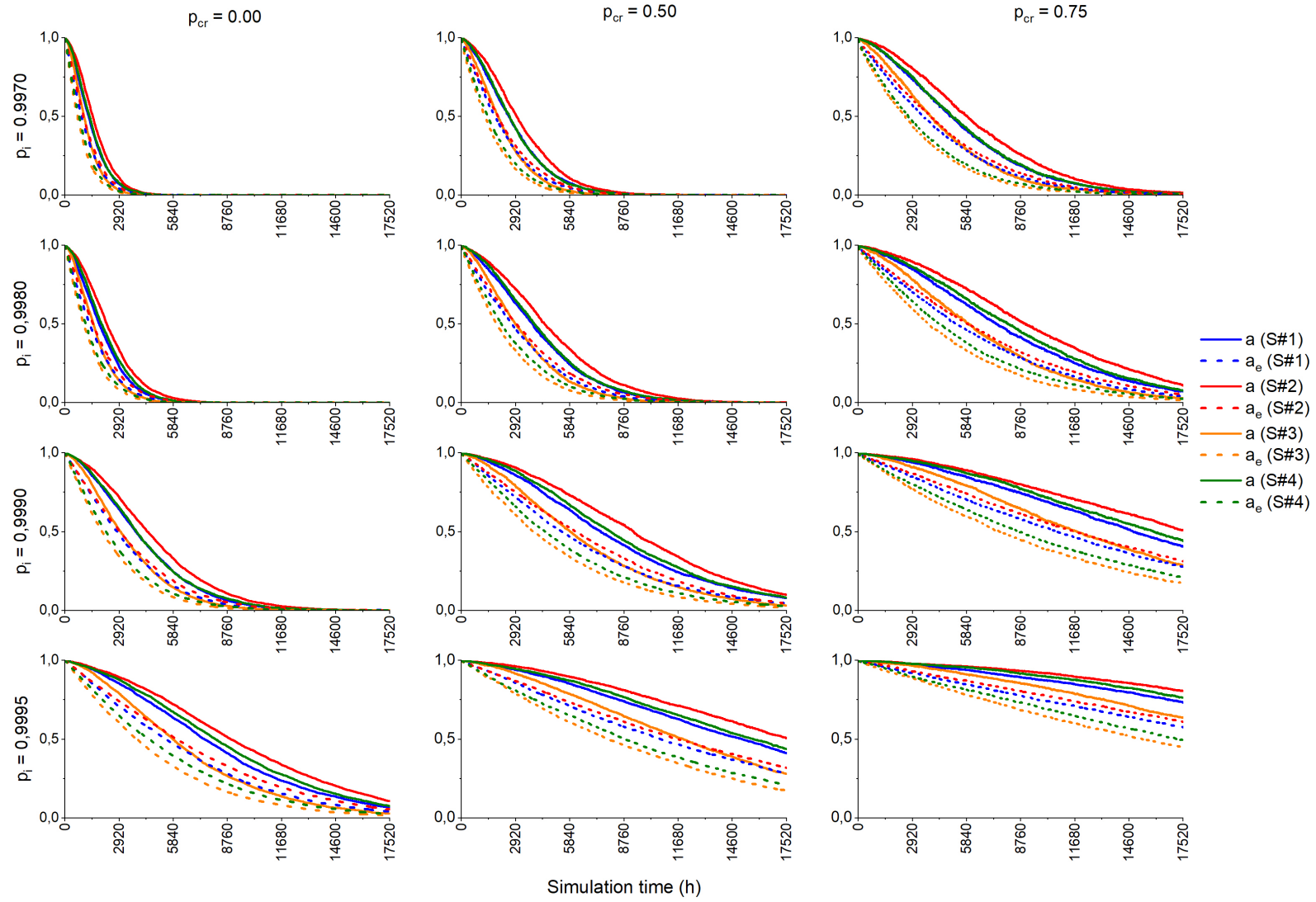
Source: Author's elaboration

Figure 44 – a and a_e decay curves for T = 5 year
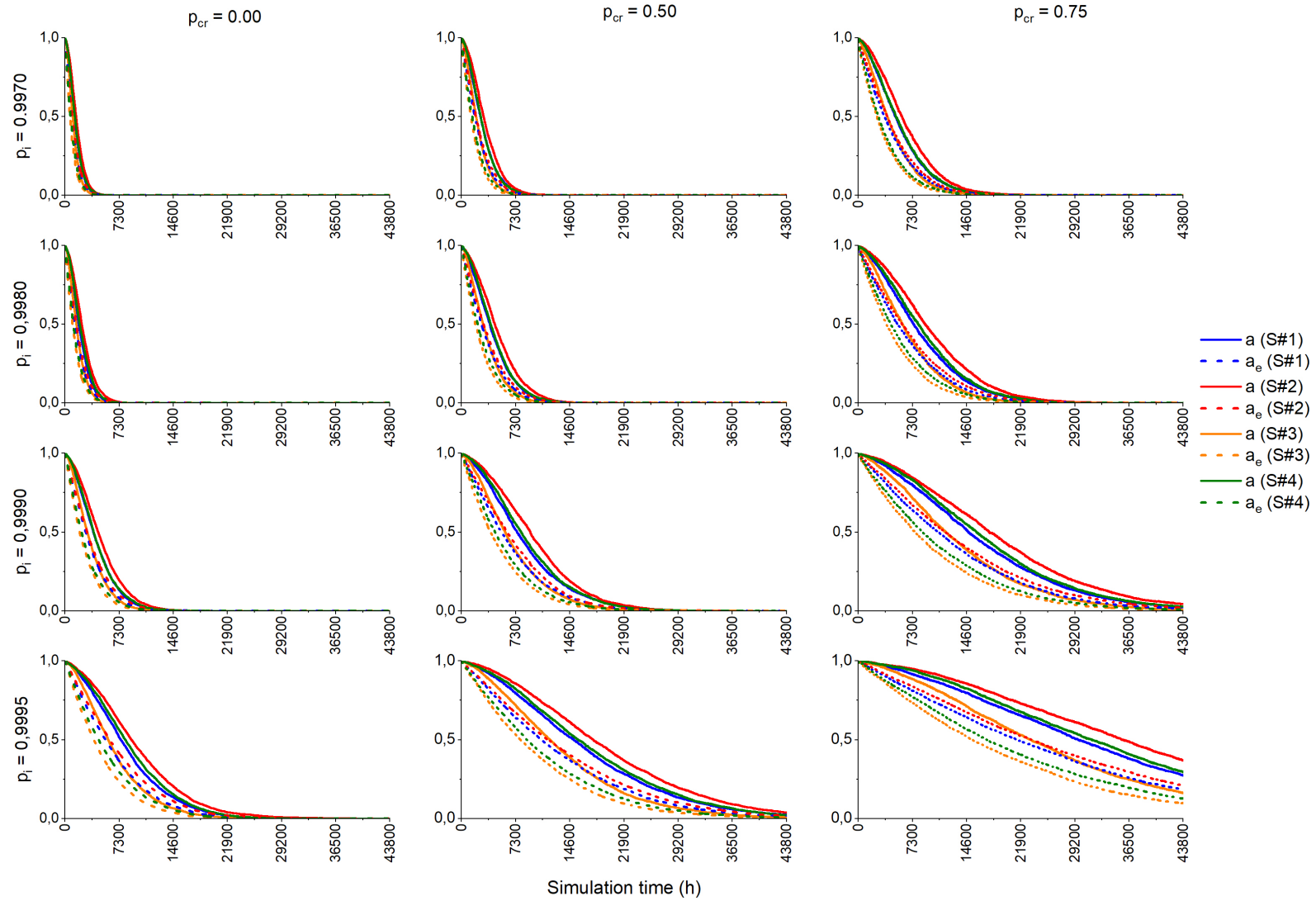
Source: Author's elaboration

Figure 45 – a and a_e decay curves for $T = 10$ year
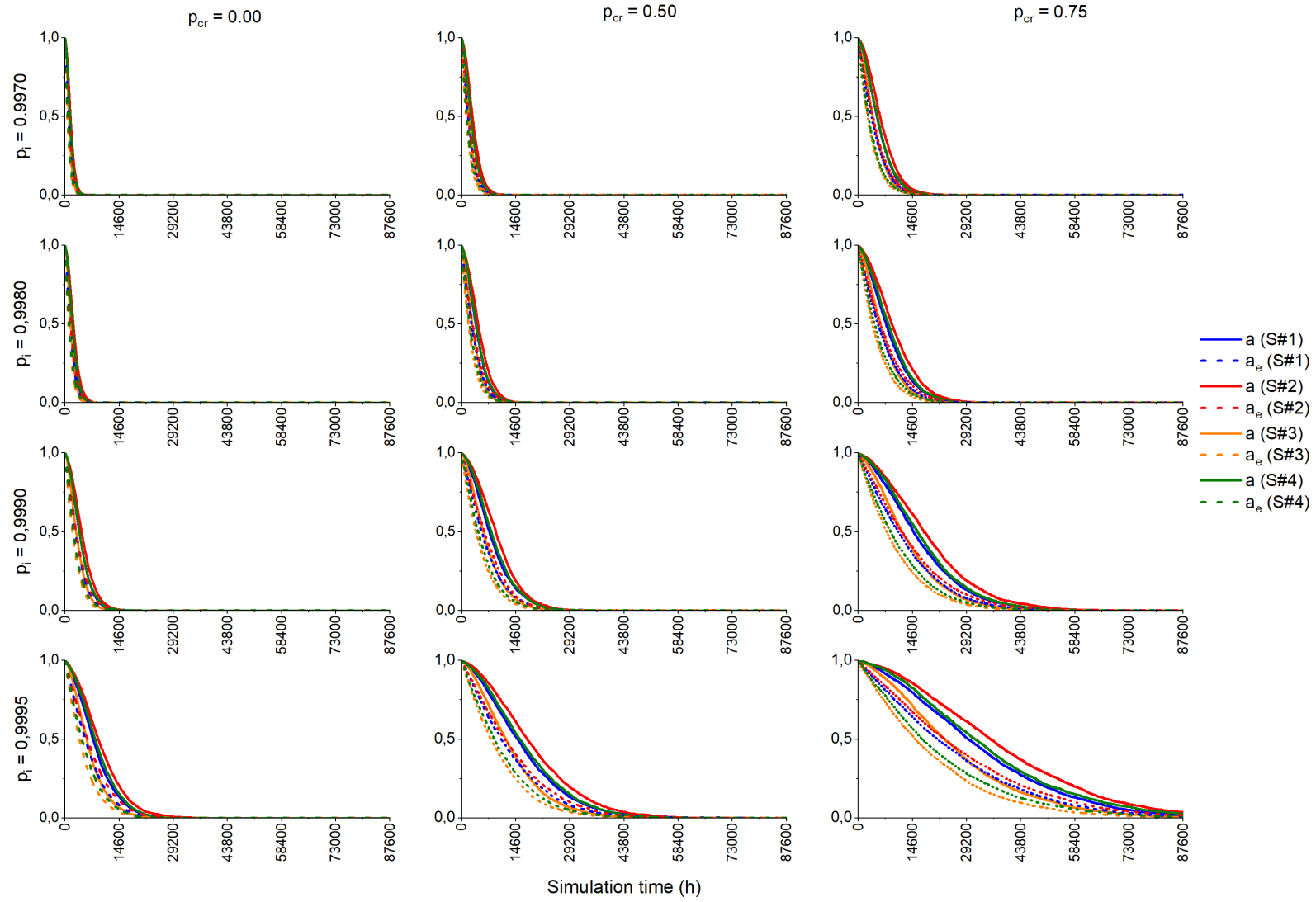
Source: Author's elaboration

Figure 46 – a and a_e decay curves for $T = 15$ year
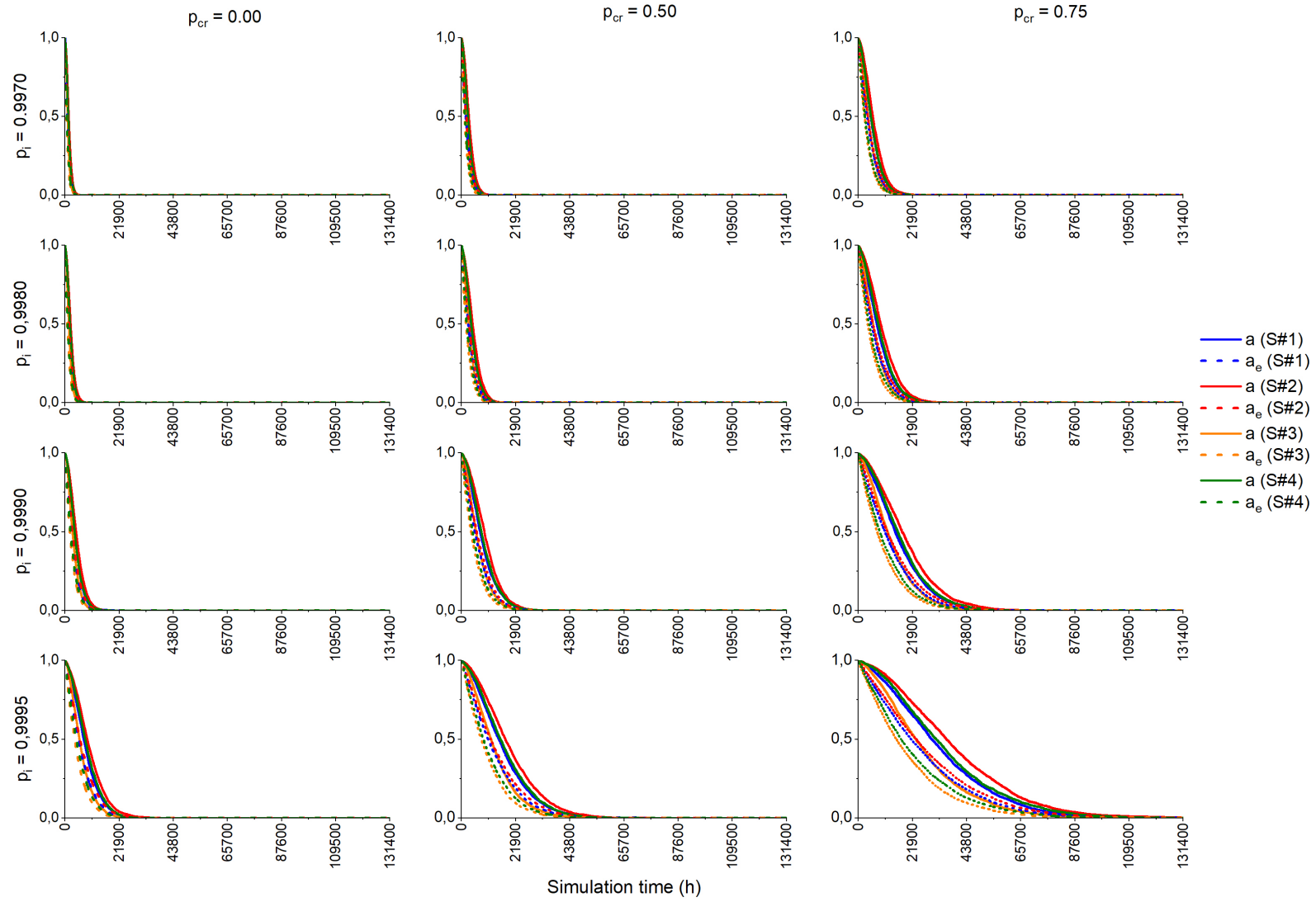
Source: Author's elaboration

Figure 47 – a and a_e decay curves for $T = 20$ year
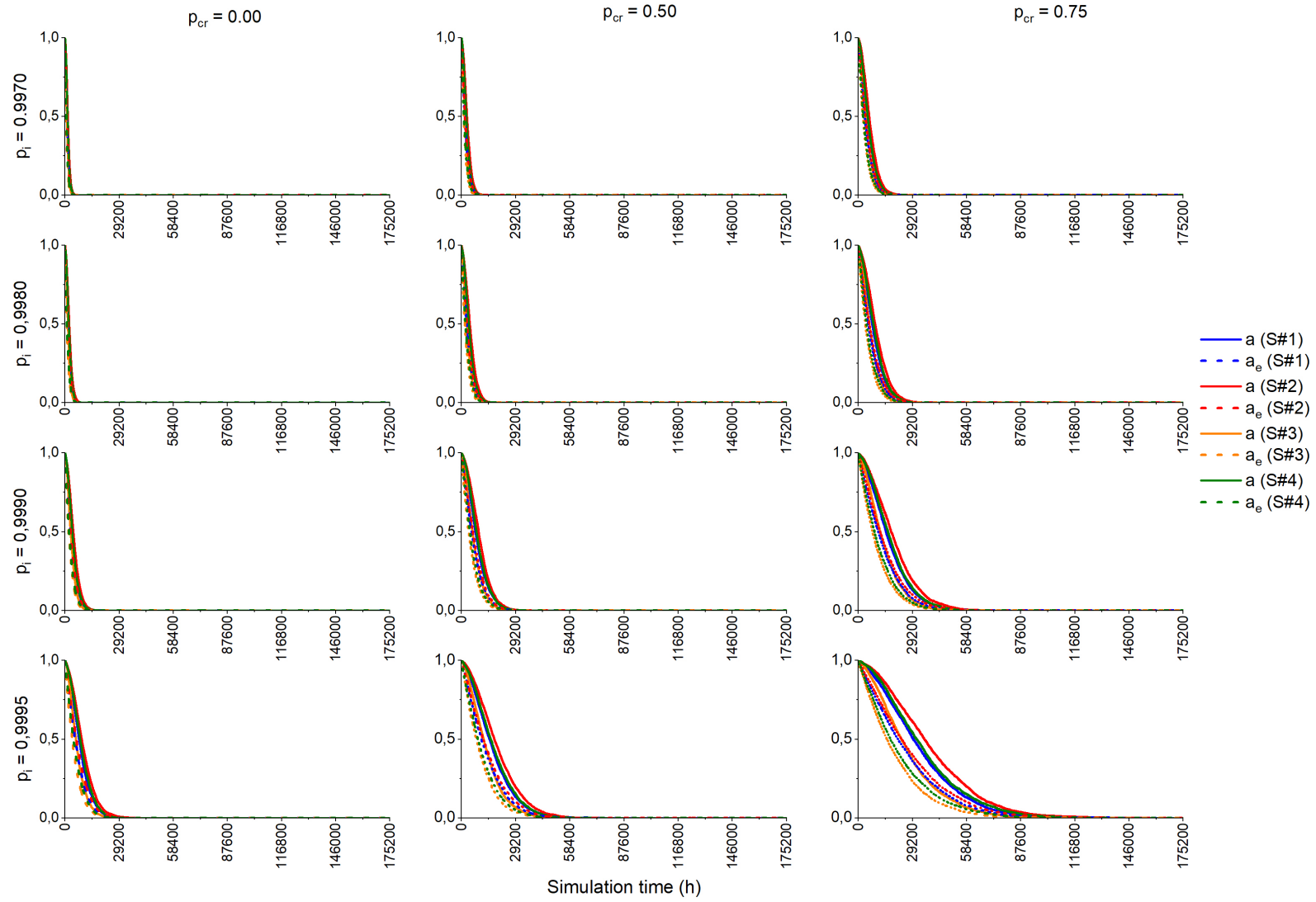
Source: Author's elaboration

As the quantitative metrics, all the curves point to S#2 as the most resilient system and S#3 as the least resilient one. S#2 is not only the system that can remain functional for longer periods, as indicated by a, but also the one that can generate more energy throughout its operation, as it can be seen through a_e values.

For a specific system, the parameter a presents always higher values compared to a_e, regardless the simulated condition. However, the difference between the curves becomes almost imperceptible under adverse conditions, specially with higher T, when all the curves cover a smaller area with more accentuated decays. On the other hand, the 1-year a curves (Figure 42) behave almost as a horizontal line when p_i and p_{cr} are admitted as their maximum simulated values, while a_e exhibits a notable decline. It can be inferred that a not only exhibits superior values compared to a_e, but it is also the most affected parameter under more beneficial scenarios. It leads to the conclusion that investment in more favorable conditions seems to impact more the system availability than its energy generation as a whole, pointing these two aspects as independent of each other.

In Figure 43 (2-year operation), it is interesting the visual perception of the influence of repair probability and probability of normal operation. Starting with the most adverse condition ($p_i = 0.9970$ and $p_{cr} = 0$), higher values of p_{cr} (to the right on the figure) assure better performances, but with significant decrease at the beginning, recovering at the end of the curve. On the other hand, by increasing p_i, the curves retard the initial decline, being the systems able to operate and generate energy with higher availabilities for longer. If these curves represented a real design phase, it would be better to invest in decrease the failure probability rather than repairing actions in this situation.

The behavior of the decays tends to be similar for all cases, anticipating or postponing some points depending on T, p_i, and p_{cr} values. The a curve starts moving in a slight angle – even achieving the horizontal behavior in some beneficial conditions –, and then it presents a significant drop, weakly recovering before it fails or reaches the lifetime. The a_e pattern points to a notable decrease at the beginning of its course, only attenuating the decay near the end of the trajectory. This analysis indicates that the first hours of operation are crucial to system and energy availabilities. Strategies to enhance both parameters should focus on retarding the decline start point for a and reducing the decay angle for a_e. In Figure 42, when $p_{cr} = 0.75$ and $p_i = 0.9995$, it is perceptible that the availability decline start points for all systems are located after the expected lifetime (i.e., outside the graph), along with a substantial reduction of energy availability decay angles.

Another procedure to analyse the behavior of the decay curves is to derive them. Two graphics are obtained by the derivation of a and a_e curves and expressed in Figure 48 and Figure 49, respectively. The figures have the same scale and are developed for a lifetime of 20 years.

Figure 48 – Derivative of a for $T = 20$ year
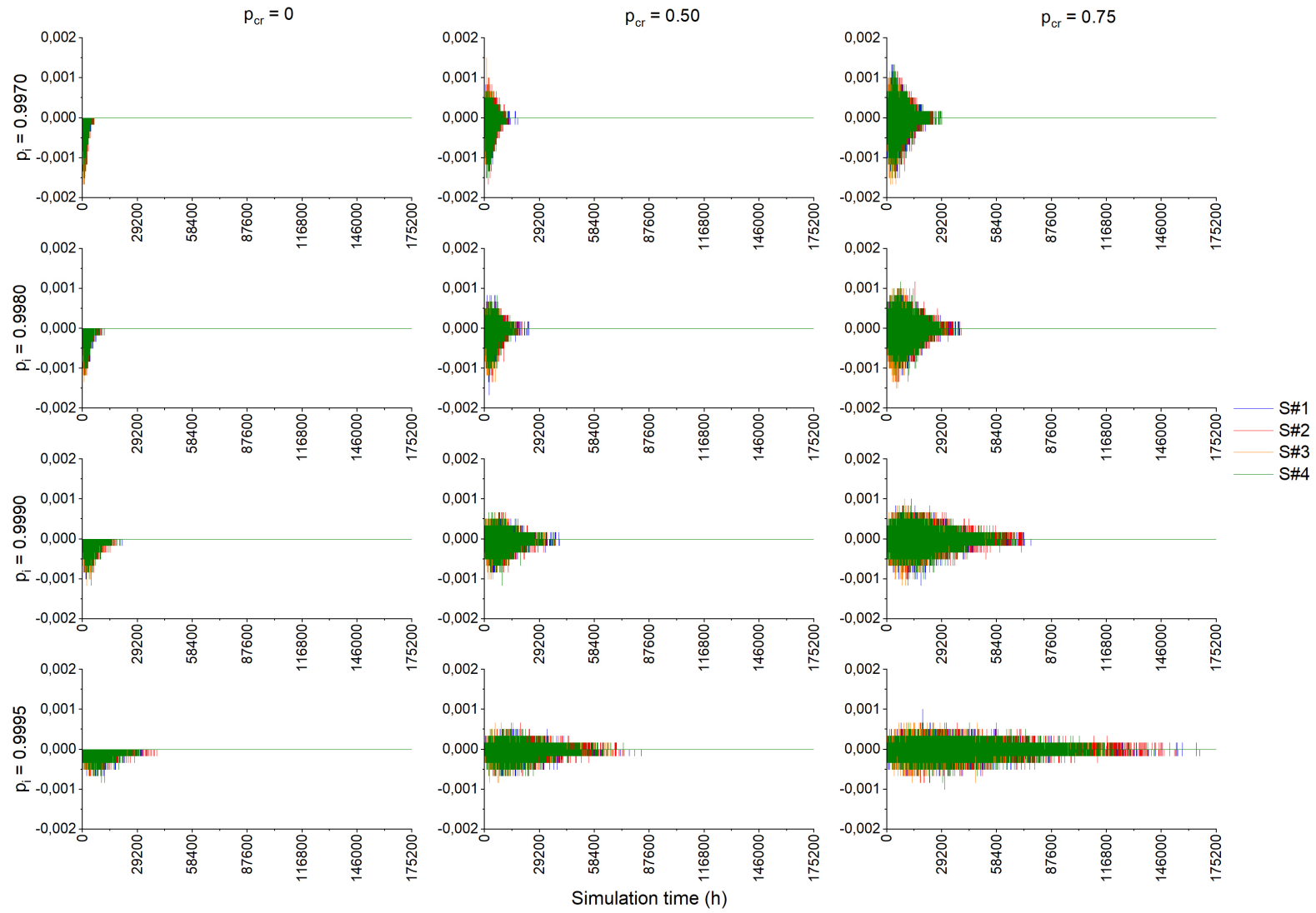
Source: Author's elaboration

Figure 49 – Derivative of a_e for T = 20 year
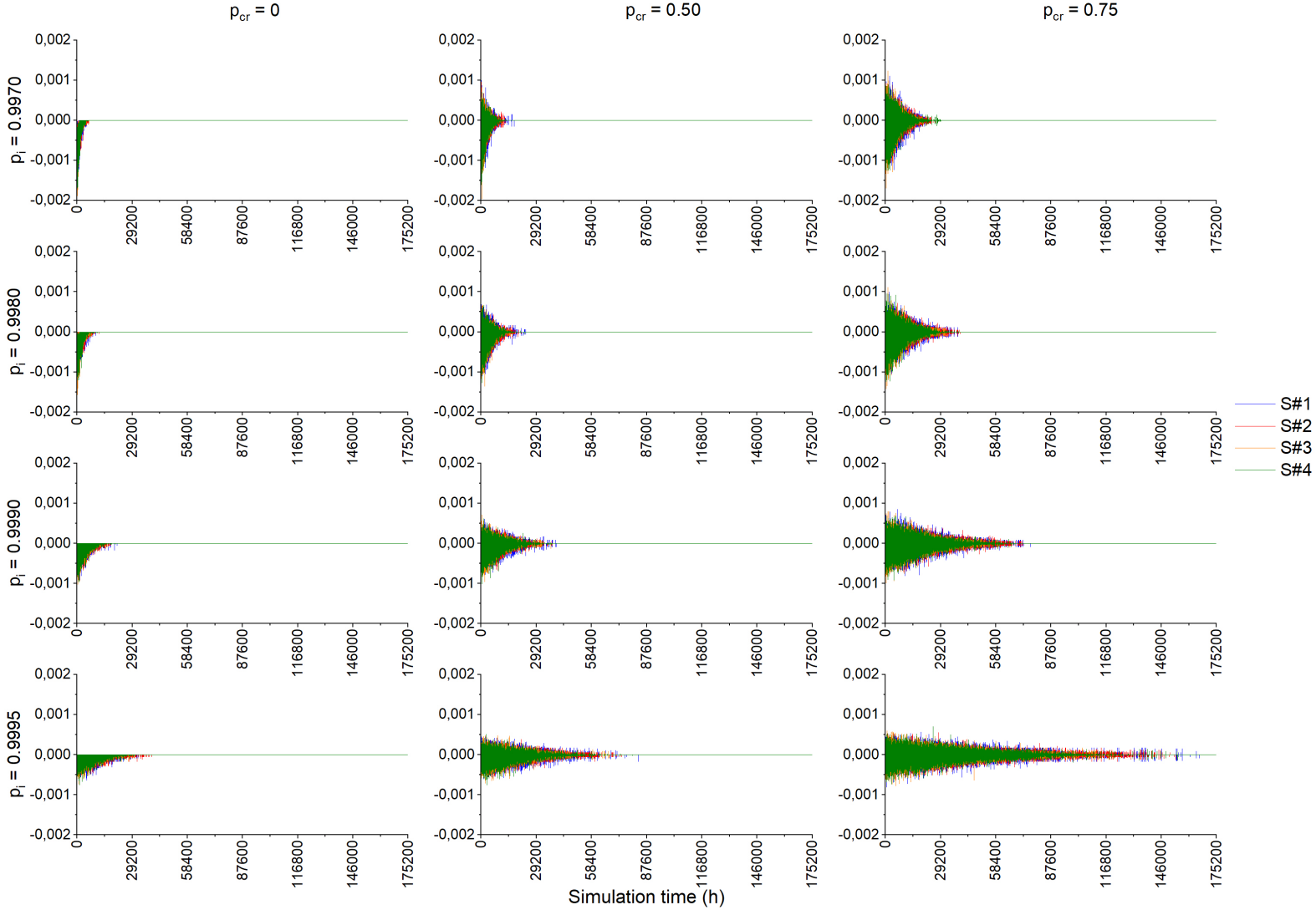
Source: Author's elaboration

A significant visual perception of the derivatives is that neither a nor a_e can recover with no repair actions, since there are no positive values in this condition, which exposes the vulnerability of the systems in this case. In other words, as low as the failure probability can be in a operation environment, a minimum failure can compromise the entire system, with the only difference that as higher the probability of normal operation, the longer the time until failure. When $p_{cr} = 0$, the derivative values in a and a_e curves show a minimum value as soon as the operation starts, then gradually returning to zero. Both parameters, however, exhibit different behavior for higher p_i: while a_e diminish the initial amplitude and distribute the remaining negative values along a higher operation time, a, along with the reduction of the peak amplitude, also postpones the peak, being able to considerably reduce its initial degradation and retarding the critical moment.

It is notable a region of instability in each curve, in which the peaks are higher, indicating sharp oscillation of a and a_e in a certain moment. The increase in p_{cr} seems not to attenuate the derive peak, but to extend the instability region, stretching the area covered by the curve. It means a longer operating time, but with low operational stability. The reduction of the failure probability (by increasing p_i) is responsible for attenuating the peaks, leading to a more stable operation. This analysis elucidates the consequences of investing in component repair and a lower frequency of failure.

An interesting difference between a and a_e behaviors is the response to more beneficial conditions. The curves representing a exhibit a peak retardation under better scenarios, with lower amplitude oscillation when $p_{cr} = 0.75$ and $p_i = 0.9995$, which indicates a predictable performance of system availability throughout its operation. On the other hand, the energy availability curves keep their region of instability at the beginning in all cases. This points to a higher degradation in energy generation in the first hours of operation, regardless the scenario.

In both figures, it is perceptible that S#2 and S#4, respectively represented by red and green lines, are the systems that keep their derivatives for longer periods, in convergence with the decay curves. Although the derivatives have seemingly the same shapes, the graphs of the systems presenting higher resilience are shifted to the right.

Another interesting aspect is the relative area covered by the a and a_e decay curves. This parameter is the relation between the area under the graph – calculated by integrating the curve from 0 to T – and the maximum value of the area, which is T itself. For the system availability, the relative area represents the amount of time that the system is able to operate at some functional level in relation to its expected lifetime; while for energy availability, this ratio indicates the generated energy in relation to an uninterrupted fully normal operation. A relative area equals to one implies a fully functional system during the whole operation for a, and an undisturbed generation for a_e. Therefore, in both cases the the closer the relations get to the unity, the higher the associated resilience. Tables 23 and 24 present the relative areas of a and a_e for the different input parameters. As in section 4.3, a darker green indicates a higher value throughout the whole table.

Table 23 – Relative area covered by a decay curves

p_i	p_{cr}	1 year				2 years				5 years				10 years				15 years				20 years			
		S#1	S#2	S#3	S#4	S#1	S#2	S#3	S#4	S#1	S#2	S#3	S#4	S#1	S#2	S#3	S#4	S#1	S#2	S#3	S#4	S#1	S#2	S#3	S#4
0.9970	**0**	0.162	0.187	0.132	0.167	0.081	0.093	0.066	0.083	0.032	0.037	0.026	0.033	0.016	0.019	0.013	0.017	0.011	0.012	0.009	0.011	0.008	0.009	0.007	0.008
	0.50	0.325	0.374	0.256	0.328	0.163	0.188	0.128	0.164	0.065	0.075	0.051	0.066	0.033	0.038	0.026	0.033	0.022	0.025	0.017	0.022	0.016	0.019	0.013	0.016
	0.75	0.581	0.649	0.488	0.588	0.321	0.368	0.259	0.325	0.129	0.148	0.104	0.130	0.064	0.074	0.052	0.065	0.043	0.049	0.035	0.043	0.032	0.037	0.026	0.033
0.9980	**0**	0.235	0.283	0.195	0.252	0.117	0.141	0.098	0.126	0.047	0.057	0.039	0.050	0.023	0.028	0.020	0.025	0.016	0.019	0.013	0.017	0.012	0.014	0.010	0.013
	0.50	0.468	0.537	0.378	0.481	0.241	0.281	0.191	0.249	0.096	0.113	0.076	0.100	0.048	0.056	0.038	0.050	0.032	0.038	0.025	0.033	0.024	0.028	0.019	0.025
	0.75	0.727	0.795	0.646	0.753	0.467	0.542	0.383	0.491	0.193	0.228	0.155	0.203	0.097	0.114	0.078	0.102	0.064	0.076	0.052	0.068	0.048	0.057	0.039	0.051
0.9990	**0**	0.472	0.533	0.388	0.478	0.243	0.279	0.197	0.247	0.097	0.112	0.079	0.099	0.049	0.056	0.039	0.049	0.032	0.037	0.026	0.033	0.024	0.028	0.020	0.025
	0.50	0.736	0.806	0.645	0.762	0.471	0.542	0.384	0.493	0.196	0.226	0.156	0.204	0.098	0.113	0.078	0.102	0.065	0.075	0.052	0.068	0.049	0.056	0.039	0.051
	0.75	0.888	0.917	0.844	0.906	0.730	0.788	0.648	0.755	0.380	0.437	0.311	0.398	0.192	0.223	0.156	0.201	0.128	0.148	0.104	0.134	0.096	0.111	0.078	0.100
0.9995	**0**	0.736	0.795	0.642	0.762	0.467	0.538	0.377	0.494	0.192	0.227	0.153	0.204	0.096	0.113	0.077	0.102	0.064	0.076	0.051	0.068	0.048	0.057	0.038	0.051
	0.50	0.890	0.924	0.845	0.903	0.731	0.792	0.649	0.750	0.383	0.441	0.309	0.398	0.194	0.224	0.155	0.201	0.129	0.149	0.103	0.134	0.097	0.112	0.078	0.100
	0.75	0.953	0.971	0.936	0.966	0.887	0.923	0.843	0.907	0.650	0.721	0.555	0.674	0.377	0.440	0.306	0.398	0.254	0.298	0.204	0.268	0.190	0.223	0.153	0.201

Note[1]: Green is highlighted throughout the whole table.
Note[2]: Subtitle:

Larger area   Smaller area

Source: Author's elaboration

Table 24 – Relative area covered by a_e decay curves

p_i	p_{cr}	1 year				2 years				5 years				10 years				15 years				20 years			
		S#1	S#2	S#3	S#4	S#1	S#2	S#3	S#4	S#1	S#2	S#3	S#4	S#1	S#2	S#3	S#4	S#1	S#2	S#3	S#4	S#1	S#2	S#3	S#4
0.9970	**0**	0.125	0.135	0.097	0.107	0.063	0.068	0.049	0.053	0.025	0.027	0.019	0.021	0.013	0.014	0.010	0.011	0.008	0.009	0.006	0.007	0.006	0.007	0.005	0.005
	0.50	0.251	0.268	0.186	0.206	0.126	0.134	0.093	0.103	0.050	0.054	0.037	0.041	0.025	0.027	0.019	0.021	0.017	0.018	0.012	0.014	0.013	0.013	0.009	0.010
	0.75	0.456	0.485	0.357	0.379	0.246	0.265	0.186	0.200	0.099	0.106	0.075	0.080	0.049	0.053	0.037	0.040	0.033	0.035	0.025	0.027	0.025	0.027	0.019	0.020
0.9980	**0**	0.184	0.205	0.146	0.159	0.092	0.102	0.073	0.079	0.037	0.041	0.029	0.032	0.018	0.020	0.015	0.016	0.012	0.014	0.010	0.011	0.009	0.010	0.007	0.008
	0.50	0.365	0.392	0.278	0.310	0.186	0.202	0.140	0.157	0.075	0.081	0.056	0.063	0.037	0.040	0.028	0.031	0.025	0.027	0.019	0.021	0.019	0.020	0.014	0.016
	0.75	0.596	0.628	0.492	0.533	0.365	0.394	0.280	0.313	0.150	0.163	0.113	0.127	0.075	0.081	0.057	0.064	0.050	0.054	0.038	0.042	0.037	0.041	0.028	0.032
0.9990	**0**	0.372	0.393	0.289	0.314	0.190	0.202	0.146	0.160	0.076	0.081	0.058	0.064	0.038	0.040	0.029	0.032	0.025	0.027	0.019	0.021	0.019	0.020	0.015	0.016
	0.50	0.604	0.643	0.500	0.544	0.368	0.398	0.286	0.318	0.151	0.163	0.116	0.129	0.076	0.082	0.058	0.065	0.050	0.054	0.039	0.043	0.038	0.041	0.029	0.032
	0.75	0.778	0.803	0.693	0.726	0.597	0.629	0.493	0.532	0.294	0.319	0.227	0.250	0.148	0.161	0.114	0.126	0.099	0.107	0.076	0.084	0.074	0.080	0.057	0.063
0.9995	**0**	0.603	0.637	0.494	0.545	0.366	0.399	0.280	0.319	0.149	0.165	0.113	0.129	0.075	0.083	0.057	0.065	0.050	0.055	0.038	0.043	0.037	0.041	0.028	0.032
	0.50	0.785	0.803	0.707	0.735	0.603	0.629	0.505	0.538	0.299	0.320	0.230	0.253	0.151	0.161	0.116	0.127	0.101	0.107	0.077	0.085	0.075	0.081	0.058	0.063
	0.75	0.885	0.901	0.835	0.859	0.780	0.805	0.699	0.734	0.525	0.555	0.421	0.462	0.295	0.318	0.226	0.254	0.198	0.214	0.151	0.170	0.149	0.161	0.113	0.128

Note[1]: Green is highlighted throughout the whole table.
Note[2]: Subtitle:

Larger area   Smaller area

Source: Author's elaboration

As the previous tables of metrics in section 4.3, there is a region of concentration of darker green tones in left and down parts of the tables, confirming the importance of T and p_i in system resilience. Moreover, the prevalence of S#2 as the most resilient system and S#3 as the least one remains the same. According to the tables, S#2 is not only the system that keeps its operation for longer periods, but it is also the one presenting the highest energy generation under the proposed conditions.

An interesting point is the elucidation of the different features of the systems S#1 and S#4. In Table 23, S#4 presents higher availability than S#1, while values in Table 24 demonstrate that S#1 exhibit greater energy availability. In other words, S#4 operates for longer periods, but this fact does not assure a superior amount of energy generated during this operation. The redundancy in S#4 was able to improve both a and a_e (comparing to S#3), but the enhancement of its energy availability was not enough to reach the values of S#1. It suggests that the component failures reach those responsible for energy generation more frequently in the configurations containing gas turbine as prime movers. Therefore, this arrangement is more susceptible to have its energy generation disturbed.

The values presented in both tables clarify important aspects to be considered in the design phase. For instance, under condition of $p_i = 0.9995$, $p_{cr} = 0.75$ and $T = 5$ years, there is no significant difference in availability for S#4 and S#1, but data of a_e for the same condition point to a difference of 6% for the generated energy between them, which would certainly influence the choice between these configurations in a real project. In another example, for $p_{cr} = 0.75$ and $p_i = 0.9990$, the availability points to an acceptable operation of more than 90% of the lifetime for S#2 and S#4 for a 1-year operation scenario. However, the energy availability for S#4 is only 72.6%, almost 8% lower than S#2. The quantitative obtainment of these parameters is certainly supportive during the design phase.

The operation of 20 years, the longest lifetime contemplated herein, is not practically feasible under the examined scenarios. If these conditions would cover an actual project, it should be suggested either to develop strategies to decrease the failure probability or increase the repair probability, or even change the initial project by reducing the expected lifetime. Reaching only $a = 0.223$ and $a_e = 0.161$, S#2, the most resilient system, does not exhibit feasible values to be actually designed.

The examples cited above demonstrate the independence of these two variables. A case in which the system is functional does not necessarily mean that it is generating an acceptable amount of energy, as well as a high a_e is not inevitably associated with a high a. It is important to consider both variables in resilience analysis.

5 CONCLUSIONS

Energy systems are one of the most important parts of the critical infrastructure, and therefore any disturbance can cause severe consequences to several societal fields. With the increase of disasters worldwide, these systems became more susceptible to unexpected failures and disruptions. In this work, the context of disasters, which create situations of sudden adversities and unpredictable failures, was covered. Each type of disaster was described, along with their possible consequences to energy systems. Among important actions to mitigate the negative effects in these systems, the study of system resilience was highlighted.

Two distinct Monte Carlo-based analysis to evaluate resilience in energy systems were introduced herein. The purpose was to represent stochastic failures in components and the consequence of the failure propagation to system operational state. Seven quantitative metrics based on proposed time counters were considered, being two of them originally developed by this work. Moreover, two decay curves were described, representing both system and energy availabilities. A further investigation was conducted to appraise the influence of repairing actions in system resilience. The proposed method was codified in Python and then applied in four cogeneration plants, being the redundancies and the type of prime mover the capital differences between them.

Preliminary results of the seven metrics, considering a certain condition of lifetime T and probability of normal operation p_i, along with three different values for probability of component repair p_{cr}, were obtained. All the metrics pointed to S#2 and S#3 as the most and the least resilient systems, respectively. S#2 is the system with highest absorptivity, that better withstand a critical condition, and the one with greatest recovery. The redundancy is one of the aspects in the configuration that appears to influence resilience, but the fact that most of the metrics pointed to S#1 as a more resilient system than S#4 indicates that the configuration itself is also a crucial factor. The systems containing internal combustion engine as prime mover presented greater metric values.

There is a notable disparity between the metrics values with and without repairing actions. The initial simulation condition pointed to an inevitable collapse of all systems, which was decreased with the addition of repairable conditions, and significantly reduced with the further increase of repair probability. A quantitative analysis of the influence of repairing actions indicated that the increase in p_{cr} affected those systems presenting lowest resilience the most, implying a feasible strategy for the actual active systems.

The variation of T and p_i enabled the investigation of their influence in system resilience. The results tables pointed to a region of concentration of higher resilience with lower T and higher p_i values. An analysis of these results indicates that, at the design phase, the lifetime must be considered from resilience point of view. A system operating for shorter periods does not need plenty improvement, while those projected to operate for longer periods need a combination of strategies to enhance both probabilities of repair and normal operation.

The manipulation of input parameters also reiterated that redundancy is not the only factor influencing resilience. Even the normalized resilience index (metric v), in which S#4 presented greater

values in an initial analysis, pointed S#1 with higher associated resilience for longer expected lifetimes, i.e., more detrimental conditions. This evidences that the proposed method was necessary to overcome an untrue initial judgement that S#2 and S#4 were probably the most resilient because of their redundancies. Moreover, the comparison between the systems can change with the operational conditions.

The evaluation of the interruption prevention with the increase in repair probability for different input conditions confirmed that the least resilient systems are the most affected. The more adverse the operational condition, the higher the difference of influence between the least and the most resilient systems – S#3 and S#2, respectively. This fact demonstrates that systems already in operation can significantly reduce stagnant periods by investing in repairing actions, even if they are not projected considering resilience at the design phase. Even the most beneficial scenario investigated herein pointed to a considerable number of simulations that were able to avoid interruption.

By analyzing the system and energy availabilities decay curves, it was possible to note the behavior of these parameters in each system under different conditions. The graphs express the probability of the system to be functional, as well as the amount of energy that is expected to be delivered at some operating time, which are quite important parameters to be analyzed at the design phase. System availability seemed to be more affected by beneficial conditions than system functionality, specially by increasing p_i. By calculating the area under the curves under different conditions, it is once more perceptible a region of concentration of higher resilience for lower T and higher p_i. Moreover, this calculation expresses in percentage two specifications important in the project stage: the amount of time that the system is supposed to remain functional and the expected amount of generated energy. Both visual and integral analysis of the curves pointed to the S#2 and S#3 as the most and the least resilient systems, respectively, proving the robustness of the method as a whole. An important verification is that S#4 exhibited a greater availability, while S#1 presented a higher energy availability. The presence of redundancy in S#4 was able to increase both a and a_e, but only the first one increased enough to be superior to the value presented by S#1.

The derivative analysis of the curves indicated distinct behaviors for a and a_e. The energy availability presented a region of instability in the first operation hours in all cases, different from system availability, which was able to distribute this region throughout the curve under more beneficial conditions. Containing the initial instability of energy availability and maintaining the stability of energy availability are challenging strategies for resilience enhancement.

This work satisfactorily provided useful tools that enable the system designer not only to quantitatively evaluate metrics related to resilience in energy systems, but also to analyze the behavior of some important parameters under different conditions. The application of the method proposed herein can guide the selection of the most resilient system, as well as instruct investments in specific strategies, focusing on increase system resilience.

5.1 SUGGESTIONS FOR FUTURE WORK

As an emergent topic in energy field, the study of resilience has still important scientific gaps to be filled and some limitations to be overcome.

One of the restrictions of this work is the input data. There is limited data in scientific articles and books over components failures and their behavior under detrimental conditions, and therefore the data considered herein was admitted or suggested, while the consequences of disasters to components were originally proposed, but with no wide discussion and validation in literature. Another point to be developed is the application of this method in other systems. Since this work aimed to establish a method to be considered in design phase, the research focus was restricted to the analysis, not the subject of investigation. It is important to investigate the proposed analysis in other systems, in order to obtain a more robust validation.

Aiming to overcome the cited limitations, the following suggestions are listed. They are just some of the possible developments that arose during the progress of this work.

1. Focus on system components: This work aims to evaluate resilience considering the systems configuration, but not focusing on their components. There are certainly critical components with greater vulnerability to cascading failures, affecting both system and energy availabilities. Their identification and examination could be useful to improve resilience with minor efforts.

2. Design point at decay curves: An adequate approach that could approximate the conceptual analysis to the real system design is to adapt p_{cr} to higher values and designate a design point in the decay curves of a and a_e. Thereby, the selection of the systems could be done not considering the highest resilience (which possibly involve higher costs), but the more suitable operation required by the project.

3. Variations of NFx and IP: In Appendix B, the variation of NFx and IP for several p_{cr} values is shown. It is suggested a possible saturation point, after which efforts to increase repair probability are no longer necessary. These curves could be analyzed under different conditions, and along with the design point proposed in previous item, can compose a robust analysis at design phase.

4. Include the cost in the analysis: Having redundancies in the configuration and investing in some strategies addressed herein can enhance system resilience, but these actions also bring associated costs. Investigations over these costs are important in the design phase and can elucidate the cost benefit from resilience point of view.

5. Resilience prediction models: Some aspects to be considered at design phase, such as power plant scale, type of generation, influence of local context (local disasters frequency, study of components behavior, modification of failure and repair probabilities for actual cases, etc.), among others, can have their influence on resilience investigated and modelled.

BIBLIOGRAPHY

1   RAFIEE, A.; KHALILPOUR, K. R. Renewable hybridization of oil and gas supply chains. In: KHALILPOUR, K. R. (Ed.). **Polygeneration with Polystorage for Chemical and Energy Hubs**. [S.l.]: Academic Press, 2019. p. 331 – 372.

2   KLEMM, C.; VENNEMANN, P. Modeling and optimization of multi-energy systems in mixed-use districts: A review of existing methods and approaches. **Renewable and Sustainable Energy Reviews**, v. 135, p. 110206, 2021.

3   MIKELLIDOU, C. V. et al. Energy critical infrastructures at risk from climate change: A state of the art review. **Safety Science**, v. 110, p. 110–120, 2018.

4   HOSSAIN, N. U. I. et al. A framework for modeling and assessing system resilience using a bayesian network: A case study of an interdependent electrical infrastructure system. **International Journal of Critical Infrastructure Protection**, v. 25, p. 62–83, 2019.

5   BOIN, A.; HART, P. The crisis approach. In: RODRIGUEZ, H.; QUARANTELLI, E. L.; DYNES, R. R. (Ed.). **Handbook of disaster research**. London: Springer, 2007. p. 42–54.

6   UNITED NATIONS OFFICE FOR DISASTER RISK REDUCTION. **Disaster (Terminology)**. [S.l.], 2020. Available: https://www.undrr.org/terminology/disaster. Accessed: 09 oct 2020.

7   BAXTER, P. J. Catastrophes - natural and man-made disasters. In: _____. **Conflict and Catastrophe Medicine: A Practical Guide**. London: Springer, 2002. p. 27–48.

8   CENTRE FOR RESEARCH ON THE EPIDEMIOLOGY OF DISASTERS. **The International Disaster Database**. [S.l.], 2020. Available: https://www.emdat.be. Accessed: 08 oct 2020.

9   GLOBAL CHANGE DATA LAB. **Our World in Data**. [S.l.], 2020. Available: https://ourworldindata.org. Accessed: 08 oct 2020.

10   KEEN, M. M.; FREEMAN, M. P. K.; MANI, M. M. **Dealing with increased risk of natural disasters: challenges and options**. [S.l.]: International Monetary Fund, 2003. v. 2003. 38 p.

11   AHMADALIPOUR, A. et al. Future drought risk in africa: Integrating vulnerability, climate change, and population growth. **Science of the Total Environment**, v. 662, p. 672–686, 2019.

12   WEISÆTH, L.; JR, Ø. K.; TØNNESSEN, A. Technological disasters, crisis management and leadership stress. **Journal of Hazardous Materials**, v. 93, n. 1, p. 33–45, 2002.

13   DESARNAUD, G. Cyber attacks and energy infrastructures: Anticipating risks. 2017. Available: www.ifri.org/sites/default/files/atoms/files/desarnaud_cyber_attacks_energy_infrastructures_2017_2.pdf. Accessed: 08 oct 2020.

14   SHEN, Y.; GU, C.; ZHAO, P. Structural vulnerability assessment of multi-energy system using a pagerank algorithm. **Energy Procedia**, v. 158, p. 6466–6471, 2019.

15   RÜBBELKE, D.; VÖGELE, S. Impacts of climate change on european critical infrastructures: the case of the power sector. **Environmental science & policy**, v. 14, n. 1, p. 53–63, 2011.

16   ZARDASTI, L. et al. Review on the identification of reputation loss indicators in an onshore pipeline explosion event. **Journal of Loss Prevention in the Process Industries**, v. 48, p. 71–86, 2017.

17   ABIMBOLA, M.; KHAN, F. Resilience modeling of engineering systems using dynamic object-oriented bayesian network approach. **Computers & Industrial Engineering**, v. 130, p. 108–118, 2019.

18   BIRESSELIOGLU, M. E.; YUMURTACI, I. O. Evaluating the nature of terrorist attacks on the energy infrastructure: the periodical study for 1970-2011. **International Journal of Oil, Gas and Coal Technology**, v. 10, n. 3, p. 325–341, 2015.

19   BIE, Z. et al. Battling the extreme: A study on the power system resilience. **Proceedings of the IEEE**, v. 105, n. 7, p. 1253–1266, 2017.

20   AMIN, S. B. et al. Solar energy and natural disasters: Exploring household coping mechanisms, capacity, and resilience in bangladesh. **Energy Research & Social Science**, v. 79, p. 102190, 2021.

21   SHANDIZ, S. C. et al. Resilience framework and metrics for energy master planning of communities. **Energy**, p. 117856, 2020.

22   MAHZARNIA, M. et al. A comprehensive assessment of power system resilience to a hurricane using a two-stage analytical approach incorporating risk-based index. **Sustainable Energy Technologies and Assessments**, v. 42, p. 100831, 2020.

23   KOSAI, S.; CRAVIOTO, J. Resilience of standalone hybrid renewable energy systems: The role of storage capacity. **Energy**, v. 196, p. 117133, 2020.

24   MARTIŠAUSKAS, L.; AUGUTIS, J.; KRIKŠTOLAITIS, R. Methodology for energy security assessment considering energy system resilience to disruptions. **Energy strategy reviews**, v. 22, p. 106–118, 2018.

25   BAO, M. et al. Modeling and evaluating nodal resilience of multi-energy systems under windstorms. **Applied Energy**, v. 270, p. 115136, 2020.

26   KAMMOUH, O.; GARDONI, P.; CIMELLARO, G. P. Probabilistic framework to evaluate the resilience of engineering systems using bayesian and dynamic bayesian networks. **Reliability Engineering & System Safety**, v. 198, p. 106813, 2020.

27   PANTELI, M.; MANCARELLA, P. Modeling and evaluating the resilience of critical electrical power infrastructure to extreme weather events. **IEEE Systems Journal**, v. 11, n. 3, p. 1733–1742, 2015.

28   BAGHBANZADEH, D. et al. Resilience improvement of multi-microgrid distribution networks using distributed generation. **Sustainable Energy, Grids and Networks**, v. 27, p. 100503, 2021.

29   EASTON, E.; BERUVIDES, M.; JACKMAN, A. The modulus of resilience for critical subsystems. In: **Operations Management-Emerging Trend in the Digital Era**. London: IntechOpen, 2020.

30   MEHRPOUYAN, H. et al. Resiliency analysis for complex engineered system design. **Artificial Intelligence for Engineering Design, Analysis and Manufacturing**, v. 29, n. 1, p. 93–108, 2015.

31   FANG, Y.; SANSAVINI, G. Optimizing power system investments and resilience against attacks. **Reliability Engineering & System Safety**, v. 159, p. 161–173, 2017.

32   NEZAMODDINI, N.; MOUSAVIAN, S.; EROL-KANTARCI, M. A risk optimization model for enhanced power grid resilience against physical attacks. **Electric Power Systems Research**, v. 143, p. 329–338, 2017.

33   HOLMGREN, Å. J. Using graph models to analyze the vulnerability of electric power networks. **Risk analysis**, v. 26, n. 4, p. 955–969, 2006.

34   LIN, Y.; BIE, Z. Tri-level optimal hardening plan for a resilient distribution system considering reconfiguration and dg islanding. **Applied Energy**, v. 210, p. 1266–1279, 2018.

35   WANG, J. et al. Literature review on modeling and simulation of energy infrastructures from a resilience perspective. **Reliability Engineering & System Safety**, v. 183, p. 360–373, 2019.

36   HUPPERT, H. E.; SPARKS, R. S. J. Extreme natural hazards: population growth, globalization and environmental change. **Philosophical Transactions of the Royal Society A: Mathematical, Physical and Engineering Sciences**, v. 364, n. 1845, p. 1875–1888, 2006.

37   HOYOS, N. et al. Impact of the 2010–2011 la niña phenomenon in colombia, south america: the human toll of an extreme weather event. **Applied Geography**, v. 39, p. 16–25, 2013.

38   SAHANA, V. et al. On the rarity of the 2015 drought in India: A country-wide drought atlas using the multivariate standardized drought index and copula-based severity-duration-frequency curves. **Journal of Hydrology: Regional Studies**, v. 31, p. 100727, 2020.

39   MINATO, N.; MORIMOTO, R. Collaborative management of regional air transport during natural disasters: Case of the 2011 east japan earthquake and tsunami. **Research in Transportation Business & Management**, v. 4, p. 13–21, 2012.

40   SATTERTHWAITE, D. et al. **Words into Action guidelines: Implementation guide for local disaster risk reduction and resilience strategies**. [S.l.]: United Nations Office for Disaster Risk Reduction, 2019. 113 p.

41   CHAI, D.; WANG, M.; LIU, K. Driving factors of natural disasters in belt and road countries. **International Journal of Disaster Risk Reduction**, v. 51, p. 101774, 2020.

42   HOCHRAINER, S.; MECHLER, R. Natural disaster risk in asian megacities: A case for risk pooling? **Cities**, v. 28, n. 1, p. 53–61, 2011.

43   SEIDLER, R. et al. Progress on integrating climate change adaptation and disaster risk reduction for sustainable development pathways in south asia: Evidence from six research projects. **International journal of disaster risk reduction**, v. 31, p. 92–101, 2018.

44   TAVARES, M.; AZEVEDO, A. et al. Influences of solar cycles on earthquakes. **Natural Science**, v. 3, n. 06, p. 436, 2011.

45   PAILOPLEE, S.; CHOOWONG, M. Probabilities of earthquake occurrences in mainland southeast asia. **Arabian Journal of Geosciences**, v. 6, n. 12, p. 4993–5006, 2013.

46   COTTRELL, E. Global distribution of active volcanoes. In: SHRODER, J. F.; PAPALE, P. (Ed.). **Volcanic Hazards, Risks and Disasters**. [S.l.]: Elsevier, 2015. p. 1–16.

47   U.S. GEOLOGICAL SURVEY. **Why are we having so many earthquakes?** [S.l.], 2020. Available: https://www.usgs.gov/faqs/why-are-we-having-so-many-earthquakes-has-naturally-occurring-earthquake-activity-been. Accessed: 19 oct 2020.

48   SIMPSON, D. Triggered earthquakes. **Annual Review of Earth and Planetary Sciences**, v. 14, n. 1, p. 21–42, 1986.

49   MITCHELL, D. **Assessing and responding to land tenure issues in disaster risk management**. [S.l.]: FAO, 2011. 114 p.

50   HIDALGO, J.; BAEZ, A. A. Natural disasters. **Critical care clinics**, v. 35, n. 4, p. 591–607, 2019.

51   SERMET, Y.; DEMIR, I.; MUSTE, M. A serious gaming framework for decision support on hydrological hazards. **Science of The Total Environment**, v. 728, p. 138895, 2020.

52   AHAMED, A.; BOLTEN, J. D. A modis-based automated flood monitoring system for southeast asia. **International journal of applied earth observation and geoinformation**, v. 61, p. 104–117, 2017.

53   MOHANTY, M. P.; MUDGIL, S.; KARMAKAR, S. Flood management in india: A focussed review on the current status and future challenges. **International Journal of Disaster Risk Reduction**, p. 101660, 2020.

54   LIU, Y. et al. Development of a bayesian-copula-based frequency analysis method for hydrological risk assessment–the naryn river in central asia. **Journal of Hydrology**, v. 580, p. 124349, 2020.

55   CHAN, F. K. S. et al. Towards resilient flood risk management for asian coastal cities: Lessons learned from hong kong and singapore. **Journal of Cleaner Production**, v. 187, p. 576–589, 2018.

56   POUR, S. H. et al. Low impact development techniques to mitigate the impacts of climate-change-induced urban floods: current trends, issues and challenges. **Sustainable Cities and Society**, v. 62, p. 102373, 2020.

57   LI, S. et al. Quantitative assessment of the relative impacts of climate change and human activity on flood susceptibility based on a cloud model. **Journal of Hydrology**, v. 588, p. 125051, 2020.

58   LIN, N. et al. Physically based assessment of hurricane surge threat under climate change. **Nature Climate Change**, v. 2, n. 6, p. 462–467, 2012.

59   TU, T. et al. Coupling hydroclimate-hydraulic-sedimentation models to estimate flood inundation and sediment transport during extreme flood events under a changing climate. **Science of The Total Environment**, v. 740, p. 140117, 2020.

60   ANDRADE, L. et al. Surface water flooding, groundwater contamination, and enteric disease in developed countries: A scoping review of connections and consequences. **Environmental pollution**, v. 236, p. 540–549, 2018.

61   THAPA, S. et al. Catchment-scale flood hazard mapping and flood vulnerability analysis of residential buildings: The case of khando river in eastern nepal. **Journal of Hydrology: Regional Studies**, v. 30, p. 100704, 2020.

62   LIANG, S. Y.; MESSENGER, N. Infectious diseases after hydrologic disasters. **Emergency Medicine Clinics**, v. 36, n. 4, p. 835–851, 2018.

63   OLORUNFEMI, I. E. et al. A gis-based assessment of the potential soil erosion and flood hazard zones in ekiti state, southwestern nigeria using integrated rusle and hand models. **CATENA**, v. 194, p. 104725, 2020.

64   NOFAL, O.; LINDT, J. W.; DO, T. Q. Multi-variate and single-variable flood fragility and loss approaches for wood frame buildings. **Reliability Engineering & System Safety**, v. 202, p. 106971, 2020.

65   MEEHL, G. A. et al. Global climate projections. In: ____. **Climate Change**. London: Cambridge, UK, Cambridge University Press, 2007. p. 1009.

66   NORDHAUS, W. D. The economics of hurricanes and implications of global warming. **Climate Change Economics**, v. 1, n. 01, p. 1–20, 2010.

67   PUGATCH, T. Tropical storms and mortality under climate change. **World Development**, v. 117, p. 172–182, 2019.

68   AUMANN, H. H.; RUZMAIKIN, A.; TEIXEIRA, J. Frequency of severe storms and global warming. **Geophysical Research Letters**, v. 35, n. 19, 2008.

69   TAMARIN-BRODSKY, T.; KASPI, Y. Enhanced poleward propagation of storms under climate change. **Nature geoscience**, v. 10, n. 12, p. 908–913, 2017.

70   MENDELSOHN, R. et al. The impact of climate change on global tropical cyclone damage. **Nature climate change**, v. 2, n. 3, p. 205–209, 2012.

71   RÄDLER, A. T. et al. Frequency of severe thunderstorms across europe expected to increase in the 21st century due to rising instability. **Climate and Atmospheric Science**, v. 2, n. 1, p. 1–5, 2019.

72   TACHIIRI, K.; SHINODA, M. Quantitative risk assessment for future meteorological disasters. **Climatic Change**, v. 113, n. 3-4, p. 867–882, 2012.

73   LUCA, A. D. et al. Contribution of mean climate to hot temperature extremes for present and future climates. **Weather and Climate Extremes**, p. 100255, 2020.

74   GRANGER, K.; SMITH, D. Storm tide impact and consequence modelling: Some preliminary observations. **Mathematical and computer modelling**, v. 21, n. 9, p. 15–21, 1995.

75   LIU, Q. et al. Risk assessment of storm surge disaster based on numerical models and remote sensing. **International journal of applied earth observation and geoinformation**, v. 68, p. 20–30, 2018.

76   IONITA, M. et al. The european 2015 drought from a climatological perspective. **Hydrology and Earth System Sciences**, v. 21, p. 1397–1419, 2017.

77   BRANDO, P. M. et al. Droughts, wildfires, and forest carbon cycling: A pantropical synthesis. **Annual Review of Earth and Planetary Sciences**, v. 47, p. 555–581, 2019.

78   WANDERS, N.; WADA, Y. Human and climate impacts on the 21st century hydrological drought. **Journal of Hydrology**, v. 526, p. 208–220, 2015.

79   MISHRA, A. K.; SINGH, V. P. A review of drought concepts. **Journal of hydrology**, v. 391, n. 1-2, p. 202–216, 2010.

80   FAVA, F.; VRIELING, A. Earth observation for drought risk financing in pastoral systems of sub-saharan africa. **Current Opinion in Environmental Sustainability**, v. 48, p. 44–52, 2021.

81   WEHNER, M. et al. Droughts, floods, and wildfires. In: ____. **Climate science special report: foruth national climate assessment**. London: U.S. Global Change Research Program, 2017. v. 1, p. 470.

82   KNORR, W. et al. Wildfire air pollution hazard during the 21st century. **Atmospheric Chemistry and Physics**, v. 17, n. 14, p. 9223, 2017.

83   PIÑOL, J.; TERRADAS, J.; LLORET, F. Climate warming, wildfire hazard, and wildfire occurrence in coastal eastern spain. **Climatic change**, v. 38, n. 3, p. 345–357, 1998.

84 RICCIARDI, A.; PALMER, M. E.; YAN, N. D. Should biological invasions be managed as natural disasters? **BioScience**, v. 61, n. 4, p. 312–317, 2011.

85 HAO, L.; YANG, L.-Z.; GAO, J.-M. The application of information diffusion technique in probabilistic analysis to grassland biological disasters risk. **Ecological modelling**, v. 272, p. 264–270, 2014.

86 KARLSSON, M.; NILSSON, T.; PICHLER, S. The impact of the 1918 spanish flu epidemic on economic performance in sweden: An investigation into the consequences of an extraordinary mortality shock. **Journal of health economics**, v. 36, p. 1–19, 2014.

87 JESTER, B. et al. Historical and clinical aspects of the 1918 h1n1 pandemic in the united states. **Virology**, v. 527, p. 32–37, 2019.

88 ALONSO, W. J. et al. We could learn much more from 1918 pandemic—the (mis) fortune of research relying on original death certificates. **Annals of epidemiology**, v. 28, n. 5, p. 289–292, 2018.

89 ALWIDYAN, M. T.; TRAINOR, J. E.; BISSELL, R. A. Responding to natural disasters vs. disease outbreaks: Do emergency medical service providers have different views? **International journal of disaster risk reduction**, v. 44, p. 101440, 2020.

90 CHAN, D. W.-K. A reflection on the anti-epidemic response of covid-19 from the perspective of disaster management. **International journal of nursing sciences**, v. 7, n. 3, p. 382–385, 2020.

91 COX, P. Potential for using semiochemicals to protect stored products from insect infestation. **Journal of Stored Products Research**, v. 40, n. 1, p. 1–25, 2004.

92 TANAKA, F.; MAGARIYAMA, Y.; MIYANOSHITA, A. Volatile biomarkers for early-stage detection of insect-infested brown rice: Isopentenols and polysulfides. **Food chemistry**, v. 303, p. 125381, 2020.

93 JAMSHIDI, B. Ability of near-infrared spectroscopy for non-destructive detection of internal insect infestation in fruits: Meta-analysis of spectral ranges and optical measurement modes. **Spectrochimica Acta Part A: Molecular and Biomolecular Spectroscopy**, v. 225, p. 117479, 2020.

94 DUKES, J. S. et al. Responses of insect pests, pathogens, and invasive plant species to climate change in the forests of northeastern north america: What can we predict? **Canadian journal of forest research**, v. 39, n. 2, p. 231–248, 2009.

95 REDUCTION, U. O. for D. R. **Words into Action Guidelines: Implementation Guide for Man-made and Technological Hazards**. [S.l.], 2018. Available: https://unece.org/environment-policy/publications/words-action-guidelines-implementation-guide-man-made-and. Accessed: 08 oct 2020.

96 AL-DAHASHA, H.; KULATUNGA, U. Challenges facing the controlling stage of the disaster response management resulting from war operations and terrorism in iraq. **Procedia Engineering**, v. 212, p. 863–870, 2018.

97 TOLEDO, T. et al. Analysis of evacuation behavior in a wildfire event. **International journal of disaster risk reduction**, v. 31, p. 1366–1373, 2018.

98 AZHAR, A.; MALIK, M. N.; MUZAFFAR, A. Social network analysis of army public school shootings: Need for a unified man-made disaster management in pakistan. **International journal of disaster risk reduction**, v. 34, p. 255–264, 2019.

99   MASOOD, A. et al. Surveying pervasive public safety communication technologies in the context of terrorist attacks. **Physical Communication**, v. 41, p. 101109, 2020.

100   HODGKINSON, P. E. Psychological after-effects of transportation disaster. **Medicine, Science and the Law**, v. 28, n. 4, p. 304–309, 1988.

101   SHALUF, I. M.; AHMADUN, F.; SHARIFF, A. R. Technological disaster factors. **Journal of Loss Prevention in the Process Industries**, v. 16, n. 6, p. 513–521, 2003.

102   SCHOOLER, T. Disasters, coping with. In: SMELSER, N. J.; BALTES, P. B. (Ed.). **International Encyclopedia of the Social and Behavioral Sciences**. Oxford: Pergamon, 2001. p. 3713 – 3718.

103   YULE, W.; UDWIN, O.; BOLTON, D. Mass transportation disasters. In: GRECA, A. et al. (Ed.). **Helping children cope with disasters and terrorism**. London: American Psychological Association, 2002. p. 223–239.

104   LU, H.; CHEN, M.; KUANG, W. The impacts of abnormal weather and natural disasters on transport and strategies for enhancing ability for disaster prevention and mitigation. **Transport Policy**, v. 98, p. 2 – 9, 2020.

105   BANG, H.; MILES, L.; GORDON, R. Challenges in managing technological disasters in Cameroon: Case study of Cameroon's worst train Crash—the Eséka train disaster. **International journal of disaster risk reduction**, v. 44, p. 101410, 2020.

106   COVA, T. J.; CONGER, S. Transportation hazards. In: KUTZ, M. (Ed.). **Transportation Engineers Handbook**. New York: McGraw Hill, 2004. p. 17.1–17.24.

107   STECKE, K. E.; KUMAR, S. Sources of supply chain disruptions, factors that breed vulnerability, and mitigating strategies. **Journal of Marketing Channels**, v. 16, n. 3, p. 193–226, 2009.

108   REIS, J. et al. Accident scenarios modelling with hazardous materials in transportation infrastructures. **Proceedings of the Institution of Civil Engineers-Forensic Engineering**, v. 172, n. 4, p. 1–12, 2020.

109   RAJEEV, K. et al. Human vulnerability mapping of chemical accidents in major industrial units in Kerala, India for better disaster mitigation. **International journal of disaster risk reduction**, v. 39, p. 101247, 2019.

110   YANG, M.; KHAN, F.; AMYOTTE, P. Operational risk assessment: A case of the bhopal disaster. **Process Safety and Environmental Protection**, v. 97, p. 70–79, 2015.

111   VARMA, R.; VARMA, D. R. The bhopal disaster of 1984. **Bulletin of Science, Technology & Society**, v. 25, n. 1, p. 37–45, 2005.

112   PEK, S.; OH, C. H.; RIVERA, J. Mnc foreign investment and industrial disasters: The moderating role of technological, safety management, and philanthropic capabilities. **Strategic Management Journal**, v. 39, n. 2, p. 502–526, 2018.

113   KIM, S.; LEE, J.; KANG, C. Analysis of industrial accidents causing through jamming or crushing accidental deaths in the manufacturing industry in south korea: Focus on non-routine work on machinery. **Safety Science**, v. 133, p. 104998, 2021.

114 APOSTOLAKIS, G. E.; LEMON, D. M. A screening methodology for the identification and ranking of infrastructure vulnerabilities due to terrorism. **Risk Analysis: An International Journal**, v. 25, n. 2, p. 361–376, 2005.

115 PURSIAINEN, C. Critical infrastructure resilience: A nordic model in the making? **International journal of disaster risk reduction**, v. 27, p. 632–641, 2018.

116 TICHỲ, L. Energy infrastructure as a target of terrorist attacks from the islamic state in iraq and syria. **International Journal of Critical Infrastructure Protection**, v. 25, p. 1–13, 2019.

117 LANDUCCI, G.; KHAKZAD, N.; RENIERS, G. History of terrorist attacks to critical infrastructures involving hazardous materials. In: LANDUCCI, G.; KHAKZAD, N.; RENIERS, G. (Ed.). **Physical Security in the Process Industry**. London: Elsevier, 2020. p. 17 – 30.

118 MATSIKA, E. et al. Development of risk assessment specifications for analysing terrorist attacks vulnerability on metro and light rail systems. **Transportation research procedia**, v. 14, p. 1345–1354, 2016.

119 RODOFILE, N. R.; RADKE, K.; FOO, E. Extending the cyber-attack landscape for scada-based critical infrastructure. **International Journal of Critical Infrastructure Protection**, v. 25, p. 14–35, 2019.

120 ZHU, B.; JOSEPH, A.; SASTRY, S. A taxonomy of cyber attacks on scada systems. In: **International conference on internet of things and 4th international conference on cyber, physical and social computing**. London: IEEE, 2011. p. 380–388.

121 SÁNDOR, H. et al. Cyber attack detection and mitigation: Software defined survivable industrial control systems. **International Journal of Critical Infrastructure Protection**, v. 25, p. 152–168, 2019.

122 KOBAYASHI, A. Geographies of peace and armed conflict: Introduction. **Annals of the Association of American Geographers**, v. 99, n. 5, p. 819–826, 2009.

123 XU, J. et al. Natural disasters and social conflict: a systematic literature review. **International journal of disaster risk reduction**, v. 17, p. 38–48, 2016.

124 MAGGIO, G.; CACCIOLA, G. When will oil, natural gas, and coal peak? **Fuel**, v. 98, p. 111–123, 2012.

125 International Energy Agency. **Data and statistics**. [S.l.], 2020. Available: www.iea.org/data-and-statistics. Accessed: 26 oct 2020.

126 RIVAZ, A.; ANIJDAN, S. M.; MOAZAMI-GOUDARZI, M. Failure analysis and damage causes of a steam turbine blade of 410 martensitic stainless steel after 165000 hours of working. **Engineering Failure Analysis**, v. 113, p. 104557, 2020.

127 United States Environmental Protection Agency. **Catalog of CHP technologies**. [S.l.], 2017. Available: https://www.epa.gov/sites/production/files/2015-07/documents/catalog_of_chp_technologies.pdf. Accessed: 26 oct 2020.

128 SILVA, F. S. da; MATELLI, J. A. Exergoeconomic analysis and determination of power cost in mcfc–steam turbine combined cycle. **International Journal of Hydrogen Energy**, v. 44, n. 33, p. 18293–18307, 2019.

129   MEHRPOOYA, M. et al. Optimal design of molten carbonate fuel cell combined cycle power plant and thermophotovoltaic system. **Energy Conversion and Management**, v. 221, p. 113177, 2020.

130   MATELLI, J. A.; GOEBEL, K. Conceptual design of cogeneration plants under a resilient design perspective: Resilience metrics and case study. **Applied Energy**, v. 215, p. 736–750, 2018.

131   VIALETTO, G.; NORO, M. An innovative approach to design cogeneration systems based on big data analysis and use of clustering methods. **Energy Conversion and Management**, v. 214, p. 112901, 2020.

132   COPPITTERS, D. et al. Techno-economic feasibility study of a solar-powered distributed cogeneration system producing power and distillate water: Sensitivity and exergy analysis. **Renewable Energy**, v. 150, p. 1089–1097, 2020.

133   TOFFOLO, A.; LAZZARETTO, A. A practical tool to generate complex energy system configurations based on the synthsep methodology. **International Journal of Thermodynamics**, v. 22, n. 1, 2019.

134   TOFFOLO, A.; RECH, S.; LAZZARETTO, A. Generation of complex energy systems by combination of elementary processes. **Journal of Energy Resources Technology**, v. 140, n. 11, p. 112005, 2018.

135   SEKI, K.; TAKESHITA, K.; AMANO, Y. Development of complex energy systems with absorption technology by combining elementary processes. **Energies**, v. 12, n. 3, p. 495, 2019.

136   RIVERA-ALVAREZ, A. et al. Comparative analysis of natural gas cogeneration incentives on electricity production in latin america. **Energy Policy**, v. 142, p. 111466, 2020.

137   RODRÍGUEZ, H. et al. **Handbook of disaster research**. London: Springer, 2007. 662 p.

138   KUTZ, M. **Mechanical Engineers' Handbook: energy and power**. New York: John Wiley & Sons, 2005. 3600 p.

139   KRÄTSCHMER, D. et al. Proof of fatigue strength of nuclear components part ii: Numerical fatigue analysis for transient stratification loading considering environmental effects. **International journal of pressure vessels and piping**, v. 92, p. 1–10, 2012.

140   GIAMPAOLO, T. **Gas turbine handbook: principles and practices**. New York: Fairmount Press, 2009. 475 p.

141   KANG, C. et al. Deposition of solid particles exposed to the suction of dual pumps in the tank of a pumping station. **Powder Technology**, v. 361, p. 727–738, 2020.

142   LANZUTTI, A. et al. Failure analysis of a safety equipment exposed to eaf environment. **Engineering Failure Analysis**, v. 95, p. 107–116, 2019.

143   SENGODAN, G. A.; ALLEGRI, G.; HALLETT, S. R. Simulation of progressive failure in laminated composites under variable environmental conditions. **Materials & Design**, v. 196, p. 109082, 2020.

144   TRETHEWEY, M. W. et al. A spectral simulation approach to evaluate probabilistic measurement precision of a reactor coolant pump torsional vibration shaft crack monitoring system. **Journal of sound and vibration**, v. 310, p. 1036–1056, 2008.

145   RODRÍGUEZ, J. et al. Fatigue of steam turbine blades at resonance conditions. **Engineering Failure Analysis**, v. 104, p. 39–46, 2019.

146   SALEHNASAB, B.; POURSAEIDI, E. Mechanism and modeling of fatigue crack initiation and propagation in the directionally solidified cm186 lc blade of a gas turbine engine. **Engineering Fracture Mechanics**, v. 225, p. 106842, 2020.

147   FARSI, H.; FANIAN, A.; TAGHIYARRENANI, Z. A novel online state-based anomaly detection system for process control networks. **International Journal of Critical Infrastructure Protection**, v. 27, p. 100323, 2019.

148   ZHANG, G.-W. et al. Regional changes in extreme heat events in china under stabilized 1.5° c and 2.0° c global warming. **Advances in Climate Change Research**, v. 11, n. 3, p. 198–209, 2020.

149   BOYCE, M. P. **Handbook for cogeneration and combined cycle power plants**. London: Amer Society of Mechanical, 2010. 776 p.

150   CROWTHER, K. G. Risk-informed assessment of regional preparedness: A case study of emergency potable water for hurricane response in southeast virginia. **International Journal of Critical Infrastructure Protection**, v. 3, n. 2, p. 83–98, 2010.

151   ZHOU, L. et al. Emergency decision making for natural disasters: An overview. **International journal of disaster risk reduction**, v. 27, p. 567–576, 2018.

152   KHAN, A.; GUPTA, S.; GUPTA, S. K. Multi-hazard disaster studies: Monitoring, detection, recovery, and management, based on emerging technologies and optimal techniques. **International Journal of Disaster Risk Reduction**, v. 47, p. 101642, 2020.

153   STEWART, M. G. Risk-informed decision support for assessing the costs and benefits of counter-terrorism protective measures for infrastructure. **International Journal of Critical Infrastructure Protection**, v. 3, n. 1, p. 29–40, 2010.

154   HAN, C.-H.; PARK, S.-T.; LEE, S.-J. The enhanced security control model for critical infrastructures with the blocking prioritization process to cyber threats in power system. **International Journal of Critical Infrastructure Protection**, v. 26, p. 100312, 2019.

155   SATISHKUMAR, K.; RATHNAM, E. V.; SRIDHAR, V. Tracking seasonal and monthly drought with GRACE-based terrestrial water storage assessments over Major River basins in South India. **Science of The Total Environment**, v. 763, p. 142994, 2020.

156   MUSTAFA, D.; MCCARTHY, J. Terrorism. In: KOBAYASHI, A. (Ed.). **International Encyclopedia of Human Geography**. Second edition. Oxford: Elsevier, 2020. p. 233 – 238.

157   ARSHAD, A. et al. Vulnerability assessment of urban expansion and modelling green spaces to build heat waves risk resiliency in karachi. **International journal of disaster risk reduction**, v. 46, p. 101468, 2020.

158   YIN, S.-Y. et al. Mid-summer surface air temperature and its internal variability over china at 1.5° c and 2° c global warming. **Advances in Climate Change Research**, v. 11, p. 185–197, 2020.

159   FEARNSIDE, P. M. Uncertainty in land-use change and forestry sector mitigation options for global warming: Plantation silviculture versus avoided deforestation. **Biomass and Bioenergy**, v. 18, n. 6, p. 457–468, 2000.

160   United Nations Framework Convention on Climate Change. **Adoption of the Paris agreement: proposal by the President**. [S.l.], 2015. Available: https://unfccc.int/resource/docs/2015/cop21/eng/l09r01.pdf. Accessed: 08 oct 2020.

161   MAO, Q.; LI, N.; PEÑA-MORA, F. Quality function deployment-based framework for improving the resilience of critical infrastructure systems. **International Journal of Critical Infrastructure Protection**, v. 26, p. 100304, 2019.

162   THURSTON, R. H. On the strength, elasticity, ductility and resilience of materials of machine construction. **Journal of the Franklin Institute**, v. 97, n. 4, p. 273–292, 1874.

163   HOLLING, C. S. Resilience and stability of ecological systems. **Annual review of ecology and systematics**, v. 4, n. 1, p. 1–23, 1973.

164   BARRIOS, R. E. Resilience: A commentary from the vantage point of anthropology. **Annals of Anthropological Practice**, v. 40, n. 1, p. 28–38, 2016.

165   RUTTER, M. Resilience: some conceptual considerations. **Journal of adolescent health**, v. 14, n. 8, p. 626–631, 1993.

166   MEEROW, S.; NEWELL, J. P.; STULTS, M. Defining urban resilience: A review. **Landscape and urban planning**, v. 147, p. 38–49, 2016.

167   CONZ, E.; LAMB, P. W.; MASSIS, A. D. Practicing resilience in family firms: An investigation through phenomenography. **Journal of Family Business Strategy**, v. 11, n. 2, p. 100355, 2020.

168   RANA, I. A. Disaster and climate change resilience: A bibliometric analysis. **International Journal of Disaster Risk Reduction**, v. 50, p. 101839, 2020.

169   ZENG, Z. et al. A markov reward process-based framework for resilience analysis of multistate energy systems under the threat of extreme events. **Reliability Engineering & System Safety**, v. 209, p. 107443, 2021.

170   HAIMES, Y. Y. On the definition of resilience in systems. **Risk Analysis: An International Journal**, v. 29, n. 4, p. 498–501, 2009.

171   AZZUNI, A.; BREYER, C. Definitions and dimensions of energy security: a literature review. **Wiley Interdisciplinary Reviews: Energy and Environment**, v. 7, n. 1, p. 268, 2018.

172   FRANCIS, R.; BEKERA, B. A metric and frameworks for resilience analysis of engineered and infrastructure systems. **Reliability Engineering & System Safety**, v. 121, p. 90–103, 2014.

173   Risk Steering Committee. **DHS risk lexicon**. [S.l.], 2010. Available: https://www.cisa.gov/sites/default/files/publications/dhs-risk-lexicon-2010_0.pdf. Accessed: 08 oct 2020.

174   BERKELEY, A. R.; WALLACE, M.; COO, C. **A framework for establishing critical infrastructure resilience goals**. [S.l.], 2010. Available: https://www.dhs.gov/xlibrary/assets/niac/niac-a-framework-for-establishing-critical-infrastructure-resilience-goals-2010-10-19.pdf. Accessed: 08 oct 2020.

175   ECK, N. J. V.; WALTMAN, L. Software survey: Vosviewer, a computer program for bibliometric mapping. **Scientometrics**, v. 84, n. 2, p. 523–538, 2010.

176   GUERRERO-BOTE, V. P.; MOYA-ANEGÓN, F. A further step forward in measuring journals' scientific prestige: The sjr2 indicator. **Journal of informetrics**, v. 6, n. 4, p. 674–688, 2012.

177 RAJE, D.; MUJUMDAR, P. Reservoir performance under uncertainty in hydrologic impacts of climate change. **Advances in water resources**, v. 33, n. 3, p. 312–326, 2010.

178 SCANLON, B. R.; DUNCAN, I.; REEDY, R. C. Drought and the water–energy nexus in texas. **Environmental Research Letters**, v. 8, n. 4, p. 045033, 2013.

179 TOBIN, I. et al. Vulnerabilities and resilience of european power generation to 1.5 c, 2 c and 3 c warming. **Environmental Research Letters**, v. 13, n. 4, p. 044024, 2018.

180 HELDER, M. et al. Resilience of roof-top plant-microbial fuel cells during dutch winter. **Biomass and Bioenergy**, v. 51, p. 1–7, 2013.

181 ZHANG, Y. et al. Resilience assessment of multi-decision complex energy interconnection system. **International Journal of Electrical Power & Energy Systems**, v. 137, p. 107809, 2022.

182 WANG, J. et al. Integrated assessment for solar-assisted carbon capture and storage power plant by adopting resilience thinking on energy system. **Journal of Cleaner Production**, v. 208, p. 1009–1021, 2019.

183 ARABZADEH, V. et al. Deep decarbonization of urban energy systems through renewable energy and sector-coupling flexibility strategies. **Journal of Environmental Management**, v. 260, p. 110090, 2020.

184 JASIŪNAS, J.; LUND, P. D.; MIKKOLA, J. Energy system resilience–a review. **Renewable and Sustainable Energy Reviews**, v. 150, p. 111476, 2021.

185 THEODORIDIS, S. Monte carlo methods. In: THEODORIDIS, S. (Ed.). **Machine Learning: a Bayesian and optimization perspective**. Second edition. London: Academic Press, 2020. p. 731–769.

186 LI, W. et al. **Reliability assessment of electric power systems using Monte Carlo methods**. [S.l.]: Springer Science & Business Media, 2013.

187 Jet Brains. **Pycharm: The professional IDE for Professional Developers**. [S.l.], 2020. Available: https://www.jetbrains.com/pycharm/. Accessed: 17 nov 2020.

188 SILVA, F. S. da; MATELLI, J. A. Script for resilience analysis in energy systems: Python programming code and partial associated data of four cogeneration plants. **Data in Brief**, v. 36, p. 106986, 2021.

189 Python Software Foundation. **CSV File Reading and Writing**. [S.l.], 2021. Available: https://docs.python.org/3/library/csv.html. Accessed: 30 aug 2021.

190 The NumPy Community. **What is NumPy?** [S.l.], 2021. Available: https://numpy.org/doc/stable/user/whatisnumpy.html. Accessed: 30 aug 2021.

191 Python Software Foundation. **Miscellaneous operating system interfaces**. [S.l.], 2021. Available: https://docs.python.org/3/library/os.html. Accessed: 30 aug 2021.

192 Python Software Foundation. **Time access and conversions**. [S.l.], 2021. Available: https://docs.python.org/3/library/time.html. Accessed: 30 aug 2021.

193 Python Software Foundation. **Sound-playing interface for Windows**. [S.l.], 2021. Available: https://docs.python.org/3/library/winsound.html. Accessed: 30 aug 2021.

194 SILVA, F. S. da; MATELLI, J. A. Resilience in cogeneration systems: Metrics for evaluation and influence of design aspects. **Reliability Engineering & System Safety**, v. 212, p. 107444, 2021.

195   WU, S. Two methods to approximate the superposition of imperfect failure processes. **Reliability Engineering & System Safety**, v. 207, p. 107332, 2021.

196   LIM, J.-H.; LU, K.-L.; PARK, D. H. Bayesian imperfect repair model. **Communications in Statistics-Theory and Methods**, v. 27, n. 4, p. 965–984, 1998.

197   LIM, J.; QU, J.; ZUO, M. J. Age replacement policy based on imperfect repair with random probability. **Reliability Engineering & System Safety**, v. 149, p. 24–33, 2016.

198   ARIF, A. et al. Power distribution system outage management with co-optimization of repairs, reconfiguration, and dg dispatch. **IEEE Transactions on Smart Grid**, v. 9, n. 5, p. 4109–4118, 2017.

199   OSSAI, C. I. Remaining useful life estimation for repairable multi-state components subjected to multiple maintenance actions. **Reliability Engineering & System Safety**, v. 182, p. 142–151, 2019.

200   SRIVATHSAN, S.; VISWANATHAN, S. A queueing-based optimization model for planning inventory of repaired components in a service center. **Computers & Industrial Engineering**, v. 106, p. 373–385, 2017.

201   MARSEGUERRA, M.; ZIO, E. Optimizing maintenance and repair policies via a combination of genetic algorithms and monte carlo simulation. **Reliability Engineering & System Safety**, v. 68, n. 1, p. 69–83, 2000.

202   SILVA, J. C. D.; MATELLI, J. A.; BAZZO, E. Development of a knowledge-based system for cogeneration plant design: Verification, validation and lessons learned. **Knowledge-Based Systems**, v. 67, p. 230–243, 2014.

203   WATSON, J.-P. et al. **Conceptual framework for developing resilience metrics for the electricity oil and gas sectors in the United States**. [S.l.], 2015. Available: https://www.energy.gov/sites/default/files/2015/09/f26/EnergyResilienceReport_%28Final%29_SAND2015-18019.pdf. Accessed: 08 oct 2020.

204   LI, W. Elements of monte carlo simulation. In: **Risk assessment of power systems: models, methods, and applications**. London: John Wiley & Sons, 2014. p. 489 – 495.

205   IKONEN, T. J. et al. Large-scale selective maintenance optimization using bathtub-shaped failure rates. **Computers & Chemical Engineering**, v. 139, p. 106876, 2020.

206   GUO, H.; ZHAO, X.; CHEN, W. Analysis of time-dependent failure rate and probability of nuclear component. **Annals of Nuclear Energy**, v. 122, p. 137–145, 2018.

207   OriginLab. **Origin and OriginPro**. [S.l.], 2021. Available: https://www.originlab.com/index.aspx?go=PRODUCTS/Origin. Accessed: 30 aug 2021.

APPENDIX A – GRAPHICAL ANALYSIS SIMULATION CODES

```python
import csv
import time
from numpy import random
import os
import winsound

#entrada de dados
try:
    VidaUtil = (int(input('Informe o número de anos de operação:')) * 8760)
    NumeroSimulacoes = int(input('Informe o número de simulações: '))
except:
    print('Os dados foram informados de maneira incorreta, por favor tente
novamente e informe o valor das variáveis'
          'com dígitos no formato inteiro')

#tempo inicial
tempo_inicial = time.time()

#SISTEMAS#
#Sistema 1
sistema1 = {'EstadoOperacional' : 'normal', 'QuantidadeComponentes' : 21,
'ComponentesFalhados' : 0, 'ComponentesReparando' : 0,
'ComponentesEletricidade' : 2, 'ComponentesTermica' : 2, 'PotenciaTotal':
4074.5, 'PotenciaAtual': 4074.5, 'funcionando': 1}
componente11 = {'ID' : 1, 'Tipo' : 'gerador', 'Afeta' : [2,17],
'Redundante' : [16], 'EAfetadoPor' : [2,17], 'EstadoOperacional' :
'normal', 'Funcao' : 'eletricidade', 'Potência' : 2100, 'Reparando' :
'não', 'MediaReparo' : 80, 'TempoReparo' : 0, 'TempoGasto' : 0}
componente21 = {'ID' : 2, 'Tipo' : 'motor', 'Afeta' : [1,3,4,5,6],
'Redundante' : [], 'EAfetadoPor' : [1,3,4,5,6,17,20], 'EstadoOperacional' :
'normal', 'Funcao' : 'nenhuma', 'Potência' : 0, 'Reparando' : 'não',
'MediaReparo' : 100, 'TempoReparo' : 0, 'TempoGasto' : 0}
componente31 = {'ID' : 3, 'Tipo' : 'bomba', 'Afeta' : [2,5,6], 'Redundante'
: [4], 'EAfetadoPor' : [2,5,6,17], 'EstadoOperacional' : 'normal', 'Funcao'
: 'nenhuma', 'Potência' : 0, 'Reparando' : 'não', 'MediaReparo' : 40,
'TempoReparo' : 0, 'TempoGasto' : 0}
componente41 = {'ID' : 4, 'Tipo' : 'bomba', 'Afeta' : [2,5,6], 'Redundante'
: [3], 'EAfetadoPor' : [2,5,6,17], 'EstadoOperacional' : 'normal', 'Funcao'
: 'nenhuma', 'Potência' : 0, 'Reparando' : 'não', 'MediaReparo' : 40,
'TempoReparo' : 0, 'TempoGasto' : 0}
componente51 = {'ID' : 5, 'Tipo' : 'radiador', 'Afeta' : [2,3,4],
'Redundante' : [6], 'EAfetadoPor' : [2,3,4,17], 'EstadoOperacional' :
'normal', 'Funcao' : 'nenhuma', 'Potência' : 0, 'Reparando' : 'não',
'MediaReparo' : 60, 'TempoReparo' : 0, 'TempoGasto' : 0}
componente61 = {'ID' : 6, 'Tipo' : 'trocador de calor', 'Afeta' :
[2,3,4,7,8,9], 'Redundante' : [5], 'EAfetadoPor' : [2,3,4,7,8,9],
'EstadoOperacional' : 'normal', 'Funcao' : 'nenhuma', 'Potência' : 0,
'Reparando' : 'não', 'MediaReparo' : 60, 'TempoReparo' : 0, 'TempoGasto' :
0}
componente71 = {'ID' : 7, 'Tipo' : 'bomba', 'Afeta' : [6,9], 'Redundante' :
[8], 'EAfetadoPor' : [6,9,17], 'EstadoOperacional' : 'normal', 'Funcao' :
'nenhuma', 'Potência' : 0, 'Reparando' : 'não', 'MediaReparo' : 40,
'TempoReparo' : 0, 'TempoGasto' : 0}
componente81 = {'ID' : 8, 'Tipo' : 'bomba', 'Afeta' : [6,9], 'Redundante' :
[7], 'EAfetadoPor' : [6,9,17], 'EstadoOperacional' : 'normal', 'Funcao' :
'nenhuma', 'Potência' : 0, 'Reparando' : 'não', 'MediaReparo' : 40,
'TempoReparo' : 0, 'TempoGasto' : 0}
componente91 = {'ID' : 9, 'Tipo' : 'chiller', 'Afeta' :
[6,7,8,11,12,13,14,15,19], 'Redundante' : [10], 'EAfetadoPor' :
[6,7,8,11,12,13,14,15,17,19], 'EstadoOperacional' : 'normal', 'Funcao' :
'calor', 'Potência' : 567.7, 'Reparando' : 'não', 'MediaReparo' : 60,
```

```python
'TempoReparo' : 0, 'TempoGasto' : 0}
componente101 = {'ID' : 10, 'Tipo' : 'chiller', 'Afeta' :
[11,12,13,14,15,19], 'Redundante' : [9], 'EAfetadoPor' :
[11,12,13,14,15,17,19], 'EstadoOperacional' : 'normal', 'Funcao' : 'calor',
'Potência' : 1406.8, 'Reparando' : 'não', 'MediaReparo' : 60, 'TempoReparo'
: 0, 'TempoGasto' : 0}
componente111 = {'ID' : 11, 'Tipo' : 'bomba', 'Afeta' : [9,10,19],
'Redundante' : [12], 'EAfetadoPor' : [9,10,17,19], 'EstadoOperacional' :
'normal', 'Funcao' : 'nenhuma', 'Potência' : 0, 'Reparando' : 'não',
'MediaReparo' : 40, 'TempoReparo' : 0, 'TempoGasto' : 0}
componente121 = {'ID' : 12, 'Tipo' : 'bomba', 'Afeta' : [9,10,19],
'Redundante' : [11], 'EAfetadoPor' : [9,10,17,19], 'EstadoOperacional' :
'normal', 'Funcao' : 'nenhuma', 'Potência' : 0, 'Reparando' : 'não',
'MediaReparo' : 40, 'TempoReparo' : 0, 'TempoGasto' : 0}
componente131 = {'ID' : 13, 'Tipo' : 'torre de resfriamento', 'Afeta' :
[9,10,14,15], 'Redundante' : [9,10,14,15,17,21], 'EAfetadoPor' :
[9,10,14,15,17,21], 'EstadoOperacional' : 'normal', 'Funcao' : 'nenhuma',
'Potência' : 0, 'Reparando' : 'não', 'MediaReparo' : 60, 'TempoReparo' : 0,
'TempoGasto' : 0}
componente141 = {'ID' : 14, 'Tipo' : 'bomba', 'Afeta' : [9,10,13],
'Redundante' : [15], 'EAfetadoPor' : [9,10,13,17], 'EstadoOperacional' :
'normal', 'Funcao' : 'nenhuma', 'Potência' : 0, 'Reparando' : 'não',
'MediaReparo' : 40, 'TempoReparo' : 0, 'TempoGasto' : 0}
componente151 = {'ID' : 15, 'Tipo' : 'bomba', 'Afeta' : [9,10,13],
'Redundante' : [14], 'EAfetadoPor' : [9,10,13,17], 'EstadoOperacional' :
'normal', 'Funcao' : 'nenhuma', 'Potência' : 0, 'Reparando' : 'não',
'MediaReparo' : 40, 'TempoReparo' : 0, 'TempoGasto' : 0}
componente161 = {'ID' : 16, 'Tipo' : 'grid', 'Afeta' : [17], 'Redundante' :
[1], 'EAfetadoPor' : [17], 'EstadoOperacional' : 'normal', 'Funcao' :
'eletricidade', 'Potência' : 0, 'Reparando' : 'não', 'MediaReparo' : 40,
'TempoReparo' : 0, 'TempoGasto' : 0}
componente171 = {'ID' : 17, 'Tipo' : 'bus', 'Afeta' :
[1,2,3,4,5,7,8,9,10,11,12,13,14,15,16,17,18,19], 'Redundante' : [],
'EAfetadoPor' : [1,16,17], 'EstadoOperacional' : 'normal', 'Funcao' :
'nenhuma', 'Potência' : 0, 'Reparando' : 'não', 'MediaReparo' : 40,
'TempoReparo' : 0, 'TempoGasto' : 0}
componente181 = {'ID' : 18, 'Tipo' : 'power Load', 'Afeta' : [],
'Redundante' : [], 'EAfetadoPor' : [17], 'EstadoOperacional' : 'normal',
'Funcao' : 'nenhuma', 'Potência' : 0, 'Reparando' : 'não', 'MediaReparo' :
40, 'TempoReparo' : 0, 'TempoGasto' : 0}
componente191 = {'ID' : 19, 'Tipo' : 'chilled water load', 'Afeta' :
[9,10,11,12], 'Redundante' : [], 'EAfetadoPor' : [9,10,11,12,17],
'EstadoOperacional' : 'normal', 'Funcao' : 'nenhuma', 'Potência' : 0,
'Reparando' : 'não', 'MediaReparo' : 40, 'TempoReparo' : 0, 'TempoGasto' :
0}
componente201 = {'ID' : 20, 'Tipo' : 'linha de gás', 'Afeta' : [2],
'Redundante' : [], 'EAfetadoPor' : [], 'EstadoOperacional' : 'normal',
'Funcao' : 'nenhuma', 'Potência' : 0, 'Reparando' : 'não', 'MediaReparo' :
40, 'TempoReparo' : 0, 'TempoGasto' : 0}
componente211 = {'ID' : 21, 'Tipo' : 'linha de água', 'Afeta' : [13],
'Redundante' : [], 'EAfetadoPor' : [], 'EstadoOperacional' : 'normal',
'Funcao' : 'nenhuma', 'Potência' : 0, 'Reparando' : 'não', 'MediaReparo' :
40, 'TempoReparo' : 0, 'TempoGasto' : 0}


#Sistema 2
sistema2 = {'EstadoOperacional' : 'normal', 'QuantidadeComponentes' : 27,
'ComponentesFalhados' : 0, 'ComponentesReparando' : 0,
'ComponentesEletricidade' : 3, 'ComponentesTermica' : 2, 'PotenciaTotal' :
4875, 'PotenciaAtual' : 4875, 'funcionando' : 1}
componente12 = {'ID' : 1, 'Tipo' : 'gerador', 'Afeta' : [3,23],
```

```
'Redundante' : [2,22], 'EAfetadoPor' : [3,23], 'EstadoOperacional' :
'normal', 'Funcao' : 'eletricidade', 'Potência' : 1400, 'Reparando' :
'não', 'MediaReparo' : 80, 'TempoReparo' : 0, 'TempoGasto' : 0}
componente22 = {'ID' : 2, 'Tipo' : 'gerador', 'Afeta' : [4,23],
'Redundante' : [1,22], 'EAfetadoPor' : [4,23], 'EstadoOperacional' :
'normal', 'Funcao' : 'eletricidade', 'Potência' : 1400, 'Reparando' :
'não', 'MediaReparo' : 80, 'TempoReparo' : 0, 'TempoGasto' : 0}
componente32 = {'ID' : 3, 'Tipo' : 'motor', 'Afeta' : [1,5,6,9,11],
'Redundante' : [], 'EAfetadoPor' : [1,5,6,9,11,26,23], 'EstadoOperacional'
: 'normal', 'Funcao' : 'nenhuma', 'Potência' : 0, 'Reparando' : 'não',
'MediaReparo' : 100, 'TempoReparo' : 0, 'TempoGasto' : 0}
componente42 = {'ID' : 4, 'Tipo' : 'motor', 'Afeta' : [2,7,8,10,12],
'Redundante' : [], 'EAfetadoPor' : [2,7,8,10,12,26,23], 'EstadoOperacional'
: 'normal', 'Funcao' : 'nenhuma', 'Potência' : 0, 'Reparando' : 'não',
'MediaReparo' : 100, 'TempoReparo' : 0, 'TempoGasto' : 0}
componente52 = {'ID' : 5, 'Tipo' : 'bomba', 'Afeta' : [3,9,11],
'Redundante' : [6], 'EAfetadoPor' : [3,9,11,23], 'EstadoOperacional' :
'normal', 'Funcao' : 'nenhuma', 'Potência' : 0, 'Reparando' : 'não',
'MediaReparo' : 40, 'TempoReparo' : 0, 'TempoGasto' : 0}
componente62 = {'ID' : 6, 'Tipo' : 'bomba', 'Afeta' : [3,9,11],
'Redundante' : [5], 'EAfetadoPor' : [3,9,11,23], 'EstadoOperacional' :
'normal', 'Funcao' : 'nenhuma', 'Potência' : 0, 'Reparando' : 'não',
'MediaReparo' : 40, 'TempoReparo' : 0, 'TempoGasto' : 0}
componente72 = {'ID' : 7, 'Tipo' : 'bomba', 'Afeta' : [4,10,12],
'Redundante' : [8], 'EAfetadoPor' : [4,10,12,23], 'EstadoOperacional' :
'normal', 'Funcao' : 'nenhuma', 'Potência' : 0, 'Reparando' : 'não',
'MediaReparo' : 40, 'TempoReparo' : 0, 'TempoGasto' : 0}
componente82 = {'ID' : 8, 'Tipo' : 'bomba', 'Afeta' : [4,10,12],
'Redundante' : [7], 'EAfetadoPor' : [4,10,12,23], 'EstadoOperacional' :
'normal', 'Funcao' : 'nenhuma', 'Potência' : 0, 'Reparando' : 'não',
'MediaReparo' : 40, 'TempoReparo' : 0, 'TempoGasto' : 0}
componente92 = {'ID' : 9, 'Tipo' : 'radiador', 'Afeta' : [3,5,6],
'Redundante' : [10,11], 'EAfetadoPor' : [3,5,6,23], 'EstadoOperacional' :
'normal', 'Funcao' : 'nenhuma', 'Potência' : 0, 'Reparando' : 'não',
'MediaReparo' : 60, 'TempoReparo' : 0, 'TempoGasto' : 0}
componente102 = {'ID' : 10, 'Tipo' : 'radiador', 'Afeta' : [4,7,8],
'Redundante' : [9,12], 'EAfetadoPor' : [4,7,8,23], 'EstadoOperacional' :
'normal', 'Funcao' : 'nenhuma', 'Potência' : 0, 'Reparando' : 'não',
'MediaReparo' : 60, 'TempoReparo' : 0, 'TempoGasto' : 0}
componente112 = {'ID' : 11, 'Tipo' : 'trocador de calor', 'Afeta' :
[3,5,6,13,14,15], 'Redundante' : [9,12], 'EAfetadoPor' : [3,5,6,13,14,15],
'EstadoOperacional' : 'normal', 'Potência' : 0, 'Funcao' : 'nenhuma',
'Reparando' : 'não', 'MediaReparo' : 60, 'TempoReparo' : 0, 'TempoGasto' :
0}
componente122 = {'ID' : 12, 'Tipo' : 'trocador de calor', 'Afeta' :
[4,7,8,13,14,15], 'Redundante' : [10,11], 'EAfetadoPor' : [4,7,8,13,14,15],
'EstadoOperacional' : 'normal', 'Potência' : 0, 'Funcao' : 'nenhuma',
'Reparando' : 'não', 'MediaReparo' : 60, 'TempoReparo' : 0, 'TempoGasto' :
0}
componente132 = {'ID' : 13, 'Tipo' : 'bomba', 'Afeta' : [11,12,15],
'Redundante' : [14], 'EAfetadoPor' : [11,12,15,23], 'EstadoOperacional' :
'normal', 'Funcao' : 'nenhuma', 'Potência' : 0, 'Reparando' : 'não',
'MediaReparo' : 40, 'TempoReparo' : 0, 'TempoGasto' : 0}
componente142 = {'ID' : 14, 'Tipo' : 'bomba', 'Afeta' : [11,12,15],
'Redundante' : [13], 'EAfetadoPor' : [11,12,15,23], 'EstadoOperacional' :
'normal', 'Funcao' : 'nenhuma', 'Potência' : 0, 'Reparando' : 'não',
'MediaReparo' : 40, 'TempoReparo' : 0, 'TempoGasto' : 0}
componente152 = {'ID' : 15, 'Tipo' : 'chiller', 'Afeta' :
[11,12,13,14,17,18,19,20,21], 'Redundante' : [16], 'EAfetadoPor' :
[11,12,13,14,17,18,19,20,21,23,25], 'EstadoOperacional' : 'normal',
'Funcao' : 'calor', 'Potência' : 668.2, 'Reparando' : 'não', 'MediaReparo'
```

```
: 60, 'TempoReparo' : 0, 'TempoGasto' : 0}
componente162 = {'ID' : 16, 'Tipo' : 'chiller', 'Afeta' : [17,18,19,20,21],
'Redundante' : [15], 'EAfetadoPor' : [17,18,19,20,21,23,25],
'EstadoOperacional' : 'normal', 'Funcao' : 'calor', 'Potência' : 1406.8,
'Reparando' : 'não', 'MediaReparo' : 60, 'TempoReparo' : 0, 'TempoGasto' :
0}
componente172 = {'ID' : 17, 'Tipo' : 'bomba', 'Afeta' : [15,16,25],
'Redundante' : [18], 'EAfetadoPor' : [15,16,23,25], 'EstadoOperacional' :
'normal', 'Funcao' : 'nenhuma', 'Potência' : 0, 'Reparando' : 'não',
'MediaReparo' : 40, 'TempoReparo' : 0, 'TempoGasto' : 0}
componente182 = {'ID' : 18, 'Tipo' : 'bomba', 'Afeta' : [15,16,25],
'Redundante' : [17], 'EAfetadoPor' : [15,16,20,21,23,25],
'EstadoOperacional' : 'normal', 'Funcao' : 'nenhuma', 'Potência' : 0,
'Reparando' : 'não', 'MediaReparo' : 40, 'TempoReparo' : 0, 'TempoGasto' :
0}
componente192 = {'ID' : 19, 'Tipo' : 'torre de resfriamento', 'Afeta' :
[15,16,20,21], 'Redundante' : [], 'EAfetadoPor' : [15,16,23,27],
'EstadoOperacional' : 'normal', 'Funcao' : 'nenhuma', 'Potência' : 0,
'Reparando' : 'não', 'MediaReparo' : 60, 'TempoReparo' : 0, 'TempoGasto' :
0}
componente202 = {'ID' : 20, 'Tipo' : 'bomba', 'Afeta' : [15,16,18],
'Redundante' : [21], 'EAfetadoPor' : [15,16,19,23], 'EstadoOperacional' :
'normal', 'Funcao' : 'nenhuma', 'Potência' : 0, 'Reparando' : 'não',
'MediaReparo' : 40, 'TempoReparo' : 0, 'TempoGasto' : 0}
componente212 = {'ID' : 21, 'Tipo' : 'bomba', 'Afeta' : [15,16,18],
'Redundante' : [20], 'EAfetadoPor' : [15,16,19,23], 'EstadoOperacional' :
'normal', 'Funcao' : 'nenhuma', 'Potência' : 0, 'Reparando' : 'não',
'MediaReparo' : 40, 'TempoReparo' : 0, 'TempoGasto' : 0}
componente222 = {'ID' : 22, 'Tipo' : 'grid', 'Afeta' : [23], 'Redundante' :
[1,2], 'EAfetadoPor' : [23], 'EstadoOperacional' : 'normal', 'Funcao' :
'eletricidade', 'Potência' : 0, 'Reparando' : 'não', 'MediaReparo' : 40,
'TempoReparo' : 0, 'TempoGasto' : 0}
componente232 = {'ID' : 23, 'Tipo' : 'bus', 'Afeta' :
[1,2,3,4,5,6,7,8,9,10,13,14,15,16,17,18,19,20,21,22,24,25], 'Redundante' :
[], 'EAfetadoPor' : [1,2,22], 'EstadoOperacional' : 'normal', 'Funcao' :
'nenhuma', 'Potência' : 0, 'Reparando' : 'não', 'MediaReparo' : 40,
'TempoReparo' : 0, 'TempoGasto' : 0}
componente242 = {'ID' : 24, 'Tipo' : 'power load', 'Afeta' : [],
'Redundante' : [], 'EAfetadoPor' : [23], 'EstadoOperacional' : 'normal',
'Funcao' : 'nenhuma', 'Potência' : 0, 'Reparando' : 'não', 'MediaReparo' :
40, 'TempoReparo' : 0, 'TempoGasto' : 0}
componente252 = {'ID' : 25, 'Tipo' : 'chilled water load', 'Afeta' :
[15,16,17,18], 'Redundante' : [], 'EAfetadoPor' : [17,18,23],
'EstadoOperacional' : 'normal', 'Funcao' : 'nenhuma', 'Potência' : 0,
'Reparando' : 'não', 'MediaReparo' : 40, 'TempoReparo' : 0, 'TempoGasto' :
0}
componente262 = {'ID' : 26, 'Tipo' : 'linha de gás', 'Afeta' : [3,4],
'Redundante' : [], 'EAfetadoPor' : [], 'EstadoOperacional' : 'normal',
'Funcao' : 'nenhuma', 'Potência' : 0, 'Reparando' : 'não', 'MediaReparo' :
40, 'TempoReparo' : 0, 'TempoGasto' : 0}
componente272 = {'ID' : 27, 'Tipo' : 'linha de água', 'Afeta' : [19],
'Redundante' : [], 'EAfetadoPor' : [], 'EstadoOperacional' : 'normal',
'Funcao' : 'nenhuma', 'Potência' : 0, 'Reparando' : 'não', 'MediaReparo' :
40, 'TempoReparo' : 0, 'TempoGasto' : 0}

#Sistema 3
sistema3 = {'EstadoOperacional' : 'normal', 'QuantidadeComponentes' : 19,
'ComponentesFalhados' : 0, 'ComponentesReparando' : 0,
'ComponentesEletricidade' : 2, 'ComponentesTermica' : 2, 'PotenciaTotal' :
6680.3, 'PotenciaAtual' : 6680.3, 'funcionando' : 1}
componente13 = {'ID' : 1, 'Tipo' : 'gerador', 'Afeta' : [2,15],
```

```
'Redundante' : [14], 'EAfetadoPor' : [2,15], 'EstadoOperacional' :
'normal', 'Funcao' : 'eletricidade', 'Potência' : 3515, 'Reparando' :
'não', 'MediaReparo' : 80, 'TempoReparo' : 0, 'TempoGasto' : 0}
componente23 = {'ID' : 2, 'Tipo' : 'turbina', 'Afeta' : [1,3], 'Redundante'
: [], 'EAfetadoPor' : [1,15,18], 'EstadoOperacional' : 'normal', 'Funcao' :
'nenhuma', 'Potência' : 0, 'Reparando' : 'não', 'MediaReparo' : 100,
'TempoReparo' : 0, 'TempoGasto' : 0}
componente33 = {'ID' : 3, 'Tipo' : 'caldeira de recuperação', 'Afeta' :
[4,6,7], 'Redundante' : [], 'EAfetadoPor' : [2,4,6,7,15],
'EstadoOperacional' : 'normal', 'Funcao' : 'nenhuma', 'Potência' : 0,
'Reparando' : 'não', 'MediaReparo' : 60, 'TempoReparo' : 0, 'TempoGasto' :
0}
componente43 = {'ID' : 4, 'Tipo' : 'chiller', 'Afeta' : [3,5,9,10,11],
'Redundante' : [8], 'EAfetadoPor' : [3,5,9,10,11,12,13,15,17],
'EstadoOperacional' : 'normal', 'Funcao' : 'calor', 'Potência' : 1758.5,
'Reparando' : 'não', 'MediaReparo' : 60, 'TempoReparo' : 0, 'TempoGasto' :
0}
componente53 = {'ID' : 5, 'Tipo' : 'tanque', 'Afeta' : [4,6,7],
'Redundante' : [], 'EAfetadoPor' : [4,6,7,19], 'EstadoOperacional' :
'normal', 'Funcao' : 'nenhuma', 'Potência' : 0, 'Reparando' : 'não',
'MediaReparo' : 30, 'TempoReparo' : 0, 'TempoGasto' : 0}
componente63 = {'ID' : 6, 'Tipo' : 'bomba', 'Afeta' : [3,5], 'Redundante' :
[7], 'EAfetadoPor' : [3,5,15], 'EstadoOperacional' : 'normal', 'Funcao' :
'nenhuma', 'Potência' : 0, 'Reparando' : 'não', 'MediaReparo' : 40,
'TempoReparo' : 0, 'TempoGasto' : 0}
componente73 = {'ID' : 7, 'Tipo' : 'bomba', 'Afeta' : [3,5], 'Redundante' :
[6], 'EAfetadoPor' : [3,5,15], 'EstadoOperacional' : 'normal', 'Funcao' :
'nenhuma', 'Potência' : 0, 'Reparando' : 'não', 'MediaReparo' : 40,
'TempoReparo' : 0, 'TempoGasto' : 0}
componente83 = {'ID' : 8, 'Tipo' : 'chiller', 'Afeta' : [9,10,11],
'Redundante' : [4], 'EAfetadoPor' : [9,10,11,12,13,15,17],
'EstadoOperacional' : 'normal', 'Funcao' : 'calor', 'Potência' : 1406.8,
'Reparando' : 'não', 'MediaReparo' : 60, 'TempoReparo' : 0, 'TempoGasto' :
0}
componente93 = {'ID' : 9, 'Tipo' : 'bomba', 'Afeta' : [4,8,17],
'Redundante' : [10], 'EAfetadoPor' : [4,8,15,17], 'EstadoOperacional' :
'normal', 'Funcao' : 'nenhuma', 'Potência' : 0, 'Reparando' : 'não',
'MediaReparo' : 40, 'TempoReparo' : 0, 'TempoGasto' : 0}
componente103 = {'ID' : 10, 'Tipo' : 'bomba', 'Afeta' : [4,8,17],
'Redundante' : [9], 'EAfetadoPor' : [4,8,15,17], 'EstadoOperacional' :
'normal', 'Funcao' : 'nenhuma', 'Potência' : 0, 'Reparando' : 'não',
'MediaReparo' : 40, 'TempoReparo' : 0, 'TempoGasto' : 0}
componente113 = {'ID' : 11, 'Tipo' : 'torre de resfriamento', 'Afeta' :
[4,8,12,13], 'Redundante' : [], 'EAfetadoPor' : [4,8,12,13,15,19],
'EstadoOperacional' : 'normal', 'Funcao' : 'nenhuma', 'Potência' : 0,
'Reparando' : 'não', 'MediaReparo' : 60, 'TempoReparo' : 0, 'TempoGasto' :
0}
componente123 = {'ID' : 12, 'Tipo' : 'bomba', 'Afeta' : [4,8,11],
'Redundante' : [13], 'EAfetadoPor' : [11,15], 'EstadoOperacional' :
'normal', 'Funcao' : 'nenhuma', 'Potência' : 0, 'Reparando' : 'não',
'MediaReparo' : 40, 'TempoReparo' : 0, 'TempoGasto' : 0}
componente133 = {'ID' : 13, 'Tipo' : 'bomba', 'Afeta' : [4,8,11],
'Redundante' : [12], 'EAfetadoPor' : [11,15], 'EstadoOperacional' :
'normal', 'Funcao' : 'nenhuma', 'Potência' : 0, 'Reparando' : 'não',
'MediaReparo' : 40, 'TempoReparo' : 0, 'TempoGasto' : 0}
componente143 = {'ID' : 14, 'Tipo' : 'grid', 'Afeta' : [15], 'Redundante' :
[1], 'EAfetadoPor' : [15], 'EstadoOperacional' : 'normal', 'Funcao' :
'eletricidade', 'Potência' : 0, 'Reparando' : 'não', 'MediaReparo' : 40,
'TempoReparo' : 0, 'TempoGasto' : 0}
componente153 = {'ID' : 15, 'Tipo' : 'bus', 'Afeta' :
[1,2,3,4,6,7,8,9,10,11,12,13,14,16,17], 'Redundante' : [], 'EAfetadoPor' :
```

```python
[1,14], 'EstadoOperacional' : 'normal', 'Funcao' : 'nenhuma', 'Potência' :
0, 'Reparando' : 'não', 'MediaReparo' : 40, 'TempoReparo' : 0, 'TempoGasto'
: 0}
componente163 = {'ID' : 16, 'Tipo' : 'power load', 'Afeta' : [],
'Redundante' : [], 'EAfetadoPor' : [15], 'EstadoOperacional' : 'normal',
'Funcao' : 'nenhuma', 'Potência' : 0, 'Reparando' : 'não', 'MediaReparo' :
40, 'TempoReparo' : 0, 'TempoGasto' : 0}
componente173 = {'ID' : 17, 'Tipo' : 'chilled water load', 'Afeta' :
[4,8,9,10], 'Redundante' : [], 'EAfetadoPor' : [9,10,15],
'EstadoOperacional' : 'normal', 'Funcao' : 'nenhuma', 'Potência' : 0,
'Reparando' : 'não', 'MediaReparo' : 40, 'TempoReparo' : 0, 'TempoGasto' :
0}
componente183 = {'ID' : 18, 'Tipo' : 'linha de gás', 'Afeta' : [2],
'Redundante' : [], 'EAfetadoPor' : [], 'EstadoOperacional' : 'normal',
'Funcao' : 'nenhuma', 'Potência' : 0, 'Reparando' : 'não', 'MediaReparo' :
40, 'TempoReparo' : 0, 'TempoGasto' : 0}
componente193 = {'ID' : 19, 'Tipo' : 'linha de água', 'Afeta' : [5,11],
'Redundante' : [], 'EAfetadoPor' : [], 'EstadoOperacional' : 'normal',
'Funcao' : 'nenhuma', 'Potência' : 0, 'Reparando' : 'não', 'MediaReparo' :
40, 'TempoReparo' : 0, 'TempoGasto' : 0}

#Sistema 4
sistema4 = {'EstadoOperacional' : 'normal', 'QuantidadeComponentes' : 22,
'ComponentesFalhados' : 0, 'ComponentesReparando' : 0,
'ComponentesEletricidade' : 3, 'ComponentesTermica' : 2, 'PotenciaTotal' :
7695.5, 'PotenciaAtual' : 7695.5, 'funcionando' : 1}
componente14 = {'ID' : 1, 'Tipo' : 'gerador', 'Afeta' : [3,18],
'Redundante' : [2,17], 'EAfetadoPor' : [3,18,21], 'EstadoOperacional' :
'normal', 'Funcao' : 'eletricidade', 'Potência' : 1210, 'Reparando' :
'não', 'MediaReparo' : 80, 'TempoReparo' : 0, 'TempoGasto' : 0}
componente24 = {'ID' : 2, 'Tipo' : 'gerador', 'Afeta' : [4,18],
'Redundante' : [1,17], 'EAfetadoPor' : [4,18,21], 'EstadoOperacional' :
'normal', 'Funcao' : 'eletricidade', 'Potência' : 1210, 'Reparando' :
'não', 'MediaReparo' : 80, 'TempoReparo' : 0, 'TempoGasto' : 0}
componente34 = {'ID' : 3, 'Tipo' : 'turbina', 'Afeta' : [1,5], 'Redundante'
: [], 'EAfetadoPor' : [1,18], 'EstadoOperacional' : 'normal', 'Funcao' :
'nenhuma', 'Potência' : 0, 'Reparando' : 'não', 'MediaReparo' : 100,
'TempoReparo' : 0, 'TempoGasto' : 0}
componente44 = {'ID' : 4, 'Tipo' : 'turbina', 'Afeta' : [2,6], 'Redundante'
: [], 'EAfetadoPor' : [2,18], 'EstadoOperacional' : 'normal', 'Funcao' :
'nenhuma', 'Potência' : 0, 'Reparando' : 'não', 'MediaReparo' : 100,
'TempoReparo' : 0, 'TempoGasto' : 0}
componente54 = {'ID' : 5, 'Tipo' : 'caldeira de recuperação', 'Afeta' :
[7,9,10], 'Redundante' : [6], 'EAfetadoPor' : [3,7,9,10,18],
'EstadoOperacional' : 'normal', 'Funcao' : 'nenhuma', 'Potência' : 0,
'Reparando' : 'não', 'MediaReparo' : 60, 'TempoReparo' : 0, 'TempoGasto' :
0}
componente64 = {'ID' : 6, 'Tipo' : 'caldeira de recuperação', 'Afeta' :
[7,9,10], 'Redundante' : [5], 'EAfetadoPor' : [4,7,9,10,18],
'EstadoOperacional' : 'normal', 'Funcao' : 'nenhuma', 'Potência' : 0,
'Reparando' : 'não', 'MediaReparo' : 60, 'TempoReparo' : 0, 'TempoGasto' :
0}
componente74 = {'ID' : 7, 'Tipo' : 'chiller', 'Afeta' :
[5,6,8,12,13,14,15,16,20], 'Redundante' : [11], 'EAfetadoPor' :
[5,6,8,12,13,14,15,16,18,20], 'EstadoOperacional' : 'normal', 'Funcao' :
'calor', 'Potência' : 3868.7, 'Reparando' : 'não', 'MediaReparo' : 60,
'TempoReparo' : 0, 'TempoGasto' : 0}
componente84 = {'ID' : 8, 'Tipo' : 'tanque', 'Afeta' : [7,9,10],
'Redundante' : [], 'EAfetadoPor' : [7,9,10,22], 'EstadoOperacional' :
'normal', 'Funcao' : 'nenhuma', 'Potência' : 0, 'Reparando' : 'não',
'MediaReparo' : 30, 'TempoReparo' : 0, 'TempoGasto' : 0}
```

```python
componente94 = {'ID' : 9, 'Tipo' : 'bomba', 'Afeta' : [5,6,8], 'Redundante'
: [10], 'EAfetadoPor' : [5,6,8,18], 'EstadoOperacional' : 'normal',
'Funcao' : 'nenhuma', 'Potência' : 0, 'Reparando' : 'não', 'MediaReparo' :
40, 'TempoReparo' : 0, 'TempoGasto' : 0}
componente104 = {'ID' : 10, 'Tipo' : 'bomba', 'Afeta' : [5,6,8],
'Redundante' : [9], 'EAfetadoPor' : [5,6,8,18], 'EstadoOperacional' :
'normal', 'Funcao' : 'nenhuma', 'Potência' : 0, 'Reparando' : 'não',
'MediaReparo' : 40, 'TempoReparo' : 0, 'TempoGasto' : 0}
componente114 = {'ID' : 11, 'Tipo' : 'chiller', 'Afeta' :
[12,13,14,15,16,20], 'Redundante' : [7], 'EAfetadoPor' :
[12,13,14,15,16,18,20], 'EstadoOperacional' : 'normal', 'Funcao' : 'calor',
'Potência' : 1406.8, 'Reparando' : 'não', 'MediaReparo' : 60, 'TempoReparo'
: 0, 'TempoGasto' : 0}
componente124 = {'ID' : 12, 'Tipo' : 'bomba', 'Afeta' : [7,11,20],
'Redundante' : [13], 'EAfetadoPor' : [7,11,18,20], 'EstadoOperacional' :
'normal', 'Funcao' : 'nenhuma', 'Potência' : 0, 'Reparando' : 'não',
'MediaReparo' : 40, 'TempoReparo' : 0, 'TempoGasto' : 0}
componente134 = {'ID' : 13, 'Tipo' : 'bomba', 'Afeta' : [7,11,20],
'Redundante' : [12], 'EAfetadoPor' : [7,11,18,20], 'EstadoOperacional' :
'normal', 'Funcao' : 'nenhuma', 'Potência' : 0, 'Reparando' : 'não',
'MediaReparo' : 40, 'TempoReparo' : 0, 'TempoGasto' : 0}
componente144 = {'ID' : 14, 'Tipo' : 'torre de resfriamento', 'Afeta' :
[7,11,15,16], 'Redundante' : [], 'EAfetadoPor' : [7,11,15,16,18,22],
'EstadoOperacional' : 'normal', 'Funcao' : 'nenhuma', 'Potência' : 0,
'Reparando' : 'não', 'MediaReparo' : 60, 'TempoReparo' : 0, 'TempoGasto' :
0}
componente154 = {'ID' : 15, 'Tipo' : 'bomba', 'Afeta' : [7,11,14],
'Redundante' : [16], 'EAfetadoPor' : [7,11,14,18], 'EstadoOperacional' :
'normal', 'Funcao' : 'nenhuma', 'Potência' : 0, 'Reparando' : 'não',
'MediaReparo' : 40, 'TempoReparo' : 0, 'TempoGasto' : 0}
componente164 = {'ID' : 16, 'Tipo' : 'bomba', 'Afeta' : [7,11,14],
'Redundante' : [15], 'EAfetadoPor' : [7,11,14,18], 'EstadoOperacional' :
'normal', 'Funcao' : 'nenhuma', 'Potência' : 0, 'Reparando' : 'não',
'MediaReparo' : 40, 'TempoReparo' : 0, 'TempoGasto' : 0}
componente174 = {'ID' : 17, 'Tipo' : 'grid', 'Afeta' : [18], 'Redundante' :
[1,2], 'EAfetadoPor' : [18], 'EstadoOperacional' : 'normal', 'Funcao' :
'eletricidade', 'Potência' : 0, 'Reparando' : 'não', 'MediaReparo' : 40,
'TempoReparo' : 0, 'TempoGasto' : 0}
componente184 = {'ID' : 18, 'Tipo' : 'bus', 'Afeta' :
[1,2,3,4,5,6,7,9,10,11,12,13,14,15,16,17,19,20], 'Redundante' : [],
'EAfetadoPor' : [1,2,17], 'EstadoOperacional' : 'normal', 'Funcao' :
'nenhuma', 'Potência' : 0, 'Reparando' : 'não', 'MediaReparo' : 40,
'TempoReparo' : 0, 'TempoGasto' : 0}
componente194 = {'ID' : 19, 'Tipo' : 'power load', 'Afeta' : [],
'Redundante' : [], 'EAfetadoPor' : [18], 'EstadoOperacional' : 'normal',
'Funcao' : 'nenhuma', 'Potência' : 0, 'Reparando' : 'não', 'MediaReparo' :
40, 'TempoReparo' : 0, 'TempoGasto' : 0}
componente204 = {'ID' : 20, 'Tipo' : 'chilled water load', 'Afeta' :
[7,11,12,13], 'Redundante' : [], 'EAfetadoPor' : [7,11,12,13,18],
'EstadoOperacional' : 'normal', 'Funcao' : 'nenhuma', 'Potência' : 0,
'Reparando' : 'não', 'MediaReparo' : 40, 'TempoReparo' : 0, 'TempoGasto' :
0}
componente214 = {'ID' : 21, 'Tipo' : 'linha de gás', 'Afeta' : [1,2],
'Redundante' : [], 'EAfetadoPor' : [], 'EstadoOperacional' : 'normal',
'Funcao' : 'nenhuma', 'Potência' : 0, 'Reparando' : 'não', 'MediaReparo' :
40, 'TempoReparo' : 0, 'TempoGasto' : 0}
componente224 = {'ID' : 22, 'Tipo' : 'linha de água', 'Afeta' : [8,14],
'Redundante' : [], 'EAfetadoPor' : [], 'EstadoOperacional' : 'normal',
'Funcao' : 'nenhuma', 'Potência' : 0, 'Reparando' : 'não', 'MediaReparo' :
40, 'TempoReparo' : 0, 'TempoGasto' : 0}
```

```python
#declarar sistema como lista
sistema = list()

#declarar ciclo, pi e pcr como lista
lista_ciclo = [1, 2, 3, 4]
lista_pi = [0.997, 0.998, 0.999, 0.9995]
lista_pcnr = [1, 0.5, 0.25]

#rodar simulação para cada ciclo
for var_ciclo in range (0, len(lista_ciclo)):
    ciclo = lista_ciclo[var_ciclo]
    if ciclo == 1:
        sistema.append(sistema1)
        sistema.append(componente11)
        sistema.append(componente21)
        sistema.append(componente31)
        sistema.append(componente41)
        sistema.append(componente51)
        sistema.append(componente61)
        sistema.append(componente71)
        sistema.append(componente81)
        sistema.append(componente91)
        sistema.append(componente101)
        sistema.append(componente111)
        sistema.append(componente121)
        sistema.append(componente131)
        sistema.append(componente141)
        sistema.append(componente151)
        sistema.append(componente161)
        sistema.append(componente171)
        sistema.append(componente181)
        sistema.append(componente191)
        sistema.append(componente201)
        sistema.append(componente211)

    if ciclo == 2:
        sistema.append(sistema2)
        sistema.append(componente12)
        sistema.append(componente22)
        sistema.append(componente32)
        sistema.append(componente42)
        sistema.append(componente52)
        sistema.append(componente62)
        sistema.append(componente72)
        sistema.append(componente82)
        sistema.append(componente92)
        sistema.append(componente102)
        sistema.append(componente112)
        sistema.append(componente122)
        sistema.append(componente132)
        sistema.append(componente142)
        sistema.append(componente152)
        sistema.append(componente162)
        sistema.append(componente172)
        sistema.append(componente182)
        sistema.append(componente192)
        sistema.append(componente202)
        sistema.append(componente212)
        sistema.append(componente222)
        sistema.append(componente232)
        sistema.append(componente242)
```

```python
        sistema.append(componente252)
        sistema.append(componente262)
        sistema.append(componente272)

    if ciclo == 3:
        sistema.append(sistema3)
        sistema.append(componente13)
        sistema.append(componente23)
        sistema.append(componente33)
        sistema.append(componente43)
        sistema.append(componente53)
        sistema.append(componente63)
        sistema.append(componente73)
        sistema.append(componente83)
        sistema.append(componente93)
        sistema.append(componente103)
        sistema.append(componente113)
        sistema.append(componente123)
        sistema.append(componente133)
        sistema.append(componente143)
        sistema.append(componente153)
        sistema.append(componente163)
        sistema.append(componente173)
        sistema.append(componente183)
        sistema.append(componente193)
    if ciclo == 4:
        sistema.append(sistema4)
        sistema.append(componente14)
        sistema.append(componente24)
        sistema.append(componente34)
        sistema.append(componente44)
        sistema.append(componente54)
        sistema.append(componente64)
        sistema.append(componente74)
        sistema.append(componente84)
        sistema.append(componente94)
        sistema.append(componente104)
        sistema.append(componente114)
        sistema.append(componente124)
        sistema.append(componente134)
        sistema.append(componente144)
        sistema.append(componente154)
        sistema.append(componente164)
        sistema.append(componente174)
        sistema.append(componente184)
        sistema.append(componente194)
        sistema.append(componente204)
        sistema.append(componente214)
        sistema.append(componente224)

    #simular para cada pcnr
    for var_pcnr in range (0, len(lista_pcnr)):
        pcnr = lista_pcnr[var_pcnr]

        #simular para cada pi
        for var_pi in range (0, len(lista_pi)):
            pi = lista_pi[var_pi]
            print(f'simulação com ciclo {ciclo}, pcr {1 - pcnr} e pi {pi}')

            tempo = 1
            resiliente = 0
```

```python
            parado = 0
            cont = 1

            # Abrir arquivo com os dados do gráfico#
            f = open(f'{pi}_{1 - pcnr}_S#{ciclo}_graph.csv', 'w',
newline='')
            writer = csv.writer(f)

            while cont <= NumeroSimulacoes:
                while tempo <= VidaUtil:

                    ### Escolha aleatória do componente não falhado ###
                    if sistema[0]['EstadoOperacional'] != 'falhado':
                        comp = random.randint(1,
sistema[0]['QuantidadeComponentes'] + 1)
                        while sistema[comp]['EstadoOperacional'] !=
'normal':  # Procura um componente até que o mesmo possua estado
operacional normal para a verificação de falha
                            comp = random.randint(1,
sistema[0]['QuantidadeComponentes'] + 1)

                        ### Avaliar a probabilidade de falha e de reparo do
componente ###
                        limsup = 100000
                        falha = random.randint(0, limsup + 1) / limsup  #
probabilidade aleatoria de falha
                        if falha > pi:
                            sistema[comp]['EstadoOperacional'] = 'falhouO'
                            sistema[0]['ComponentesFalhados'] += 1

                            ### Avaliação da probabilidade de reparo ###
                            reparo = random.randint(0, limsup + 1) / limsup
# probabilidade de reparo
                            if reparo > pcnr:
                                sistema[comp]['Reparando'] = 'sim'
                                sistema[0]['ComponentesReparando'] += 1
                                novo_tr =
round(random.normal(sistema[comp]['MediaReparo'], 0.2 *
sistema[comp]['MediaReparo']))
                                sistema[comp]['TempoReparo'] = novo_tr

                            ### Avaliação da propação de falha ###
                            falhados_agora = list()
                            falhados_agora.append(comp)
                            if len(sistema[comp]['Afeta']) > 0:  # se o
componente realmente afetar outros
                                for va2 in range(0,
len(sistema[comp]['Afeta'])):
                                    afetado = sistema[comp]['Afeta'][va2]
                                    if
sistema[afetado]['EstadoOperacional'] == 'normal':

sistema[afetado]['EstadoOperacional'] = 'falhouP'
                                        falhados_agora.append(afetado)
                                        sistema[0]['ComponentesFalhados'] =
sistema[0]['ComponentesFalhados'] + 1

                                        # verificar se redundante afeta o
que falhou
                                        if len(sistema[comp]['Redundante'])
> 0:
```

```python
                                    for pos_redundante in range(0,
len(sistema[comp]['Redundante'])):
                                        redundante =
sistema[comp]['Redundante'][pos_redundante]
                                        if
sistema[redundante]['EstadoOperacional'] == 'normal':
                                            if
len(sistema[afetado]['EAfetadoPor']) > 0:
                                                for pos_afetadopor
in range(0, len(sistema[afetado]['EAfetadoPor'])):
                                                    afetadopor =
sistema[afetado]['EAfetadoPor'][pos_afetadopor]
                                                    if afetadopor
== redundante:
                                                        if afetado
in falhados_agora:

sistema[afetado]['EstadoOperacional'] = 'normal'

sistema[0]['ComponentesFalhados'] = sistema[0]['ComponentesFalhados'] - 1

falhados_agora.remove(afetado)
                                    falhados_agora.remove(comp)

                                    while len(falhados_agora) > 0:
                                        comp_verificado = falhados_agora[0]
                                        if
len(sistema[comp_verificado]['Afeta']) > 0:
                                            for va16 in range(0,
len(sistema[comp_verificado]['Afeta'])):
                                                afetado_agora =
sistema[comp_verificado]['Afeta'][va16]
                                                if
sistema[afetado_agora]['EstadoOperacional'] == 'normal':

sistema[afetado_agora]['EstadoOperacional'] = 'falhouP'

falhados_agora.append(afetado_agora)

sistema[0]['ComponentesFalhados'] = sistema[0]['ComponentesFalhados'] + 1

                                                    # verificar se redundante
afeta o que falhou
                                                    if
len(sistema[comp_verificado]['Redundante']) > 0:
                                                        for pos_redundante2 in
range(0, len(sistema[comp_verificado]['Redundante'])):
                                                            redundante2 =
sistema[comp_verificado]['Redundante'][pos_redundante2]
                                                            if
sistema[redundante2]['EstadoOperacional'] == 'normal':
                                                                if
len(sistema[afetado_agora]['EAfetadoPor']) > 0:
                                                                    for
pos_afetadopor2 in range(0, len(sistema[afetado_agora]['EAfetadoPor'])):

afetadopor2 = sistema[afetado_agora]['EAfetadoPor'][pos_afetadopor2]
                                                                        if
afetadopor2 == redundante2:
                                                                            if
afetado_agora in falhados_agora:
```

```python
                    sistema[afetado_agora]['EstadoOperacional'] = 'normal'

                    sistema[0]['ComponentesFalhados'] = sistema[0]['ComponentesFalhados'] - 1

                    falhados_agora.remove(afetado_agora)
                                        falhados_agora.remove(comp_verificado)
                                    falhados_agora.clear()

                        ##### Avaliar se tem componente sendo reparado #####
                    for componente in range(1,
sistema[0]['QuantidadeComponentes'] + 1):
                        if sistema[componente]['Reparando'] == 'sim':
                            sistema[componente]['TempoGasto'] =
sistema[componente]['TempoGasto'] + 1
                            if sistema[componente]['TempoGasto'] ==
sistema[componente]['TempoReparo']:
                                sistema[componente]['Reparando'] = 'não'
                                sistema[componente]['EstadoOperacional'] =
'normal'
                                sistema[componente]['TempoGasto'] = 0
                                sistema[0]['ComponentesReparando'] =
sistema[0]['ComponentesReparando'] - 1
                                # verificar propagação do reparo
                                falhou = list()
                                sistema[0]['ComponentesFalhados'] = 0
                                for va17 in range(1,
sistema[0]['QuantidadeComponentes'] + 1):  # passa por todos os componentes
                                    if sistema[va17]['EstadoOperacional']
== 'falhouP':  # troca de falhoup
                                        sistema[va17]['EstadoOperacional']
= 'normal'  # para normal
                                    elif sistema[va17]['EstadoOperacional']
== 'falhouO':
                                        falhou.append(va17)
                                        sistema[0]['ComponentesFalhados'] =
sistema[0]['ComponentesFalhados'] + 1
                                while len(falhou) > 0:
                                    verificado_agora = falhou[0]
                                    if
len(sistema[verificado_agora]['Afeta']) > 0:
                                        for va18 in range(0,
len(sistema[verificado_agora]['Afeta'])):
                                            afetado_agora_2 =
sistema[verificado_agora]['Afeta'][va18]
                                            if
sistema[afetado_agora_2]['EstadoOperacional'] == 'normal':

sistema[afetado_agora_2]['EstadoOperacional'] = 'falhouP'

falhou.append(afetado_agora_2)

sistema[0]['ComponentesFalhados'] = sistema[0]['ComponentesFalhados'] + 1
                                    if
len(sistema[verificado_agora]['Redundante']) > 0:
                                        for pos_redundante3 in
range(0, len(sistema[verificado_agora]['Redundante'])):
                                            redundante3 =
sistema[verificado_agora]['Redundante'][pos_redundante3]
                                            if
sistema[redundante3]['EstadoOperacional'] == 'normal':
```

```python
                                                          if
len(sistema[afetado_agora_2]['EAfetadoPor']) > 0:
                                                            for
pos_afetadopor3 in range(0, len(sistema[afetado_agora_2]['EAfetadoPor'])):

afetadopor3 = sistema[afetado_agora_2]['EAfetadoPor'][pos_afetadopor3]
                                                              if
afetadopor3 == redundante3:

                                                            if
afetado_agora_2 in falhou:

sistema[afetado_agora_2]['EstadoOperacional'] = 'normal'

sistema[0]['ComponentesFalhados'] = sistema[0]['ComponentesFalhados'] - 1

falhou.remove(afetado_agora_2)
                                        falhou.remove(verificado_agora)
                                    falhou.clear()

                    ##### Verificação da potência #####
                    potenciaatual = 0
                    for cppotencia in range(1,
(sistema[0]['QuantidadeComponentes'] + 1)):
                        if (sistema[cppotencia]['Funcao'] == 'eletricidade'
or sistema[cppotencia]['Funcao'] == 'calor') and
sistema[cppotencia]['EstadoOperacional'] == 'normal':  # se o componente
for produtor e estiver operando
                            potenciaatual = potenciaatual +
sistema[cppotencia]['Potência']
                    sistema[0]['PotenciaAtual'] = potenciaatual  #
atualizar valor de potência da planta
                    porcpot = potenciaatual / sistema[0]['PotenciaTotal']
                    if potenciaatual == 0:
                        sistema[0]['funcionando'] = 0
                        sistema[0]['EstadoOperacional'] = 'falhado'
                        if sistema[0]['ComponentesReparando'] == 0:  # se
não houver componentes reparando quer dizer que o sistema falhou
                            break
                        else:
                            parado += 1
                            sistema[0]['funcionando'] = 0
                    else:
                        sistema[0]['funcionando'] = 1
                        if sistema[0]['ComponentesFalhados'] == 0:
                            sistema[0]['EstadoOperacional'] = 'normal'
                        elif sistema[0]['ComponentesFalhados'] > 0:
                            sistema[0]['EstadoOperacional'] = 'resiliente'
                            resiliente += 1
                    writer.writerow((tempo, sistema[0]['funcionando'],
porcpot, cont))

                    # Contagem de tempo#
                    tempo += 1

                tempo = 1
                resiliente = 0
                parado = 0
                sistema[0]['EstadoOperacional'] = 'normal'
                sistema[0]['ComponentesFalhados'] = 0
                sistema[0]['ComponentesReparando'] = 0
                sistema[0]['funcionando'] = 1
```

```python
                for i in range(1, sistema[0]['QuantidadeComponentes'] + 1):
                    sistema[i]['EstadoOperacional'] = 'normal'
                    sistema[i]['TempoGasto'] = 0
                    sistema[i]['Reparando'] = 'não'
                cont += 1
            f.close()
    sistema.clear()


for var_ciclo_2 in range (0, len(lista_ciclo)):
    ciclo_2 = lista_ciclo[var_ciclo_2]

    for var_pcnr_2 in range (0, len(lista_pcnr)):
        pcnr_2 = lista_pcnr[var_pcnr_2]

        for var_pi_2 in range (0, len(lista_pi)):
            pi_2 = lista_pi[var_pi_2]

            file = open(f'graf_{pi_2}_{1 - pcnr_2}_S#{ciclo_2}.csv', 'w',
newline='')
            writer2 = csv.writer(file)  # do pacote csv chamar o metodo
writer
            writer2.writerow(('tempo', 'probabilidade funcionamento',
'mediapotencia'))

            x = [0] * VidaUtil
            y = [0] * VidaUtil
            z = [0] * VidaUtil
            soma = [0]*VidaUtil
            contador = [0] * VidaUtil
            contador2 = [0] * VidaUtil

            for va4 in range(1, (VidaUtil + 1)):
                y[va4 - 1] = va4

            with open(f'{pi_2}_{1 - pcnr_2}_S#{ciclo_2}_graph.csv', 'r') as
csvfile:
                plots = csv.reader(csvfile, delimiter=',')
                for row in plots:

                    temponovo = int(row[0])
                    soma[temponovo-1] = soma[temponovo - 1] + float(row[2])
                    contador[temponovo - 1] += 1

                    if int(row[1]) == 1:
                        contador2[temponovo - 1] += 1

            for va5 in range(0, VidaUtil):
                if contador[va5] != 0:
                    x[va5] = contador2[va5] / NumeroSimulacoes
                    z[va5] = soma[va5]/NumeroSimulacoes
                else:
                    x[va5] = 0
                    z[va5] = 0
                writer2.writerow((y[va5], x[va5], z[va5]))

            file.close()
            os.remove(f'{pi_2}_{1 - pcnr_2}_S#{ciclo_2}_graph.csv')

tempo_final = time.time()
##### Cálculo do tempo de execução #####
```

```python
tempo_total_horas = (tempo_final - tempo_inicial) // 3600
tempo_total_minutos = ((tempo_final - tempo_inicial) % 3600) // 60
tempo_total_segundos = ((tempo_final - tempo_inicial) % 3600) % 60
if tempo_total_horas > 0:
    print(f"a simulação acabou em {tempo_total_horas} horas,
{tempo_total_minutos} minutos e {tempo_total_segundos:.0f} segundos ")
elif tempo_total_minutos > 0:
    print(f"a simulação acabou em {tempo_total_minutos} minutos e
{tempo_total_segundos:.0f} segundos ")
else:
    print(f"a simulação acabou em {tempo_total_segundos:.0f} segundos ")

winsound.Beep(1000, 2000)


#26/07/2021
```

The variation of NFx and its IP with different repair probabilities are shown in Figure 50 and Figure 51, respectively. The calculation of IP is done considering each 10% increase in p_{cr}. The simulations considered the initial condition of $p_i = 0.9970$ and $T = 1$ year. The aim of these figures is to observe the behavior of these parameters under several p_{cr} conditions, although its extreme values are not an acceptable assumption in practice.

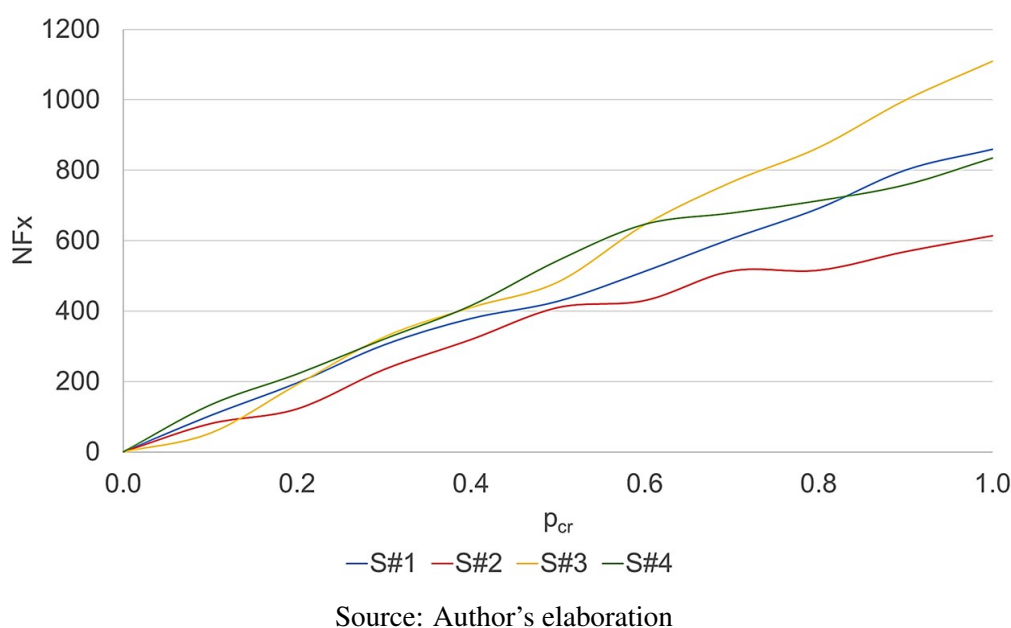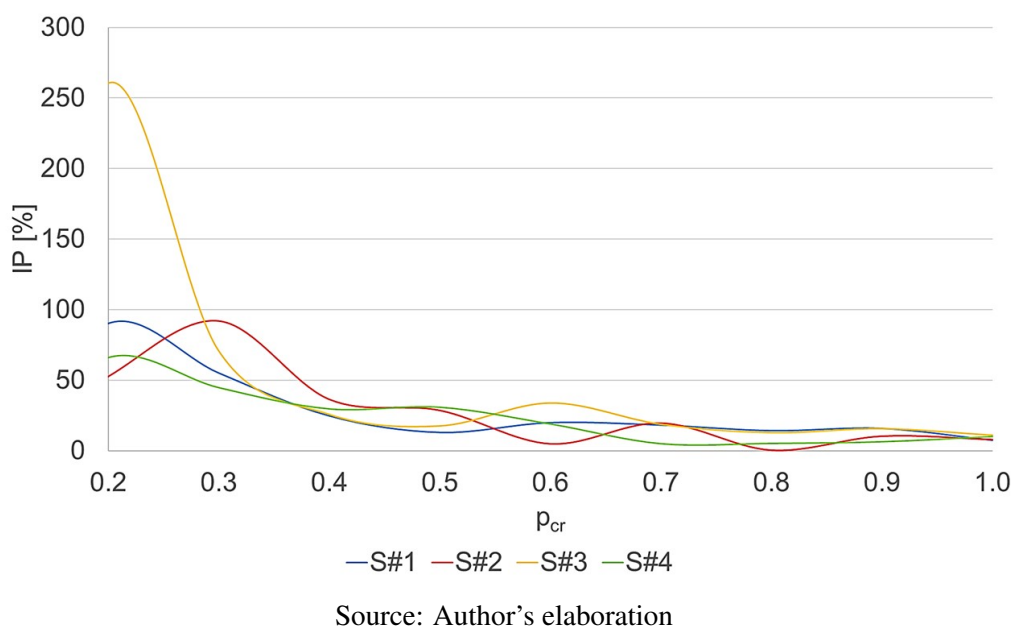Figure 50 – NFx variation with different p_{cr}

Source: Author's elaboration

Figure 51 – IP variation with different p_{cr}

Source: Author's elaboration

The first curve shown in Figure 50 exhibit an unstoppable growth with the increase of p_{cr}. S#3, the least resilient system indicated by all the metrics and graphical analysis, presents a more inclined curve,

which indicates a greater influence of p_{cr} increasing, as discussed before. It is interesting that this variation diminishes the inclination of S#2, the most resilient system, along the curve trajectory. This suggests a possible p_{cr} saturation point, in which the its increase does not avoid more interruptions. This could be more explored by further investigations.

Figure 51 exhibits the IP variation along different p_{cr} values, and it can be seen that a simple introduction of a repairable condition was able to avoid a high number of interruptions in S#3 during its operation. The increase of this parameter induces lower IP values, with a curious oscillation, converging to close to zero.

These results are preliminaries and need further development, including simulations with different conditions and comparison of the curves behavior, and therefore they were described in appendix.